JACC: CARDIOVASCULAR IMAGING VOL. ■, NO. ■, 2024

iREVIEW

STATE-OF-THE-ART REVIEW

Myocardial Strain Imaging

Theory, Current Practice, and the Future

Otto A. Smiseth, MD, PhD,[a] Oliver Rider, BA, BMBCh, DPhil,[b] Marta Cvijic, MD, PhD,[c,d] Ladislav Valkovič, PhD,[b,e] Espen W. Remme, MSc, PhD,[a,f] Jens-Uwe Voigt, MD, PhD[g,h]

ABSTRACT

Myocardial strain imaging by echocardiography or cardiac magnetic resonance (CMR) is a powerful method to diagnose cardiac disease. Strain imaging provides measures of myocardial shortening, thickening, and lengthening and can be applied to any cardiac chamber. Left ventricular (LV) global longitudinal strain by speckle-tracking echocardiography is the most widely used clinical strain parameter. Several CMR-based modalities are available and are ready to be implemented clinically. Clinical applications of strain include global longitudinal strain as a more sensitive method than ejection fraction for diagnosing mild systolic dysfunction. This applies to patients suspected of having heart failure with normal LV ejection fraction, to early systolic dysfunction in valvular disease, and when monitoring myocardial function during cancer chemotherapy. Segmental LV strain maps provide diagnostic clues in specific cardiomyopathies, when evaluating LV dyssynchrony and ischemic dysfunction. Strain imaging is a promising modality to quantify right ventricular function. Left atrial strain may be used to evaluate LV diastolic function and filling pressure. (JACC Cardiovasc Imaging. 2024;■:■–■)

Strain is a term that originates from the field of continuum mechanics and may be used to describe deformations of any structure, including the heart. In cardiac imaging, the term *strain* is used to describe myocardial shortening and thickening, which are the fundamental features of myocardial fiber function. **Figure 1A** illustrates the most commonly measured myocardial strains. These include left ventricular (LV) longitudinal and circumferential shortening strains and radial thickening strain. Both longitudinal and circumferential strains contribute to LV wall thickening. In addition to these orthogonal normal strains, a complete characterization of LV deformation includes 3 shear strains that are less commonly measured: circumferential-longitudinal shear, or so-called twist, results from 2 short-axis planes rotating relative to each other, as illustrated in **Figure 1B**;

From the [a]Institute for Surgical Research, Division of Cardiovascular and Pulmonary Diseases, Oslo University Hospital, Rikshospitalet, and University of Oslo, Oslo, Norway; [b]Oxford Centre for Clinical Magnetic Resonance Research, RDM Cardiovascular Medicine, University of Oxford, Oxford, United Kingdom; [c]Department of Cardiology, University Medical Centre Ljubljana, Ljubljana, Slovenia; [d]Faculty of Medicine, University of Ljubljana, Ljubljana, Slovenia; [e]Department of Imaging Methods, Institute of Measurement Science, Slovak Academy of Sciences, Bratislava, Slovakia; [f]The Intervention Center, Oslo University Hospital, Rikshospitalet, Oslo, Norway; [g]Department of Cardiovascular Diseases, University Hospitals Leuven, Leuven, Belgium; and the [h]Department of Cardiovascular Sciences, KU Leuven-University of Leuven, Leuven, Belgium.
The authors attest they are in compliance with human studies committees and animal welfare regulations of the authors' institutions and Food and Drug Administration guidelines, including patient consent where appropriate. For more information, visit the Author Center.

Manuscript received February 27, 2024; revised manuscript received July 1, 2024, accepted July 3, 2024.

ISSN 1936-878X https://doi.org/10.1016/j.jcmg.2024.07.011

ABBREVIATIONS AND ACRONYMS

2D = 2-dimensional

3D = 3-dimensional

CMR = cardiac magnetic resonance

EF = ejection fraction

FT = feature tracking

GLS = global longitudinal strain

LA = left atrial/atrium

LV = left ventricle/ventricular

LVEF = left ventricular ejection fraction

ROI = region of interest

RV = right ventricle/ventricular

STE = speckle-tracking echocardiography

circumferential-radial shear can be described as the subendocardium is rotating more or less than the epicardium; and radial-longitudinal shear involves the subendocardium is moving more or less longitudinally than the epicardium.

When calculating myocardial strain, it is most common to use a Lagrangian description that uses the end-diastolic length as a reference (L_o and T_o in Figure 1) and expresses the change in length as a percentage of this reference length. A Eulerian description uses the deformed configuration as a reference. Historically, this was the first type of strain that was introduced in echocardiographic software, as it was calculated by integrating strain rate from tissue velocity measurements, but it is less used today. When strain based on the Eulerian (ε_E) and Lagrangian approach (ε_L) are expressed as fractions, they are related as $\varepsilon_E = \ln(1 + \varepsilon_L)$, where ln is the natural logarithm.

Strain imaging provides complementary information to LV ejection fraction (LVEF), as it allows the quantification of segmental as well as global function and can be used to assess both systolic and diastolic function. Whereas myocardial strain imaging has traditionally been applied to study the LV, it is currently implemented also as a tool for the quantification of right ventricular (RV) and left atrial (LA) function. In this paper we review the theory behind strain as a measure of myocardial function, current clinical applications of strain imaging, and prospects for the technology. The Central Illustration summarizes the current strain technologies and applications.

FIGURE 1 Definition of Myocardial Strain

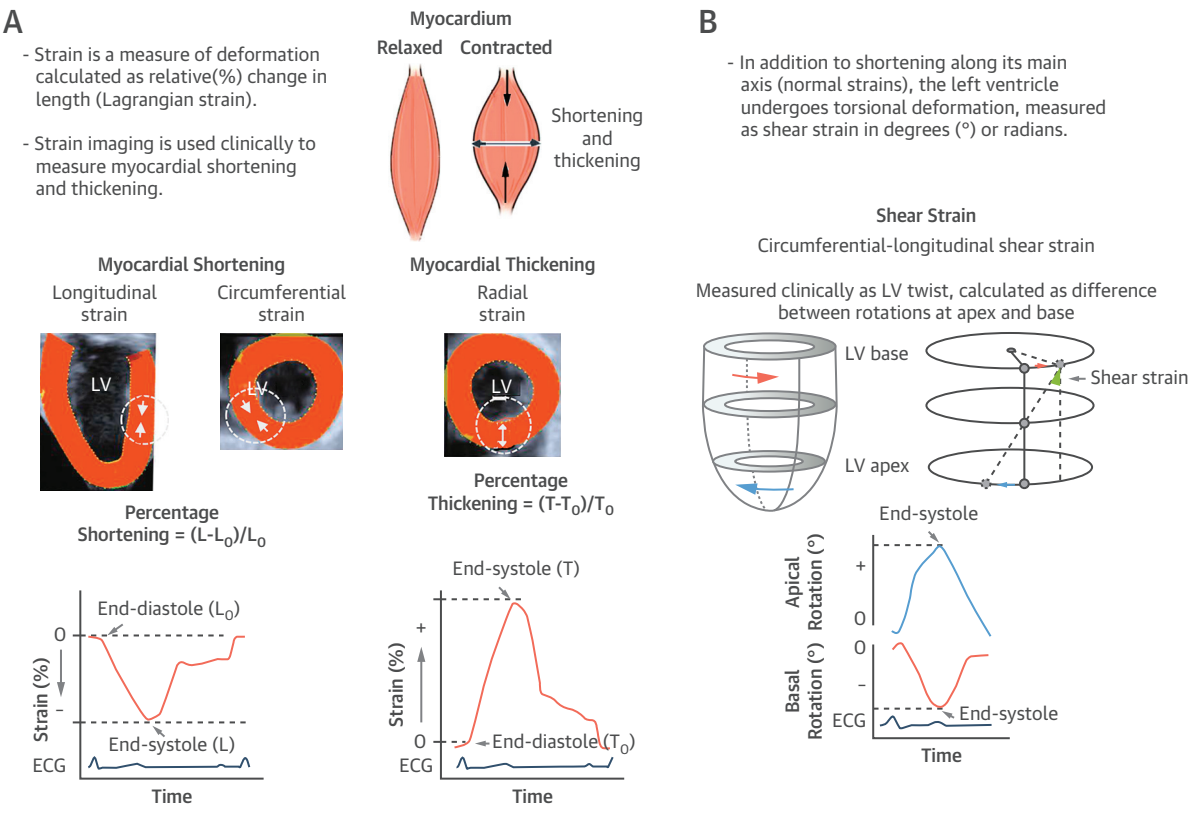

Myocardial strain imaging quantifies cardiac deformation. (A) The most widely used left ventricular (LV) strain measures are myocardial shortening in the longitudinal and circumferential directions and thickening in the radial direction (normal strains). (B) Illustration of LV circumferential-longitudinal shear or so-called twist, calculated as the difference between rotations at the apex and base. ECG = electrocardiogram.

CENTRAL ILLUSTRATION **Strain Imaging: Technologies and Clinical Applications**

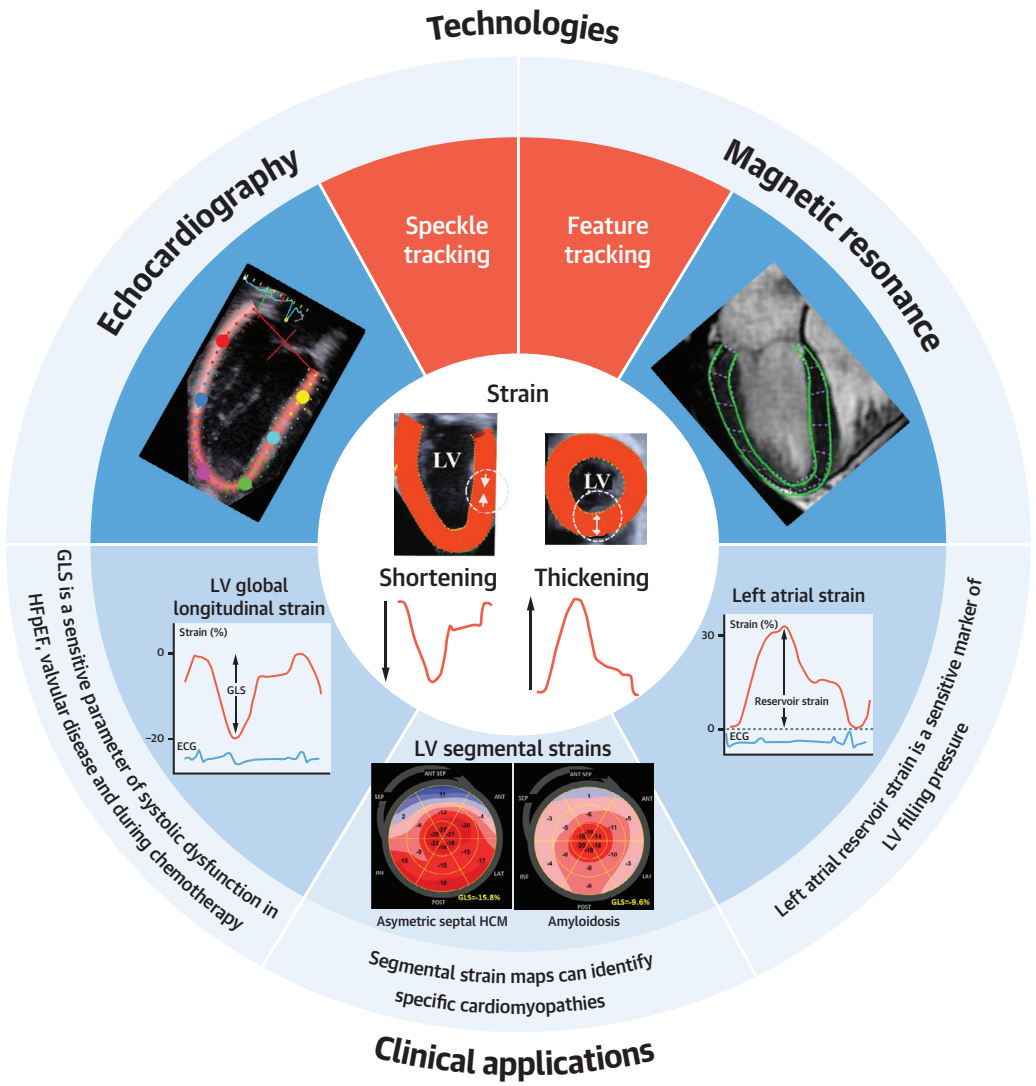

Smiseth OA, et al. JACC Cardiovasc Imaging. 2024;■(■):■–■.

GLS = global longitudinal strain; HCM = hypertrophic cardiomyopathy; HFpEF = heart failure with preserved ejection fraction; LA = left atrium; LV = left ventricle/ventricular; RV = right ventricle.

MYOCARDIAL STRAIN: HISTORY OF THE TECHNOLOGY

The quantification of myocardial deformation has been available for a long time in cardiac physiology using implanted ultrasonic dimension crystals[1] (**Figure 2**) or radiopaque markers implanted in a grid pattern so their 3-dimensional (3D) movement could be tracked by high-speed biplane cineradiography to derive the deformations.[2] Myocardial strain imaging as a clinical modality is rooted in cardiac magnetic resonance (CMR). The earliest CMR methods used radiofrequency pulses and multiple saturation planes, which resulted in distinct lines in the myocardium that could be used as a means of tissue tagging, as they follow myocardial deformation throughout the cardiac cycle.[3] By the late 1980s, this had been refined to produce a 3D grid of tags known

FIGURE 2 History of Myocardial Strain Technologies

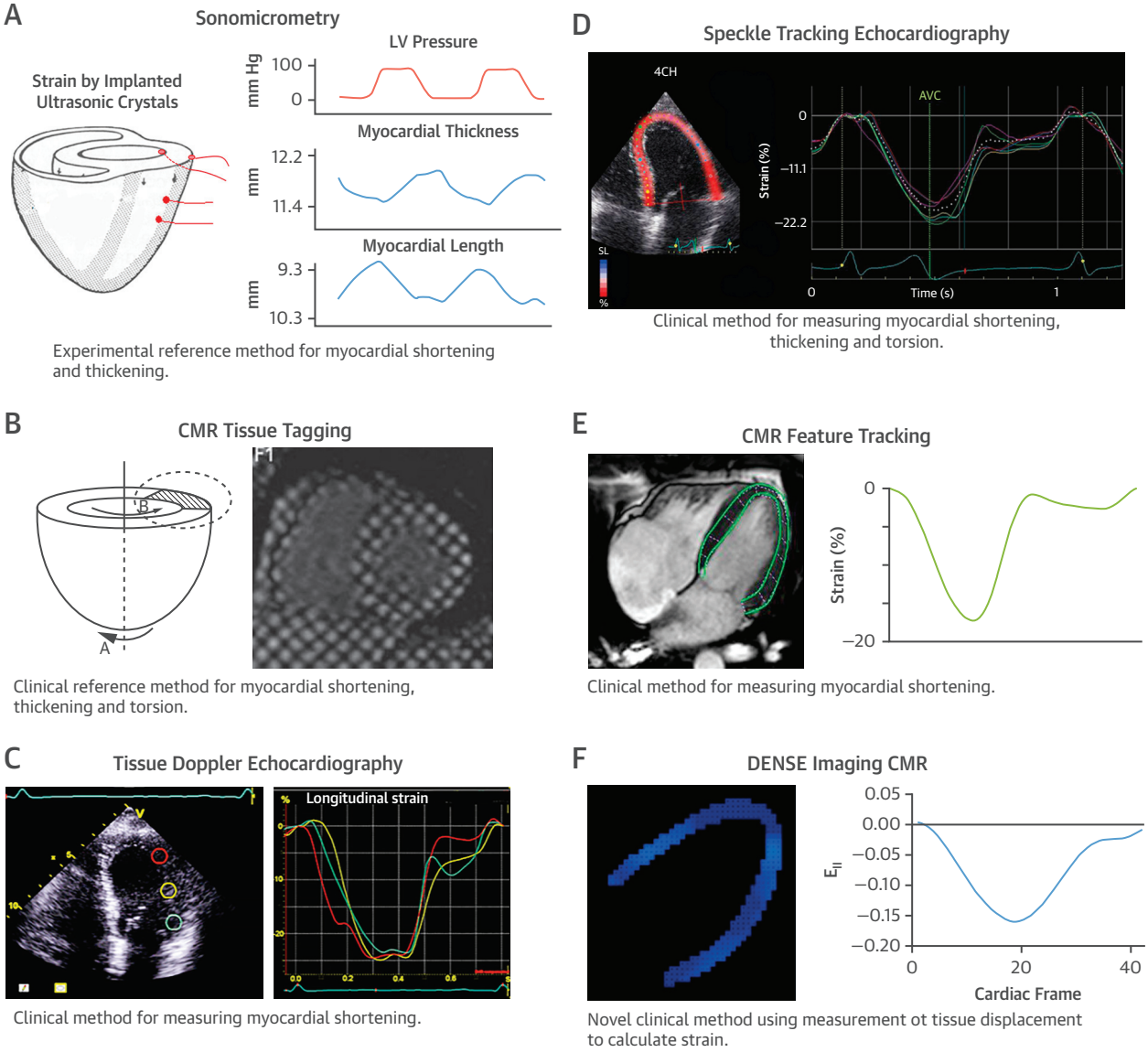

Graphical illustration of the history of strain imaging. (A) Data from an experimental study in which sonomicrometry was used to measure myocardial percentage shortening and thickening. Adapted with permission from Bugge-Asperheim et al.[1] (B) Illustration of left ventricular (LV) strain measured by cardiac magnetic resonance (CMR) with tissue tagging. Adapted under CC BY-NC-ND 4.0 license from Shehata et al.[234] (C) Illustration of LV strain measured using tissue Doppler echocardiography. (D) Illustration of LV strain measured using speckle-tracking echocardiography. (E) Illustration of strain by CMR feature tracking. Adapted under CC BY 4.0 license from Backhaus et al.[235] (F) Displacement encoding with stimulated echoes (DENSE) imaging CMR is an emerging clinical method for strain measurement. Adapted under CC BY-NC-ND 4.0 license from Auger et al.[236] 4CH = 4-chamber view; AVC = aortic valve closure.

as spatial modulation of magnetization,[4] and it was applied to interrogate myocardial velocities in 1991.[5] This method enabled characterizations of segmental strains in both healthy and diseased myocardium, with early studies focusing mainly on the infarcted or hypertrophied myocardium.[4,6,7] This method, which is primarily a research tool, is considered the clinical gold standard for the validation of new strain methods such as those based on echocardiography. Contemporaneously with the development of spatial

FIGURE 3 Strain by Myocardial Tissue Tagging

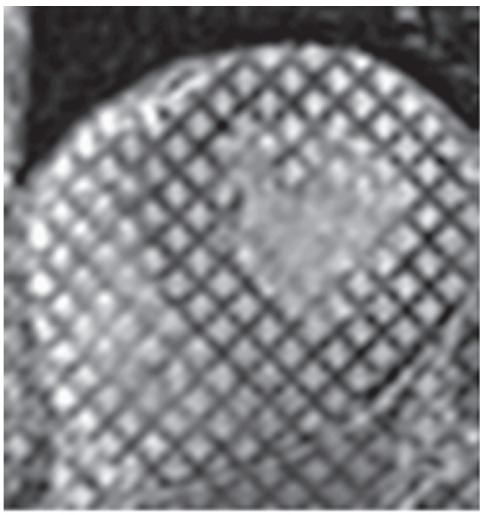

Image showing myocardial tagging: a grid of dark tag lines applied across a short-axis image.

modulation of magnetization tagging methods, CMR tissue phase velocity mapping methods for strain imaging also surfaced.[8] This technique in general has not been adopted widely, because of lower temporal resolution. This was overcome by the development of navigated high-temporal resolution sequences by 2006,[9] but long acquisition times have limited its use.

Strain rate and strain by echocardiography were first introduced as a 1-dimensional tissue Doppler imaging-based method.[10,11] For routine clinical use, this method was later superseded by 2-dimensional (2D) speckle-tracking echocardiography (STE), which provides multidirectional strains.[12-15] Currently, strain by STE is the most commonly used method.

The next phase of CMR strain imaging built on this echocardiography approach, which was applied to standard CMR cine images as feature tracking (FT). Despite greater variability and some discrepancy from the earlier "gold standard" tagging methods, as a result of the simplicity of postprocessing of standard cine images FT CMR is now the dominant strain method used by the CMR community. More recently, other methods have emerged, including 3D FT and techniques such as displacement encoding with stimulated echoes and strain-encoded magnetic resonance imaging. The latter has superior spatial and temporal resolution compared with tagging[16] and affords the opportunity of real-time imaging.

STE has also been applied to 3D data sets, theoretically overcoming the problem of through-plane motion of 2D speckle tracking and allows a comprehensive description of the deformation of the entire ventricle. Nevertheless, challenging data acquisition as well as the lower temporal and spatial resolution of 3D STE limit its clinical use.

Interestingly, a recent study showed that the analysis of myocardial deformation is also feasible on time-resolved 3D cardiac computed tomographic images.[17] The method is based on the calculations of global strain based entirely on the 3D displacement of the segmental myocardial volumes over the cardiac cycle using a deformable image registration-based tracking approach. The proposed method was reported to allow automatic and robust tracking of the LV myocardium using clinical computed tomographic image sequences, but data on clinical applications are still lacking.

METHODOLOGY: CMR

A wide range of CMR methods are available to assess myocardial strain. These methods offer various approaches to quantify strain, enabling clinicians and researchers to comprehensively analyze cardiac mechanics. Brief descriptions of the main approaches (myocardial tagging and FT) are provided in the following sections, with the main focus on imaging of the LV. More detailed information can be found elsewhere.[18,19]

MYOCARDIAL TAGGING. With this method, perturbing the magnetization with radiofrequency saturation pulses creates a grid of visible markers ("tags") in the tissue (**Figure 3**). Myocardial strain is measured by tracking these markers during the cardiac cycle (Video 1). Tags are typically applied at end-diastole, with imaging being performed across the whole cardiac cycle. At lower heart rates, the tags can fade during early diastole, which limits diastolic functional assessment. Higher field strength 3-T magnets can result in longer tag duration throughout the cardiac cycle.

CMR TAGGING SEQUENCES. All CMR tagging sequences consist of 2 main parts, the tagging part and the image acquisition part. It is the differences in how tagging and data acquisition are performed that make each of the techniques unique.

The simplest and most commonly used method for tagging is called spatial modulation of magnetization. Its tagging part consists of 2 nonselective radiofrequency pulses (usually 90°), separated by a tagging gradient (**Figure 4**). After the first pulse, the tagging

FIGURE 4 A Representative Tagging Sequence

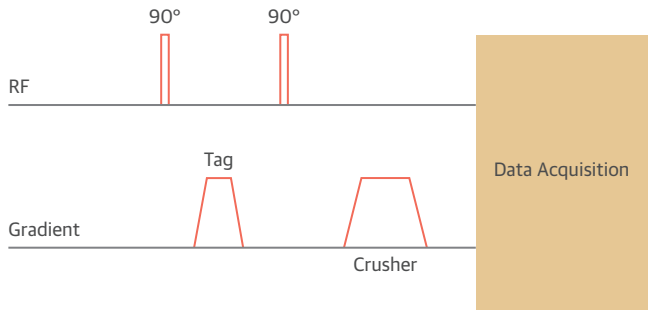

RF = radiofrequency pulse.

gradient disperses the excited spins, creating a modulation on the basis of incremental phase shifts. The second pulse then stores the modulated spins in the longitudinal plane, and a spoiler gradient is then applied to remove any remaining transverse magnetization. Spatial modulation of magnetization uses conventional data acquisition for imaging.

More advanced CMR tagging techniques use a combination of modulation and demodulation gradients to better store strain information. One example is the displacement encoding with stimulated echoes technique, which uses a stimulated echo acquisition mode sequence for tagging (Figure 5). Stimulated echo acquisition mode consists of 3 90° pulses to generate a stimulated echo. Equal-magnitude displacement encoding (modulation) and decoding (demodulation) gradients are added after the first and third pulses of the stimulated echo acquisition mode sequence, respectively. To eliminate any remaining transverse magnetization, crusher gradients are applied during the mixing period in between modulation and demodulation. Similar to spatial modulation of magnetization, the acquisition part uses conventional imaging readout. Displacement encoding with stimulated echoes provides higher spatial resolution and uses pixel-by-pixel displacement, making it possible to draw representative displacement vectors, with vector magnitude and direction representing the displacement value and orientation. Figure 6 shows an example of displacement encoding with stimulated echoes imaging CMR.

FIGURE 5 A Representative Displacement Encoding With Stimulated Echoes Sequence

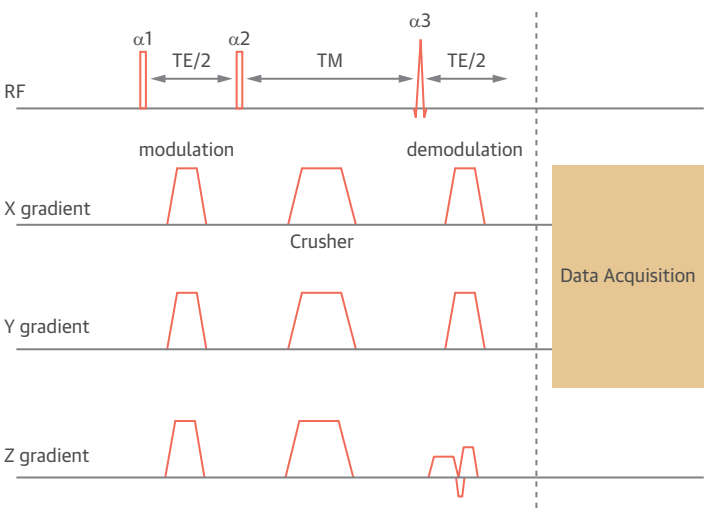

The time between the first and second radiofrequency pulses (RFs; α1 and α2) is equal to the time between the third RF pulse (α3) and data acquisition (echo time [TE]/2).
TM = mixing time.

Another example of advanced tagging sequence is strain-encoded imaging, which uses similar tagging part as spatial modulation of magnetization, but in this case, the tagging gradients are applied parallel to and inside the imaging plane to capture through-plane strain (Figure 7). During the imaging part of strain-encoded magnetic resonance imaging, further demodulation (tuning) gradients are applied between the section selection and data readout gradients to reduce scan time. Two sets of demodulated images are ultimately acquired. The low-tuning images represents static tissue, and the high-tuning images represent contracting tissue, exhibiting a high modulation frequency caused by tissue contraction. By comparing the image pixel by pixel and comparing the low-tuning and high-tuning images, myocardial strain can be quantified into a strain map.

Another CMR tagging technique is called tissue phase mapping. It uses velocity-encoded bipolar gradients to encode the tissue velocity in the phase of the signal. This allows the calculation of the velocities of different points within the myocardium. Myocardial velocities are then integrated in 3 directions (and over time) to show myocardial displacement and allow the evaluation of regional strains in the longitudinal, circumferential, and radial directions. As this method involves long imaging times, which can result in motion artifacts, strain derivation is thus potentially less accurate, and 3D velocity data are typically reported rather than the strain (Figure 8).

FT. CMR FT is a postprocessing method for quantifying tissue deformation that uses routinely acquired contrast-free CMR cine images (Figure 9). It is based

FIGURE 6 **CMR Displacement Encoding With Stimulated Echoes Imaging**

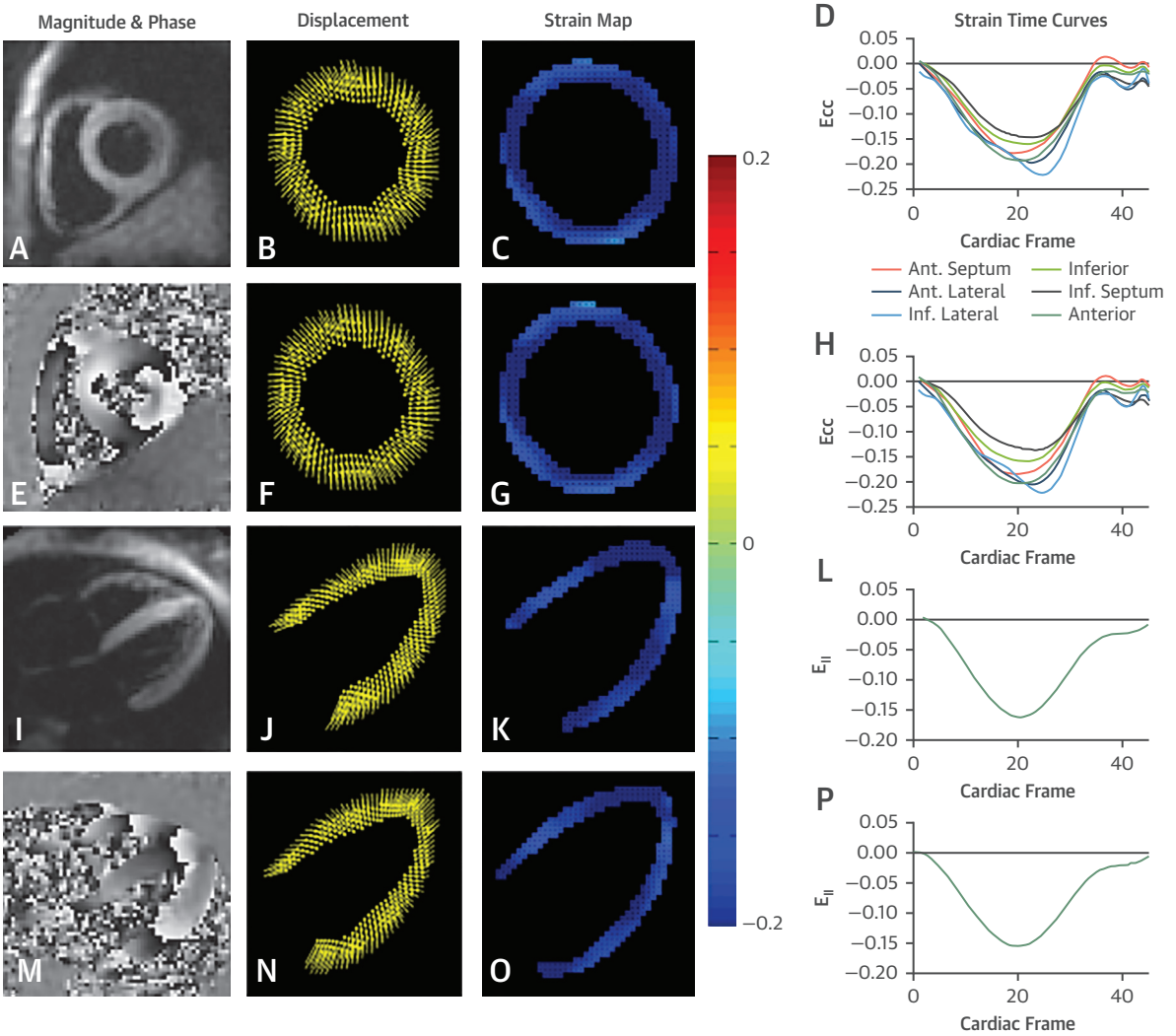

Reproduced with permission under CC BY-NC-ND 4.0 license from Auger et al.[236] Ant. = anterior; Inf. = inferior; other abbreviation as in Figure 2.

on tracking small image features (eg, details of the endocardial contour) from frame to frame. Combining information on the direction and magnitude of the displacement of several features makes it possible to calculate tissue deformation in all directions within the image plane. When considering frame rate in addition, the method provides information on velocity and strain rate. FT CMR requires high-quality image acquisition with adequate temporal and spatial resolution.

FT postprocessing begins with defining a region of interest (ROI), usually comprising the endocardial and epicardial borders on short- or long-axis cine images (Figure 9). In the following step, the software detects and tracks features and produces a 2D strain map. Myocardial deformation can then be visualized through graphical markers on the image or quantified via strain curves. Three-dimensional data sets allow the simultaneous estimation of radial, circumferential, and longitudinal strain parameters.

METHODOLOGY: ECHOCARDIOGRAPHY

TISSUE DOPPLER vs SPECKLE TRACKING. Echocardiography is currently the method of choice for strain assessment in clinical practice.

FIGURE 7 A Representative Strain-Encoding Sequence

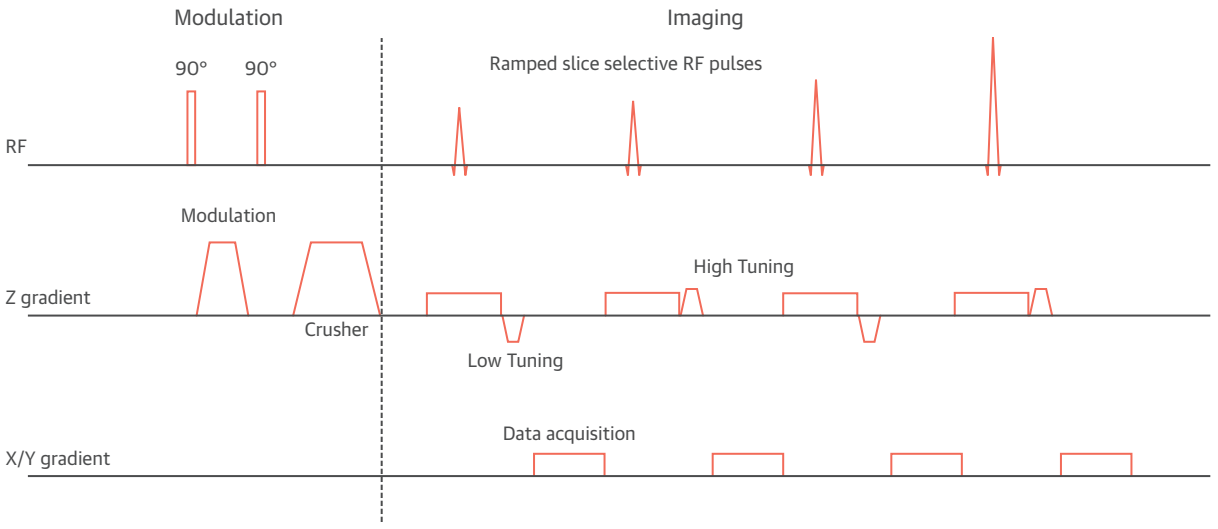

RF = radiofrequency pulse.

Measurements of strain are obtained by STE using dedicated speckle-tracking software during post-processing of regular image loops. Strain based on tissue Doppler imaging is also feasible in clinical settings but is not widely used, as it requires dedicated acquisitions, is dependent on the angle of insonation, and is more time consuming when analysis in multiple directions and image planes is required. Nevertheless, tissue Doppler imaging enables higher temporal resolution than STE, allows a more reliable assessment of strain rate and a better recognition of short-lived events, and can be faster for a focal analysis of a certain myocardial region.

FIGURE 8 CMR Tissue Phase Mapping

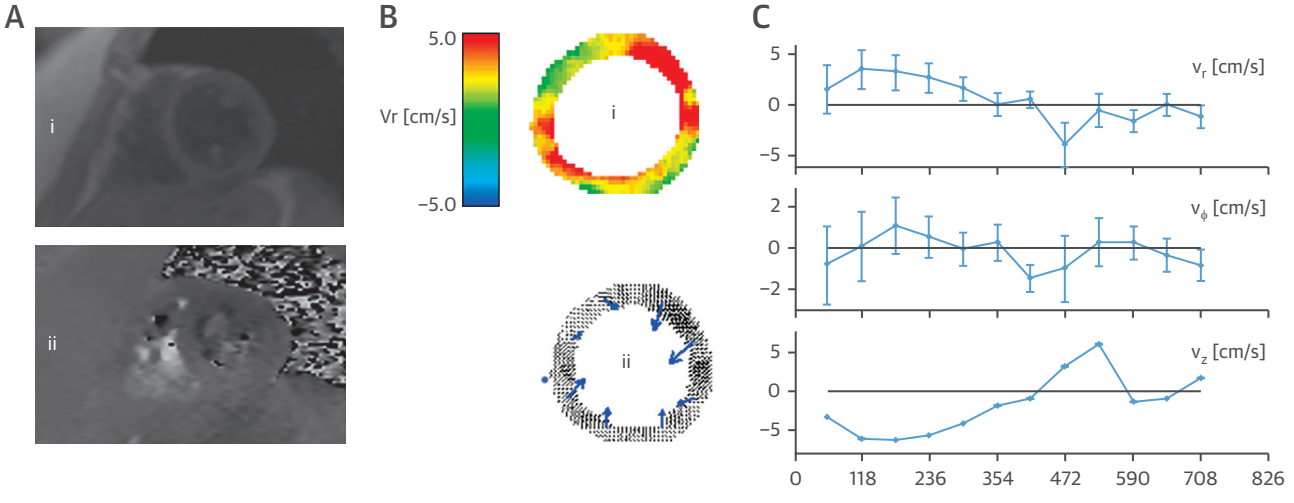

(A) Magnitude (i) and phase (ii) images from the tissue phase mapping sequence. (B) Velocity (i) and displacement (ii) maps. (C) Velocity maps in the radial, circumferential, and longitudinal directions obtained. V = velocity; other abbreviation as in Figure 2.

FIGURE 9 **CMR Feature Tracking: Circumferential Strain**

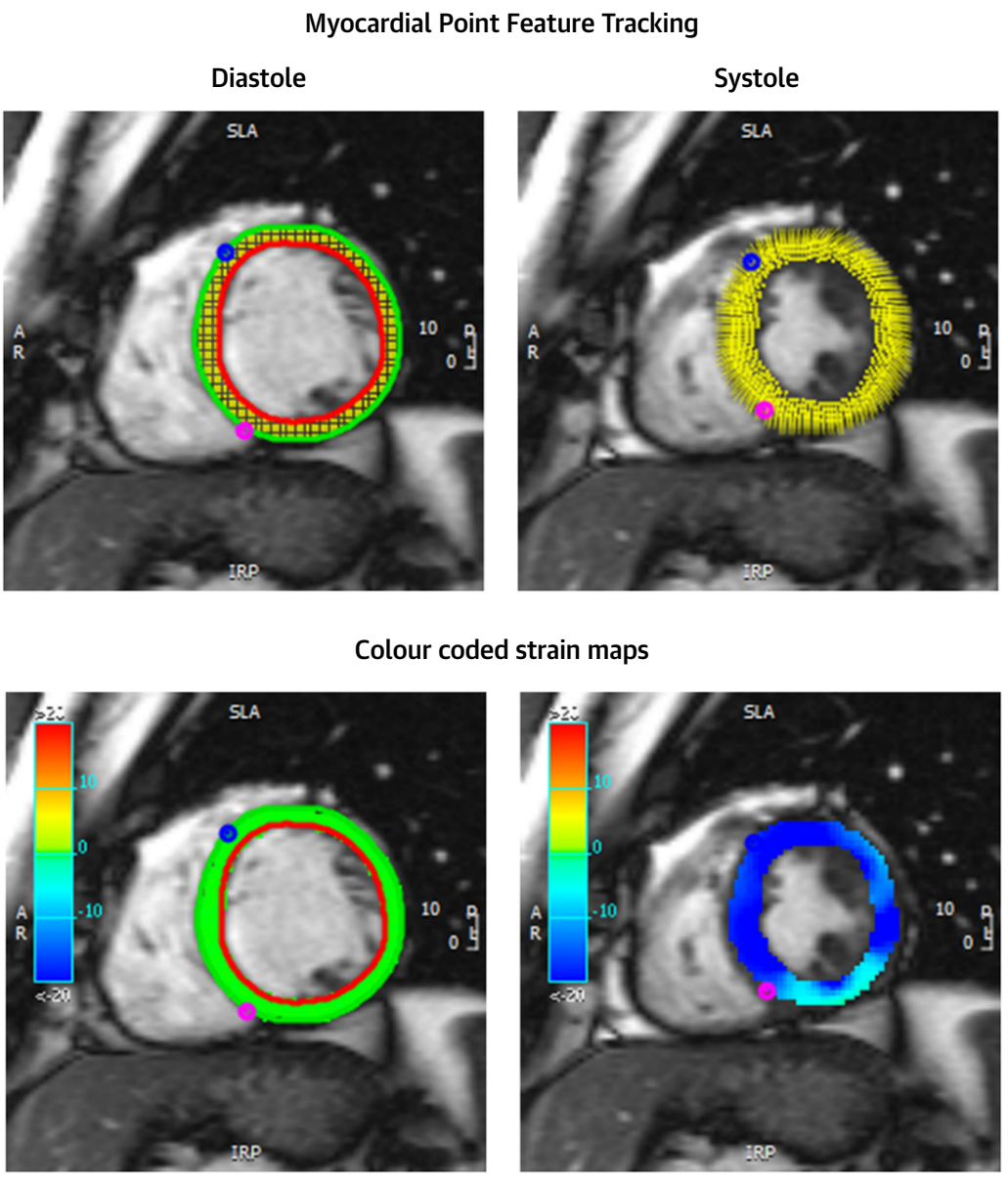

The top panels show the feature points that are tracked, and the bottom panels show resultant displacement by colored strain maps (below) across the cardiac cycle. Abbreviation as in Figure 2.

STE is based on tracking bright and dark dots ("speckles") in the myocardium. Speckles do not represent tissue structure but represent interference patterns that have been shown to move together with the tissue for a limited time and distance so that they can be used as features for tracking.[20,21] In contrast, CMR FT tracks predominantly the endocardial border, which explains some of the differences in results found in direct comparisons of STE and CMR FT (Table 1).[22]

Reliable and meaningful tracking requires an appropriate placement of the ROI and enough trackable features within it. Tracking is performed by some software solutions by using a relatively thin ROI in the subendocardial and sometimes in addition in the midwall and in the subepicardial myocardium.

TABLE 1 Summary of Technical Characteristics of Clinically Used Strain Methods

	CMR FT	2D STE	3D STE
Dominant features used for tracking	Endocardial borders	Myocardial speckles and contour	Myocardial speckles and contour
Signal-to-noise ratio	High	Moderate	Low
Temporal resolution	30 phases per heart cycle	40-80 frames/s	34-50 frames/s
Spatial resolution	Reasonable (1-2 mm in plane and 8-10 mm through plane)	Good (submillimeter radial; lateral depends on number of beams and image depth)	Poor (at least 3-4 times <2D STE)
Out-of-plane motion	Yes	Yes	No
Feasibility	Very high	High (80%-97%)[a]	Moderate (60%-83%)[a]
Reproducibility	High	High	Moderate
Intervendor differences	Significant	Relatively small	Significant

[a]Data for left ventricular strain.[14,237-239]
2D = 2-dimensional; 3D = 3-dimensional; CMR = cardiac magnetic resonance; FT = feature tracking; STE = speckle-tracking echocardiography.

Despite the inclusion of approximately one-third of the wall thickness, this region is often displayed only as a thin line. Other software solutions try to use all available speckles within the wall ("full wall tracking"). Notably, as explained later, measured strain values from endocardial vs full wall tracking may differ substantially, particularly in ventricles with thick walls. Analysis of thin structures such as atrial walls or separate layers of the LV wall is technically more challenging,[23,24] resulting in less robust strain estimates compared with full wall tracking. Furthermore, full wall tracking is less susceptible to foreshortened images, and there is less influence from regional myocardial shape abnormalities, such as regional bulging.[25,26] These issues are discussed in the section "Tips and Pitfalls When Measuring LV Strain."

Although speckles can be tracked in any direction within a 2D or 3D data set, the quality of strain estimates is not the same in all directions.[20,21] Better tracking quality is achieved in the direction of the scan lines, where spatial resolution is higher than perpendicular to them. Consequently, apical views are most suitable for tracking longitudinal myocardial function but may not allow reliable estimates in radial direction. Additionally, as image quality and line density deteriorate with the distance from the ultrasound probe, tracking is better in the near field of the probe.

High-quality image data sets from standardized echocardiographic views are crucial for good tracking quality and reliable strain analysis.[20,24] Suboptimal images with shadowing artifacts, ultrasound dropouts, and reverberations prevent a reliable assessment of speckle motion. Out-of-plane motion of speckles is another potential source of error affecting more short-axis views than apical views.[27] Tracking quality should not be judged from the strain curves, as pathology may also result in abnormal curve shapes. It is therefore of utmost importance to visually compare the results of the tracking process, best displayed as an overlay of several dots, directly with the motion of the underlying myocardium.[20]

The temporal resolution of regular 2D grayscale images is sufficient for measuring systolic motion and strain with STE but is insufficient for a reliable analysis of short-lived events and accurate measurement of the high myocardial strain rates that occur during isovolumic contraction and relaxation.[23] Acquisition of 3D data sets is done with substantially lower temporal and spatial resolution than with 2D imaging, which is a limitation for 3D speckle tracking.[22,28] A minimum frame rate of 40 to 50 frames/s should be maintained.[29] However, despite theoretical advantages, limitations in image quality as well as temporal and spatial resolution and lack of standardization still prevent the wide use of 3D STE in daily clinical practice.[21,22,30]

STRAIN RATE. Potentially, peak systolic strain rate may be superior to peak strain as a measure of LV contractility because it is less influenced by changes in cardiac load and structure.[31,32] Furthermore, STE with frame rates ranging from 40 to 80 frames/s does not allow reliable assessment of the highest strain rates. As suggested by experimental studies, there are important deformations during isovolumic contraction and relaxation that cannot be measured with the frame rates used in current speckle-tracking echocardiographic technologies.[33,34] Tissue Doppler has a higher temporal resolution up to 300 to 400 frames/s and may be used alternatively. Furthermore, there are promising developments within high-frame rate echocardiography that allow STE at frame rates that exceed those of tissue Doppler.[35,36] It remains to be

FIGURE 10 **LV Rotation, Twist, and Torsion**

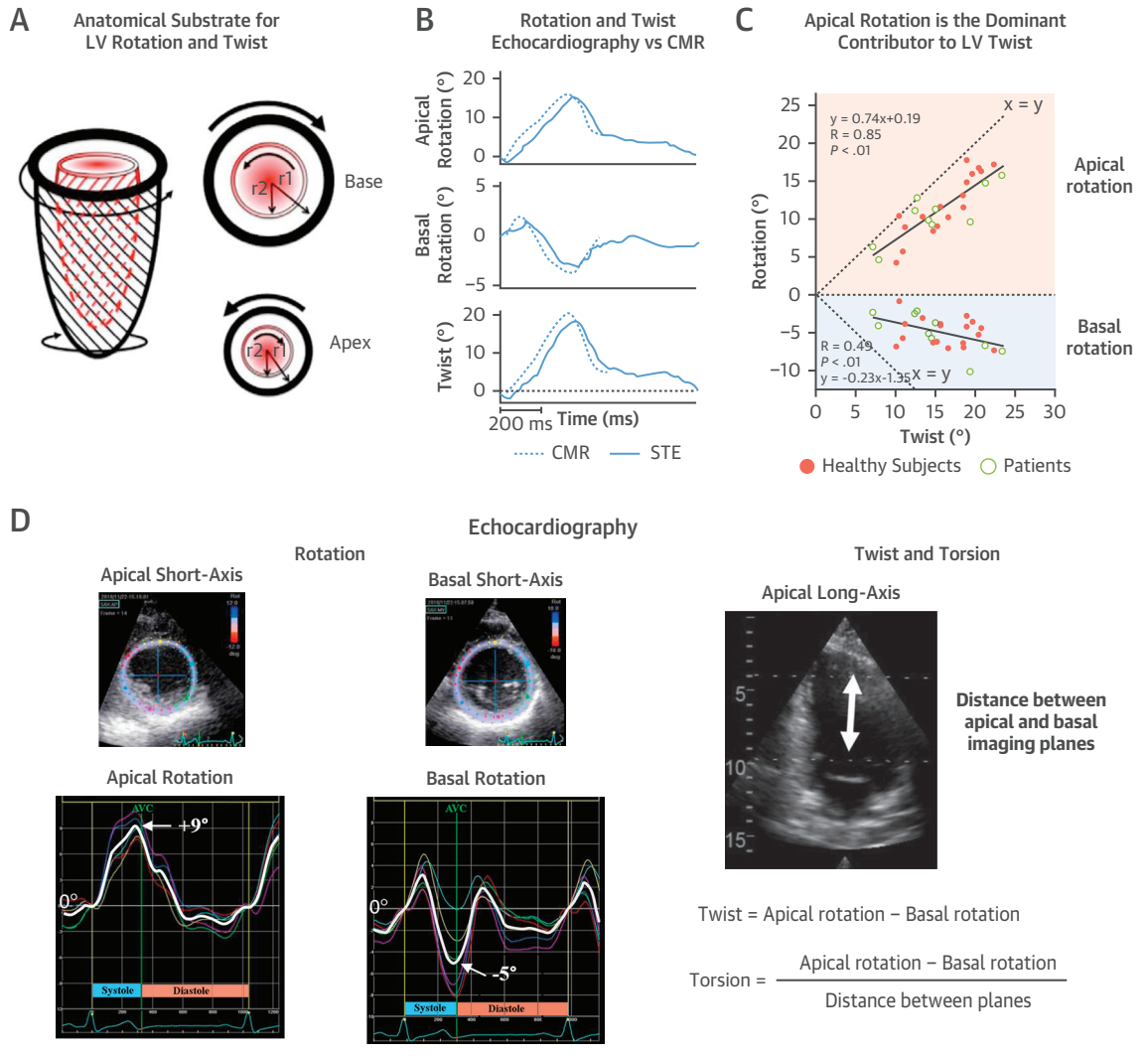

(A) Schematic illustration of LV myocardial fiber orientation. The structural basis for LV rotation and twist is a spiral architecture of myofibers, with subendocardial and subepicardial fibers arranged in right-handed and left-handed helices, respectively. Larger r1 than r2 indicates longer lever arm and larger torque in the subepicardium. Adapted with permission from Omar et al.[240] (B) Representative example of rotation and twist by speckle-tracking echocardiography (STE) and CMR tagging in a healthy subject. Rotation by CMR was not feasible for a complete heart cycle because of tag fading. Adapted with permission from Helle-Valle et al.[50] (C) Relationships between LV twist and apical and basal rotation by CMR in a clinical study. The magnitude of LV twist is determined primarily by apical rotation. Adapted with permission from Opdahl et al.[53] (D) Measurement of LV rotation, twist, and torsion by echocardiography. Abbreviations as in Figures 1 and 2.

shown, however, that these very high sampling rates provide clinically important information.

Strain components. A full description of the complex 3D deformation of the heart requires 3 normal (meaning that they are perpendicular to one another) strains that describe longitudinal, radial, and circumferential shortening and lengthening and may also include shear strains. In clinical practice, however, evaluation is commonly limited to measuring longitudinal strain only. As shown by Risum et al,[37] measurements of radial and circumferential strains from the short-axis views are less feasible and have

FIGURE 11 Measurement of LV Apical Rotation and Back-Rotation: Clinical Cases

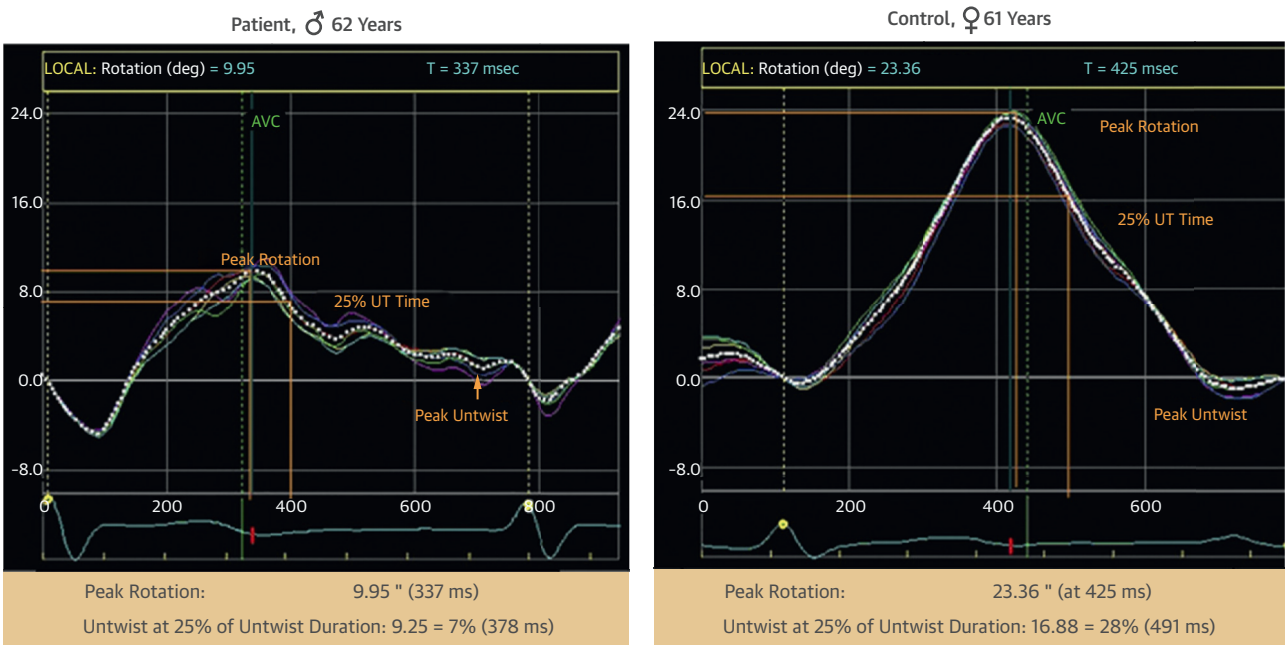

Peak apical rotation and back-rotation (untwist) in a patient (left) and a control subject (right) showing magnitude of peak apical rotation and timing of untwist (25% of total untwist duration). (Left) Male patient with heart failure and normal left ventricular ejection fraction. (Right) Female control subject. The y-axis depicts rotation in degrees, and the x-axis depicts time. Reproduced with permission from Tan et al.[241] AVC = aortic valve closure; UT = untwisting; other abbreviation as in Figure 1.

higher variability than longitudinal strain. In the latter study, variability was higher for radial than for circumferential strain.

Longitudinal strain has been shown to be highly feasible, robust, and reproducible, superior to many other conventional echocardiographic parameters.[23,24,37-42] Shear strains can be assessed by measuring twist or torsion, but low feasibility and high variability have prevented widespread clinical use so far. Likewise, although 3D STE would allow a fast and comprehensive evaluation of multiple strain components of all LV or RV segments from a single 3D data set,[39,43] it is hardly used for the same reasons.[44-46]

MEASUREMENT OF LV ROTATION, TWIST, AND TORSION. When viewed from the LV apex toward the base, the apex rotates counterclockwise during systole, and the base rotates in the opposite direction. LV twist is measured as difference between apical and basal rotations and is expressed as twist angle (degrees or radians). Torsion is the twist angle normalized to (divided by) the distance between the imaging planes.

Torsion of the ventricle allows uniform distribution of fiber stress across the wall and contributes to efficient systolic contraction. Furthermore, elastic energy, which is stored in the myocardium in systole, is released in early diastole by rapid untwisting and contributes to filling by active suction of blood into the ventricle.[47,48]

The structural basis for torsion is the spiral architecture of myocardial fibers with subendocardial and subepicardial fibers arranged in a right-handed and left-handed helix, respectively. Because of a larger lever arm and therefore larger torque in the subepicardium, normal hearts have systolic counterclockwise rotation of the apex (Figure 10).

LV rotation and twist can be measured using several methods, including CMR and STE.[49-51] Reference values for LV twist in healthy subjects are reported from the NORRE (Normal Reference Ranges for Echocardiography) study.[52] Figure 10 illustrates measurements of LV rotation and twist. Because rotation increases progressively toward the apex, it is important to include the distal apex in the image. The optimal distal cross-sectional image plane should include only a small part or no part of the RV. Furthermore, out-of-plane motion of the LV base caused by longitudinal motion is a significant limitation. Because 2D echocardiography does not provide

FIGURE 12 Transmural Gradient of LV Strains

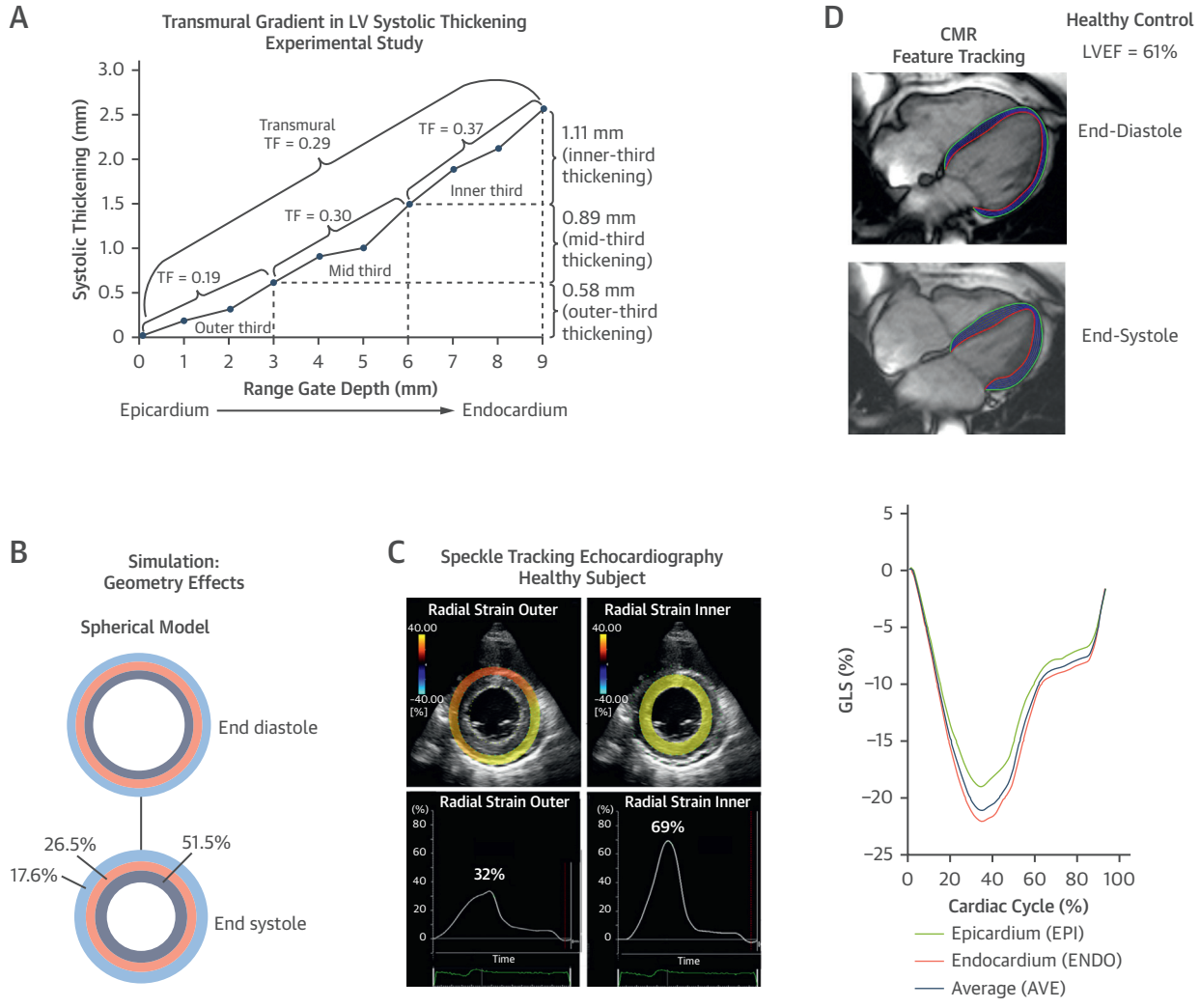

(A) Experimental study showing measurement of systolic thickening (radial strain) in different layers of the LV wall by Doppler transit time. Myocardial thickening increased progressively from the outer to the inner layer in the LV wall. Reproduced with permission from Zhu et al.[242] (B) Theoretical model showing that transmural difference in radial strain can be attributed to a pure geometric effect, as reduction in the external diameter of a passive circular structure leads to more thickening of inner than outer layers. The figure simulates reduction of inner radius by 25%, and the numbers indicate the resulting thickening in inner, mid, and outer wall layers.[243] (C) Recordings by speckle-tracking echocardiography from a healthy subject in an LV short-axis view showing much higher radial strains in inner than outer layer. Adapted under CC BY-NC 4.0 license from Smiseth et al.[244] (D) Layer-specific global longitudinal strain (GLS) by CMR feature tracking in a healthy subject. Adapted under CC BY-NC-ND 4.0 license from Xu et al.[245] LVEF = left ventricular ejection fraction; TF = thickening fraction; other abbreviations as in **Figures 1 and 2**.

accurate measures of distance between the 2 image planes, it is difficult to measure torsion in a clinical setting. As illustrated in **Figure 10C**, rotation at the apex makes the largest contribution to LV twist. Therefore, it was suggested by Opdahl et al[53] to use apical rotation as a simplified bedside index of LV twist.

Figure 11 illustrates the assessment of LV diastolic function by measuring LV back-rotation (untwisting rate). Untwisting has been shown to reflect LV relaxation and restoring forces.[47,48,54]

There are several potential applications of assessing LV rotation and twist in clinical diagnostics,[55] including the assessment of both systolic and diastolic function. There are, however, unresolved issues regarding feasibility, standardization, and vendor dependency that currently limit the use of rotation and twist as clinical measures.

FIGURE 13 Transmural Strain Gradients in Normal and Infarcted Left Ventricles

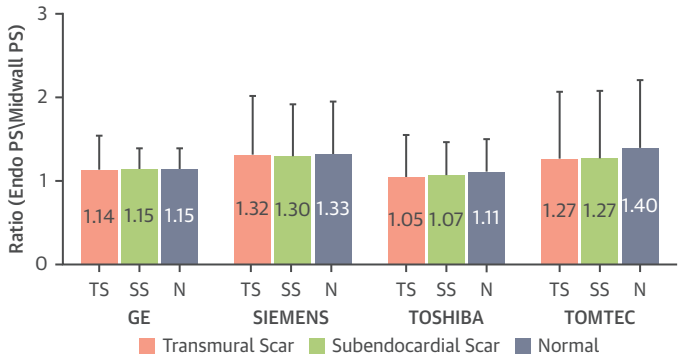

Comparison of the endocardial (Endo)–to-midwall ratio (transmural gradient) of peak systolic strain (PS) in normal segments (N) and segments with subendocardial scar (SS) or transmural scar (TS). No statistical significance was found. The test was done using tracking software from 4 different vendors. Reproduced with permission from Unlu et al.[56]

LV LAYER-SPECIFIC STRAIN. It has been suggested that LV transmural differences in strain may provide incremental diagnostic information. As shown in Figure 12, strains in a normal LV are higher in the subendocardium than in the subepicardium, and the gradient is most pronounced for radial and circumferential strains. This can be explained by geometric effects and does not imply a difference in contractility between the inner and outer wall layers. For LV longitudinal strain, the difference between strain in the inner and outer layers is much smaller than for strain in short-axis images, reflecting the much larger radius of curvature in the longitudinal direction of the ventricle.

The rationale for using layer-specific longitudinal strain analysis as a diagnostic approach is not obvious, as the different layers are mechanically connected (tethered). Therefore, motion in one layer will be reflected in motion in all wall layers within the same segment. Furthermore, the lateral resolution of apical echocardiographic images is suboptimal for differentiating between strains in different layers of the LV wall. An echocardiographic study that measured layered longitudinal strain could not identify any differential behavior of layers between normal and infarcted segments. The result was the same with software from 4 different vendors (Figure 13).[56]

At the present time, there is not sufficient evidence to recommend layer-specific LV strain for clinical use. Similar considerations apply to layer-specific FT by CMR.

MODIFIERS OF LV STRAIN. The magnitude of myocardial strain is influenced by loading conditions (preload and afterload), heart rate, and chamber size and geometry.[57-63] How strain values should be interpreted in the context of these factors was previously discussed in detail.[28]

Figure 14 illustrates reduction in global longitudinal strain (GLS) in response to a moderate increase in systolic arterial pressure induced by mental stress in patients on cancer chemotherapy and in healthy control subjects.[64] The reduction in GLS during mental stress was associated with a compensatory increase in myocardial work, and the increase was most marked in healthy control subjects. Importantly, none of the patients showed a relative reduction in GLS that exceeded 15%, which is the currently recommended cutoff value for suspecting cardiotoxic effect of chemotherapy. The study shows the importance of recording blood pressure at the time of the imaging study. Furthermore, to avoid this "white-coat effect on LV strain," communication about stressful topics should be avoided during an echocardiographic study.

STRAIN VS MITRAL ANNULAR PLANE SYSTOLIC EXCURSION AND TRICUSPID ANNULAR PLANE SYSTOLIC EXCURSION. M-mode-derived mitral annular plane systolic excursion and tricuspid annular plane systolic excursion are alternative measures of LV and RV longitudinal systolic function.[65] Some investigators have proposed that mean global mitral annular plane systolic excursion normalized to end-diastolic LV length might be an equivalent to GLS.[66] However, the correlation between GLS and normalized mitral annular plane systolic excursion was only moderate. Although mitral annular plane systolic excursion is less dependent on image quality and can be easily measured without additional postprocessing, the clinical data on this approach are limited.

Støylen et al[65] showed how global LV strains can be measured directly from LV 2D or M-mode recordings. This approach, however, does not provide segmental strains and therefore has limited ability to identify regional dysfunction. Furthermore, errors in strain estimates caused by angle dependency are a limitation.

FIGURE 14 Afterload Sensitivity of LV GLS

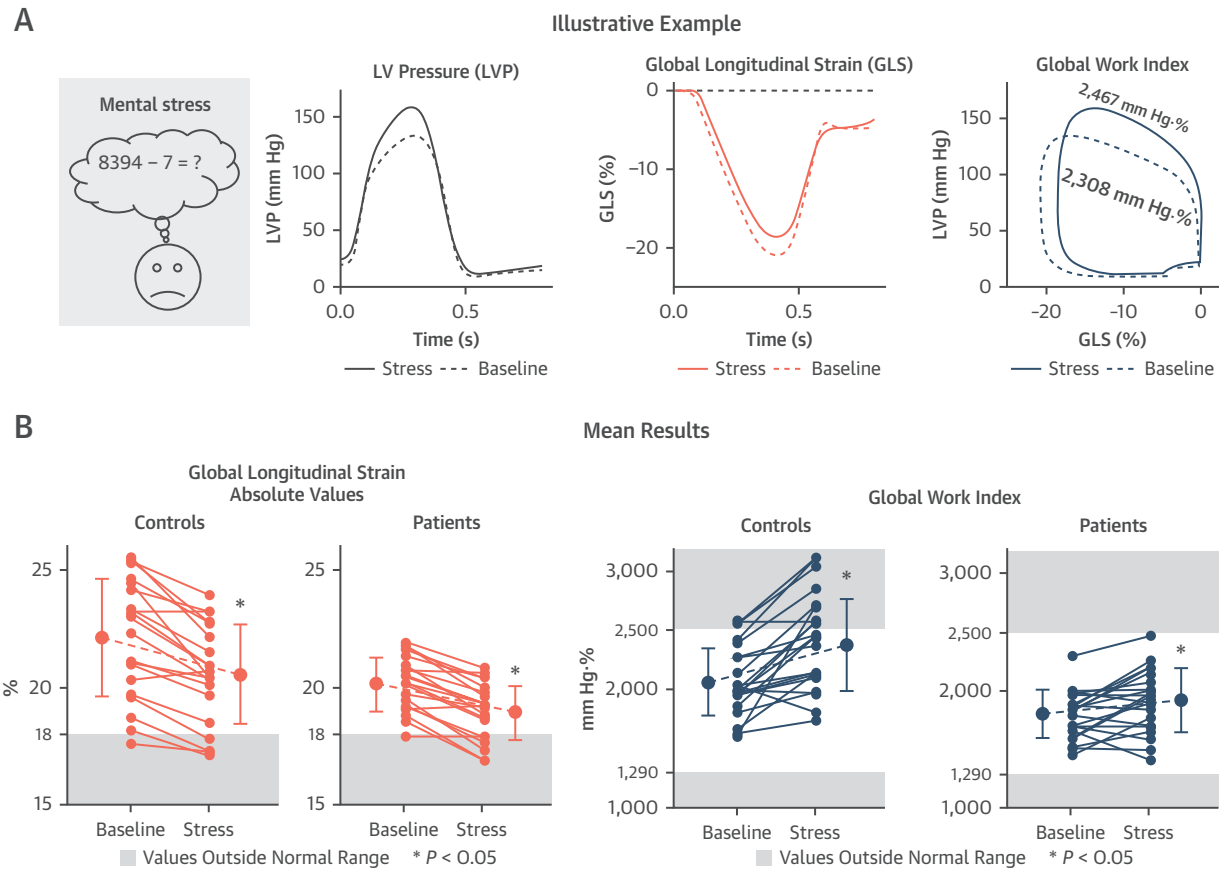

Responses to mental arithmetic stress were tested in a group of patients on cardiotoxic chemotherapy and in healthy control subjects. (A) Data from a patient on chemotherapy. Mental stress caused elevation of peak left ventricular pressure (LVP) and reduction in absolute GLS, whereas the myocardial work index showed a slight increase. (B) Individual data and mean ± SD from control subjects and patients during baseline and mental stress. There were significant reductions in absolute GLS in both groups, with no significant difference between the groups in GLS response. Mental stress caused significant increments in global LV work index, most marked in the control subjects. LVP was estimated noninvasively. Adapted with permission from Sletten et al.[64] Abbreviations as in Figures 1 and 12.

However, for bedside echocardiography in intensive units, where image quality might be an issue, mitral annular plane systolic excursion or mitral annular plane systolic excursion normalized to LV length could be used as an alternative index for assessing LV function. It has been shown that the simplicity and feasibility of these alternative parameters enable the detection of LV systolic dysfunction also in critical ill patients.[67]

DERIVED METHODS. Myocardial work. Noninvasive myocardial work index is a recent modality that combines LV strain with an estimate of LV pressure[68] (Figure 15). The method uses the principle that the area of LV pressure-dimension loops reflects external myocardial work, as suggested by Suga[69] for global LV function and by Tyberg et al[70] for regional LV function (Figure 15A). The inspiration to translate these basic principles into a clinical method originates from collaboration between one of the inventors of the work index method (O.A.S.) and John Tyberg.

There are 2 different methods to calculate external myocardial work from LV strain and a noninvasive estimate of LV pressure. First, analogous to the calculation of LV stroke work as the area of the LV pressure-volume loop, segmental LV work can be calculated as area of the segmental pressure-strain loop (mm Hg %). Figures 15A and 15B illustrate this

FIGURE 15 Methods to Estimate Myocardial Work by LV Pressure-Strain Analysis

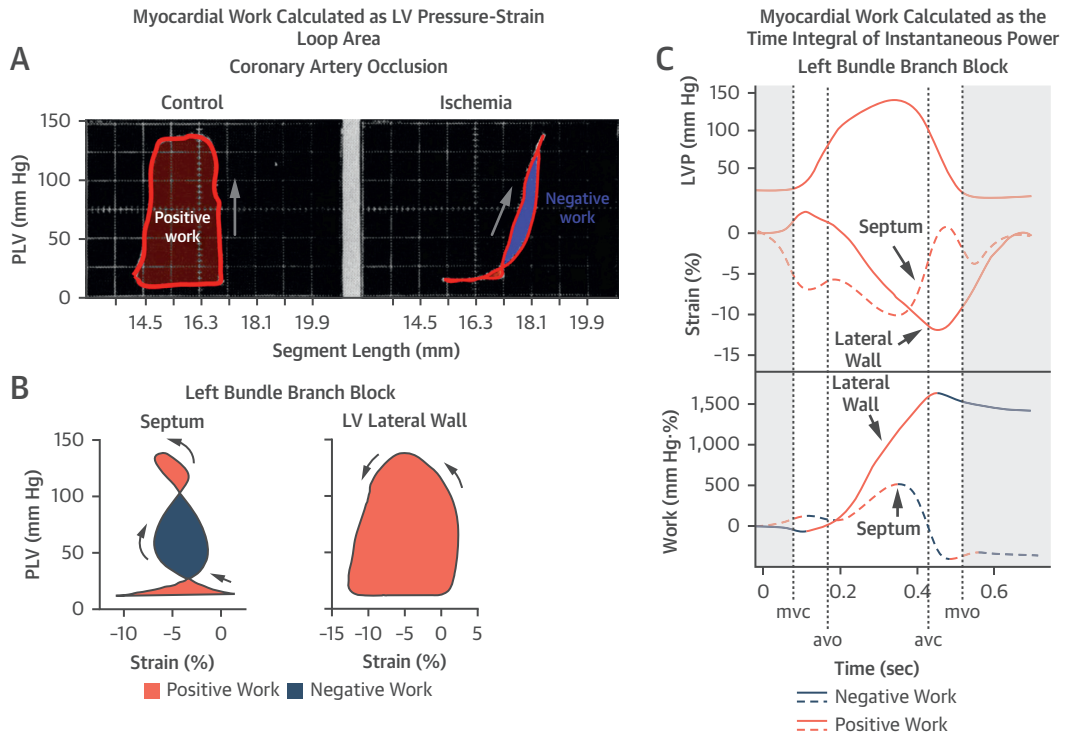

Two different methods to calculate myocardial work by LV pressure-strain analysis. (A,B) Myocardial work calculated as the LV pressure-strain loop area. (A) An experimental study showing positive work in a nonischemic segment (left) and negative work in an ischemic segment (right). Counterclockwise rotation of the pressure-dimension coordinates indicates positive work, and clockwise rotation indicates negative work. Segmental work is calculated as net loop area by summation of areas with positive and negative work. Adapted with permission from Tyberg et al.[70] (B) A patient with left bundle branch block, showing a dysfunctional septum with predominantly negative work. Reproduced under CC BY-NC-ND 4.0 license from Smiseth and Aalen.[246] (C) Myocardial work calculated as the time integral of instantaneous power. Negative and positive work during systole is marked as red and black lines, respectively. Adapted with permission from Russell et al.[71] avc = aortic valve closure; avo = aortic valve opening; mvc = mitral valve closure; mvo = mitral valve opening; PLV = left ventricular pressure; other abbreviations as in Figures 1 and 14.

method. In a validation study, Russell et al[68] showed that noninvasive LV pressure combined with LV strain by STE could be applied to construct LV pressure-strain loops clinically. In a subsequent study, Russell et al[71] introduced an alternative, and currently more widely used, clinical method to measure myocardial work indexes. The method is illustrated in Figure 15C.

The myocardial work index is calculated for individual segments and as a global parameter as the average value for all the segments. In addition, several indexes are also calculated for each LV segment and globally. Constructive work is defined as work performed by a segment during shortening in systole and includes the small amount of work during lengthening in isovolumic relaxation. Wasted work represents energy not contributing to LV ejection and is calculated as work performed on a segment that lengthens in systole. Shortening during isovolumic relaxation is also considered wasted work, as it costs energy but makes no contribution to LV ejection. Myocardial work efficiency is calculated as the percentage ratio of constructive work divided by the sum of constructive and wasted work.

In patients with aortic stenosis, brachial cuff pressure does not reflect peak LV pressure, and therefore a modification of the method is needed to obtain LV pressure.[72] When estimating peak LV pressure as the sum of cuff pressure and the aortic pressure gradient, the work index could be estimated with good accuracy in patients with aortic stenosis.[73,74] In a recent study by Ribic et al[75] in patients with aortic stenosis, it was shown how the LV pressure estimate could be improved by

FIGURE 16 Myocardial Work Index in Aortic Stenosis

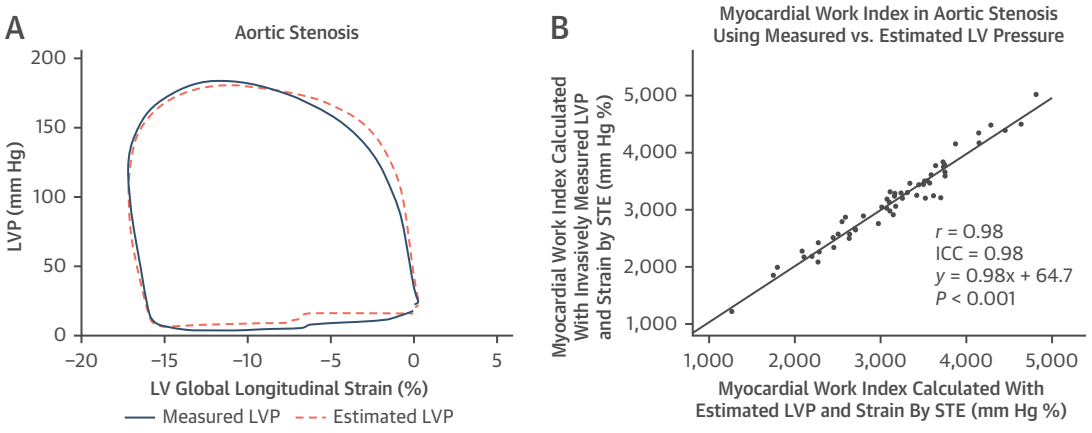

(A) Comparison of estimated LVP with invasively measured LVP by micromanometer in a patient with aortic stenosis. Noninvasive LVP was estimated using a specific approach for aortic stenosis.[75] (B) Correlation between global LV work index using noninvasive vs invasive LVP in aortic stenosis. Both panels are adapted under CC BY-NC 4.0 license from Ribic et al.[75] ICC = intraclass correlation coefficient; other abbreviations as in Figures 1 and 14.

incorporating aortic diastolic pressure in the analysis (Figure 16). In general, however, the original method of Russell et al[68] may be applied to measure LV work in aortic stenosis, with the exception that the transaortic pressure gradient must be added to cuff pressure when estimating peak LV pressure. Similarly, in patients with hypertrophic obstructive cardiomyopathy, it was suggested to calculate myocardial work using the sum of brachial cuff pressure and an estimate of the intraventricular pressure gradient to represent peak systolic LV pressure.[72]

An advantage of assessing myocardial work compared with just measuring strain is that work indexes incorporate afterload. Furthermore, whereas GLS provides a measure at only 1 time point during the heart cycle, work uses strain values from the entire systole from onset contraction until the onset of LV filling. In addition, this modality includes a measure of mechanical efficiency and therefore provides more comprehensive data on LV function than by just measuring strain. Furthermore, regional differences in myocardial work appear to reflect myocardial glucose metabolism.[68,76]

Limitations of noninvasive myocardial work (by both methods) compared with work in appropriate physical units are the use of pressure instead of force and relative instead of absolute dimensions. Estimation of force, which would be a more appropriate parameter than pressure, would require measurement of LV radii of curvature and wall thickness. One should also be aware that the current method to calculate myocardial work indexes does not take into consideration individual differences in LV diastolic pressure.

Readers are referred to Manganaro et al[77] for normal reference values for myocardial work indexes.

There are promising data on the application of myocardial work indexes in several clinical conditions. It remains to be shown, however, whether clinical decisions based on the assessment of myocardial work will improve health outcomes.

Mechanical dispersion. As observed in patients with long-QT syndrome, large intersegmental variability in contraction duration, called mechanical dispersion, is associated with increased risk for ventricular arrhythmias.[78,79] Mechanical dispersion is calculated as the SD of contraction duration measured from the peak Q wave or the start of the R wave on electrocardiography to peak shortening strain in multiple LV segments.[78] Mechanical dispersion is associated with risk for ventricular arrhythmias in other diseases as well, including patients with previous myocardial infarction and nonischemic cardiomyopathy.[80-82]

In patients with long-QT syndrome, mechanical dispersion is presumably caused by regional differences in action potential duration, which lead to spatial nonuniformity in contraction duration. In ischemic heart disease and cardiomyopathies, several

FIGURE 17 **LV LS, CS, and RS in a Healthy Subject**

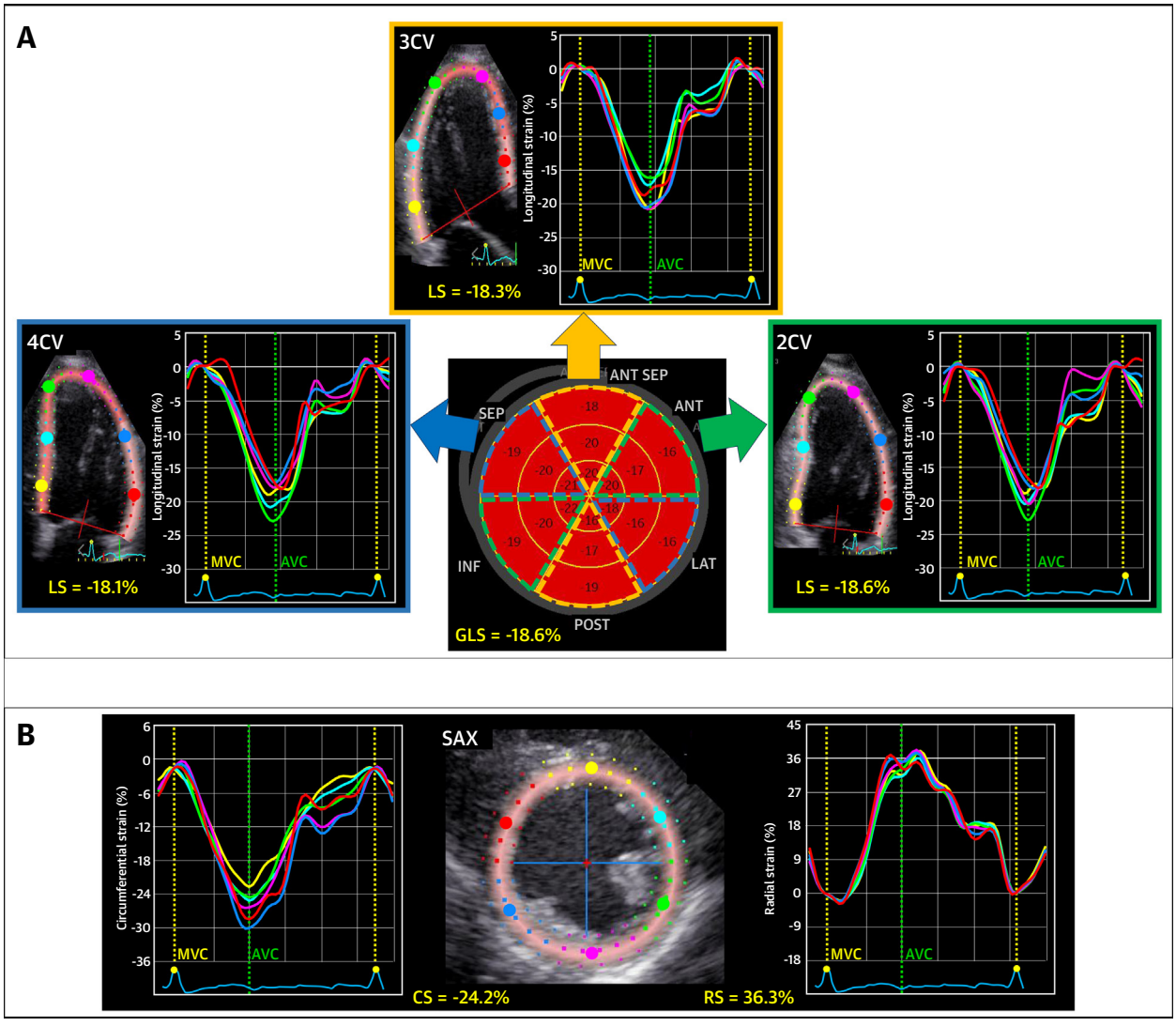

Typical recordings of longitudinal strain (LS), circumferential strain (CS) and radial strain (RS) from the left ventricle in a healthy subject. (A) Three apical views of the left ventricle with corresponding LS and bull's-eye plot. (B) Parasternal short-axis view (SAX) with corresponding CS and RS. Colors of the strain traces correspond to the color labels in the respective longitudinal and apical cross-sectional images. 2CV = 2-chamber view; 3CV = 3-chamber view; 4CV = 4-chamber view; ANT = anterior; INF = inferior; LAT = lateral; MVC = mitral valve closure; POST = posterior; SEP = septal; other abbreviations as in Figures 2 and 12.

different mechanisms may potentially explain intersegmental differences in contraction duration, including local delays in electromechanical activation, segmental contractile dysfunction, myocardial scar, fibrosis or nonuniform loading conditions.

Mechanical dispersion is a promising parameter for assessment of risk. There is, however, need for further validation in prospective outcome studies before a potential role in clinical routine can be decided.

STRAIN MEASUREMENTS IN CARDIAC CHAMBERS. The LV. Systolic function can be assessed by GLS,[83] which has been shown to be a sensitive marker of systolic dysfunction in a broad spectrum of cardiac diseases, as addressed in subsequent sections of this

review. Circumferential and radial strains may provide incremental information but are currently not widely implemented in clinical routine, because of limitations previously discussed. **Figure 17** illustrates measurements of LV longitudinal, circumferential, and radial strains.

Practically, depending on the software used, analysis starts with a check of the electrocardiographic trigger that defines end-diastole. If needed, the time point is adjusted to mitral valve closure. Next, an ROI is defined manually or automatically that covers the entire myocardium and avoids the echo-dense pericardium. If possible, the ROI is regionally adapted to the actual wall thickness. Larger, abrupt changes in wall thickness (bulging) should be avoided or excluded (**Figure 18**). Tracking is initiated manually or automatically, and the tracking result is carefully checked. For this, an overlay of markers indicating the tracked motion (ideally several dots per segment) is compared with the motion of the underlying myocardium. Improvements should be attempted only when necessary and only by adjusting either the end-systolic or the end-diastolic contour. When the definition of end-systole is correct, peak strain values can be accepted. Otherwise, end-systole needs to be manually set to aortic valve closure.

Currently, there is no generally applicable lower normal value for GLS. Instead, vendor-dependent normal ranges of GLS have been proposed.[84] Recent studies demonstrated that GLS also varies with age, sex, body weight, and blood pressure.[84-86] An individual patient meta-analysis suggested that regardless of vendors or clinical covariates, absolute GLS <16% likely indicates significant myocardial dysfunction. This is consistent with the lower limit of normal of 15.7% reported in a recent study on a large population of presumably healthy individuals with guideline-directed chamber-specific recordings, thereby limiting systematic and random variability.[87] Importantly, loading conditions have an impact on strain values and should be considered when using GLS as parameter of systolic function.

Absolute GLS in the range ≥16% to <18% is considered in a gray zone. Further grading of GLS would be somewhat arbitrary, as there are not yet sufficient data available to make firm recommendations. Studies of the prognostic impact of different levels of GLS and validation by invasive contractility measures would be helpful when defining criteria for grading. As imaging reports are often received by nonexperts in echocardiography, a verbal interpretation of the measured strain values, considering pathology and the specifics of the software used, is recommended to be included in echocardiography reports.

LV GLS measurements obtained on 2D STE showed very good reproducibility, with test-retest errors within acceptable limits for clinical use (<10% relative error).[40,88] For segmental longitudinal strains, reproducibility was not as good as for GLS, making

FIGURE 18 Practical Considerations When Measuring Myocardial Strain

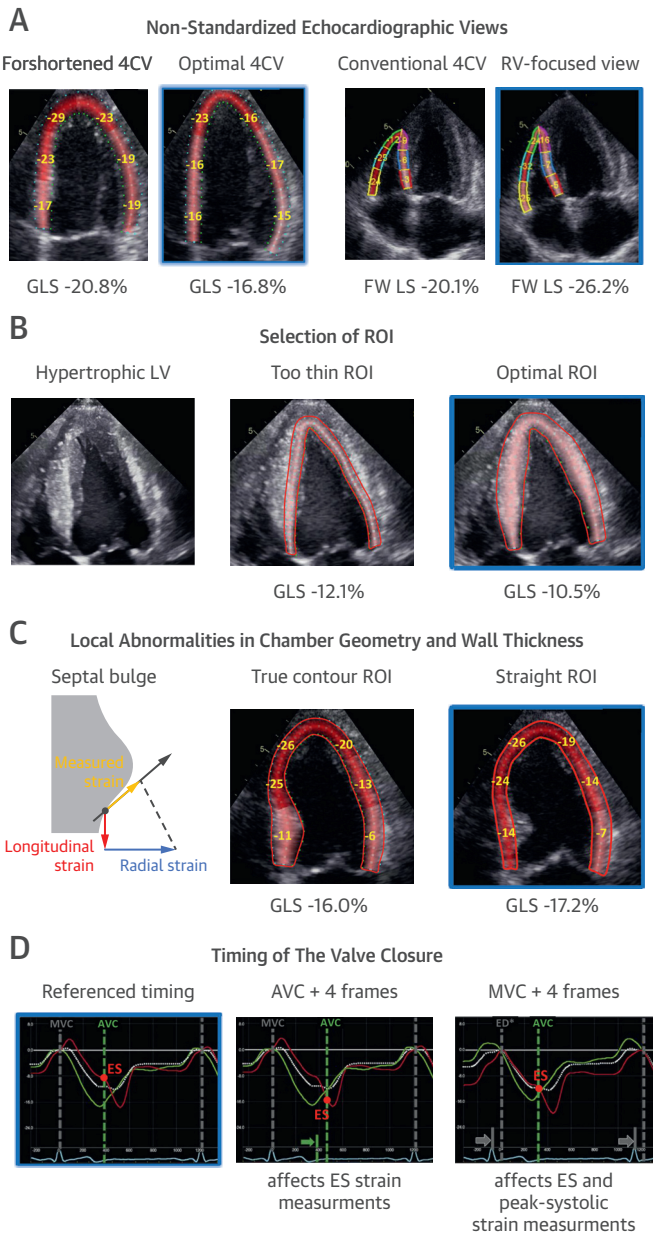

Continued on the next page

the clinical use of numerical segmental strain values challenging; nevertheless, strain curves and patterns can provide important diagnostic information.[89]

TIPS AND PITFALLS WHEN MEASURING LV STRAIN. Commercially available versions of speckle-tracking software enable an easy and fast semiautomatic or fully automatic strain analysis of all cardiac chambers. Detailed practical step-by-step recommendations have been published.[90-92] In the following, we focus on common technical issues that can affect strain estimates and consequently lead to measurement errors (Figure 18).

- Using nonstandardized echocardiographic views for STE may significantly affect strain values (Figure 18). Foreshortening of the 2D LV apical views can result in overestimation of absolute GLS of approximately 10% to 20%, with a predominant effect on longitudinal strain in the apical segments and in the endocardial layer.[26] RV strain measurements obtained from the recommended RV-focused apical 4-chamber view are greater in absolute magnitude than those obtained from a conventional 4-chamber view.[42] This difference may be related to the assessment of different areas of the RV free wall and the fact that the segments of the RV free wall more distant to the interventricular septum (corresponding to the largest RV basal diameter) undergo the greatest longitudinal deformation.
- Strain values are influenced by the selection of the ROI, as illustrated in Figure 18. Modern software determines ROIs (semi)automatically, but sometimes the regions need to be manually adjusted. For full wall tracking, the entire wall should be incorporated in the analysis, but not more. In hearts with thick walls, a too thin (too endocardial) ROI will result in an overestimation of the absolute strain values compared with a correctly placed ROI. Including bright pericardium will tether the ROI to this nonmoving feature and lead to reduced strain estimates. For both endocardial and full wall tracking, care must be taken to avoid the inclusion of papillary muscles or valve leaflet structures. Using fully automated software without manual editing options is therefore not recommended. A correct definition of the ROI as well as images with low noise and artifact burden are of highest importance for accurate strain estimates.[93]
- Local abnormalities in chamber geometry and wall thickness, such as septal bulging or sigmoid septum, may influence both segmental and global strain measurements (Figure 18C). Including a septal bulge in the ROI results in a clinically relevant underestimation of the absolute value of longitudinal strain, especially when endocardial tracking software is used, compared with full wall tracking software, in which strain measurements are less affected.[25] When including a septal bulge or similar structure in other locations in the ventricle, radial strain may dominate and cause net positive systolic strain when applying STE on images recorded from apical views. Therefore, to correctly assess longitudinal shortening in the presence of local thickening of the LV wall, the ROI is best drawn straight and in the longitudinal direction, excluding major local bulges. However, when a marked wall thickening extends over more than 1 full segment, we recommend that the ROI include the thickening.
- The exact definition of timing of cardiac events has a major impact on the accuracy of strain measurements, especially in pathology (Figure 18D).[94] End-diastole, and with it zero strain, should correspond to mitral valve closure. Most vendors approximate end-diastole using the QRS trigger on the electrocardiogram. As this is often programmed to detect just a steep slope within the QRS complex, true end-diastole may be missed in case of a distorted QRS complex (eg, in conduction delays). End-systole is commonly determined either on the basis of peak global deformation or an electrocardiographic analysis. Also, this approach may fail to represent properly the traditional physiological

FIGURE 18 Continued

Recommended views or methods are marked with a blue frame. (A) A particularly foreshortened echocardiographic view causes an overestimation of absolute values of apical LS and GLS. A dedicated right ventricular (RV) view should be used for assessing RV free wall (FW) LS and RV global strain. (B) Correct placement of the region of interest (ROI), selecting the whole thickness of the left ventricular wall is crucial for correct strain measurements. Particularly in hypertrophied hearts, a too thin ROI that tracks only the endocardium may lead to a significant overestimation of absolute GLS. (C) In hearts with regional septal bulging (here at the basal septum), the measured endocardial strain along the endocardial contour (yellow arrow) is a projection of a combination of longitudinal shortening (red) and radial thickening (blue) and may lead to underestimation of the true longitudinal shortening of the myocardium. Full wall tracking is affected to a lesser extent, but also here, drawing a straight ROI leads to a more accurate assessment of segmental LS and GLS. (D) Impact of timing on the accuracy of regional strain measurements in normal segment (green strain curve) and infarcted segment (red strain curve). Assumed MVC and AVC are indicated by dotted lines. Green and gray arrows point at the true timing of the events. The red dot indicates the measured end-systolic (ES) strain value. (Left) Correct measurement (ES strain −8%). (Middle) An incorrect setting of AVC results in overestimation of absolute ES strain (−16%). (Right) An incorrect setting of end-diastole affects the definition of zero strain and affects the ES strain measurement (ES strain −11%). Modified with permission from Mada et al.[94] Abbreviations as in Figures 2, 12, and 17.

FIGURE 19 LA Strain by Speckle-Tracking Echocardiography

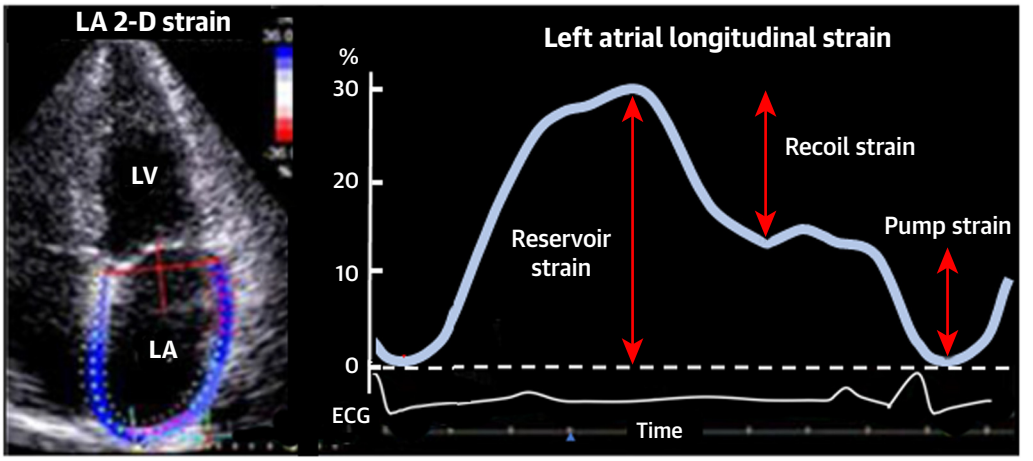

(Left) Apical 4-chamber image with color-coded region of interest for left atrial (LA) strain. (Right) The global LA strain trace is illustrated. Arrows indicate reservoir strain, recoil strain, and pump strain. 2-D = 2-dimensional; other abbreviations as in Figure 1.

definition of end-systole as aortic valve closure. T-wave analysis of the electrocardiogram can be only a rough approximation, and peak deformation may be delayed after aortic valve closure if several pathologic (eg, infarcted) segments are in the image. Timing should therefore be manually corrected if deemed necessary using direct observation of closure of the mitral and aortic valves or a spectral Doppler evaluation thereof.[23] In RV strain analysis, timing should be adjusted to corresponding valve events in the right heart.[24]

Global and regional strain. All 3 strain components can be applied for describing LV global (global strain) or regional (segmental strain) function of a chamber. GLS is a very reproducible measurement, as the value is obtained from a large part of the ventricle, and averaging data from multiple segments reduces effects of random signal noise and artifacts. Tracking segmental strain is performed in a much smaller myocardial region, which makes it also more susceptible to regional image artifacts and results in a high degree of measurement variability.[40,89,95] Accordingly, single-segment strain values should be used with caution.

When several adjacent segments have abnormal strains, these may be used to raise suspicion of regional pathology (specific cardiomyopathies or myocardial ischemia). It is important to note that qualitative analysis of the patterns of segmental strain curves, as well as the bull's-eye display, should be the preferred method for assessing regional strain. Detailed analysis of pattern of segmental strain curves, especially assessment of the time course of myocardial contraction, such as postsystolic shortening in ischemic segments or typical strain pattern of mechanical dyssynchrony, provide important diagnostic information.[32,96-99] The extent to which qualitative strain curve shape analysis or relative comparison between regions could compensate for the relatively poor segmental strain reproducibility remains to be determined.

The LA. Practically, LA strain analysis is performed on a nonforeshortened apical 4-chamber view of the LA and optionally also on an apical 2-chamber view.[24] The ROI is drawn from mitral ring to mitral ring. Available software extrapolates strain across the entries of the pulmonary veins and across the base of the appendage, which complicates the interpretation of segmental strains. In clinical routine, LA strain is assessed as GLS. The use of dedicated tracking software for LA strain is preferable, as it significantly improves measurement reproducibility.[100]

During LV systole, the LA serves as a reservoir that collects blood from the pulmonary veins, and during diastole, the reservoir volume is ejected into the LV by passive LA contraction (recoil) in early diastole and by active contraction in late diastole. During diastole the atrium also functions as a conduit for transport of blood from the pulmonary veins to the LV, and this transport continues until it is interrupted by active atrial contraction. A more extensive explanation of the different components of LA function and how

they relate to pulmonary venous flow and LV function is provided in a review by Hoit.[101]

For measurement of LA reservoir strain, it was recommended by a joint European Association of Cardiovascular Imaging and American Society of Echocardiography task force to use ventricular end-diastole to define the zero baseline.[24] With this definition, reservoir strain is measured as the difference between peak strain and strain at ventricular end-diastole. An alternative would be to use the onset of LA contraction as zero baseline. An advantage of using end-diastole as zero is that this definition applies to all patients, including those in atrial fibrillation. In patients with wide QRS complex, as in bundle branch block, which complicates the definition of end-diastole, one may use the presystolic nadir of the atrial strain trace as zero reference. LA pump strain is measured as difference between strain values at ventricular end-diastole and the onset of atrial contraction. Technically, LA pump strain has a negative sign but is most often reported as an absolute value. **Figure 19** shows a typical LA strain trace.

Whereas LA reservoir and pump function can be assessed using strain imaging, the conduit function is not reflected in LA strains. LA conduit function represents the volume of blood that passes through the LA that cannot be attributed to reservoir or booster pump functions.[102] Conduit volume can be computed using 3D echocardiography or CMR, in the absence of significant mitral or aortic regurgitation, as [LV stroke volume – (maximum LA volume – minimum LA volume)],[103] but this is cumbersome and is rarely done clinically.[104,105] Conduit function is reflected in the D wave of antegrade pulmonary venous flow velocity.[106] Sometimes the term *conduit strain* is used for deformations in the LA in early diastole, but the passive LA contraction after mitral valve opening is not a measure of conduit function, and therefore calling it conduit strain may lead to misunderstandings. As proposed previously, a more appropriate term for this passive early diastolic contraction would be *recoil strain*.[107] As recoil strain approximates the difference between LA reservoir strain and pump strain, one may question the utility of measuring and reporting it as a separate parameter.

The reported ranges of normal LA strains are rather wide, which in part is caused by normal biological variability but may also reflect imaging from non-dedicated LA views and manual tracing instead of semiautomated tracking software to define atrial endocardium. Median values for normal LA reservoir and pump strain have been reported as 42% and 14%, respectively,[108] while the lower limits of normal are 17% and 6%, respectively.[87] There is age dependency of normal values for LA strain, with reduction in reservoir strain and increase in pump strain with ageing.[108] There are only minor differences in LA strain between sexes, and there appear to be no differences among ethnic groups.[108] Regardless of age and sex, reservoir strain $<$ 20% to 23% is considered abnormally low.

As demonstrated in several studies, LA strain by STE has high feasibility and quite good reproducibility.[109-112] Together with LV GLS, LA reservoir strain was found to be among the most reliable parameters compared with several other echocardiographic parameters in an intercenter reproducibility study.[113]

Most studies of the reproducibility of LA strain have been performed using echocardiography with software developed for measuring LV strains. Some of the vendors have developed dedicated semi-automated software for measuring LA strain.

The terminology used to describe LA strain varies somewhat in current published reports. One can argue that the terminology for LA strain should be consistent with that used for LV strain. One option would be to use LA GLS as an equivalent to LV GLS. However, names that refer to the function that is being measured facilitate communication, and therefore the terms *LA reservoir strain* and *pump strain* are preferable.

The RV. Software developments as well as increasing evidence supporting the clinical usefulness of RV strain measurements have led to growing interest in RV strain over the past few years. RV longitudinal strain is useful to assess RV function in several cardiomyopathies and offers incremental functional information and prognostic value over the conventional echocardiographic indexes of RV systolic function in various cardiovascular diseases.[114]

Practically, special care should be taken to use an RV-focused apical 4-chamber view for achieving a standardized RV display with clearly visualized myocardium of the free wall.[24] RV-focused views result in higher reproducibility of strain measurements compared with conventional apical 4-chamber views.[42] The ROI should be adjusted to the thin RV free wall (3-5 mm).[115] A layer-specific analysis is not possible. RV deformation can be reported as global strain, including septum and RV free wall, but RV free wall longitudinal strain, which comprises only the 3 free wall segments, is commonly recommended for clinical practice.[24] The 2 measurements are not interchangeable, as RV free wall strain has a larger

FIGURE 20 Why GLS Is a More Sensitive Measure of LV Function Than EF

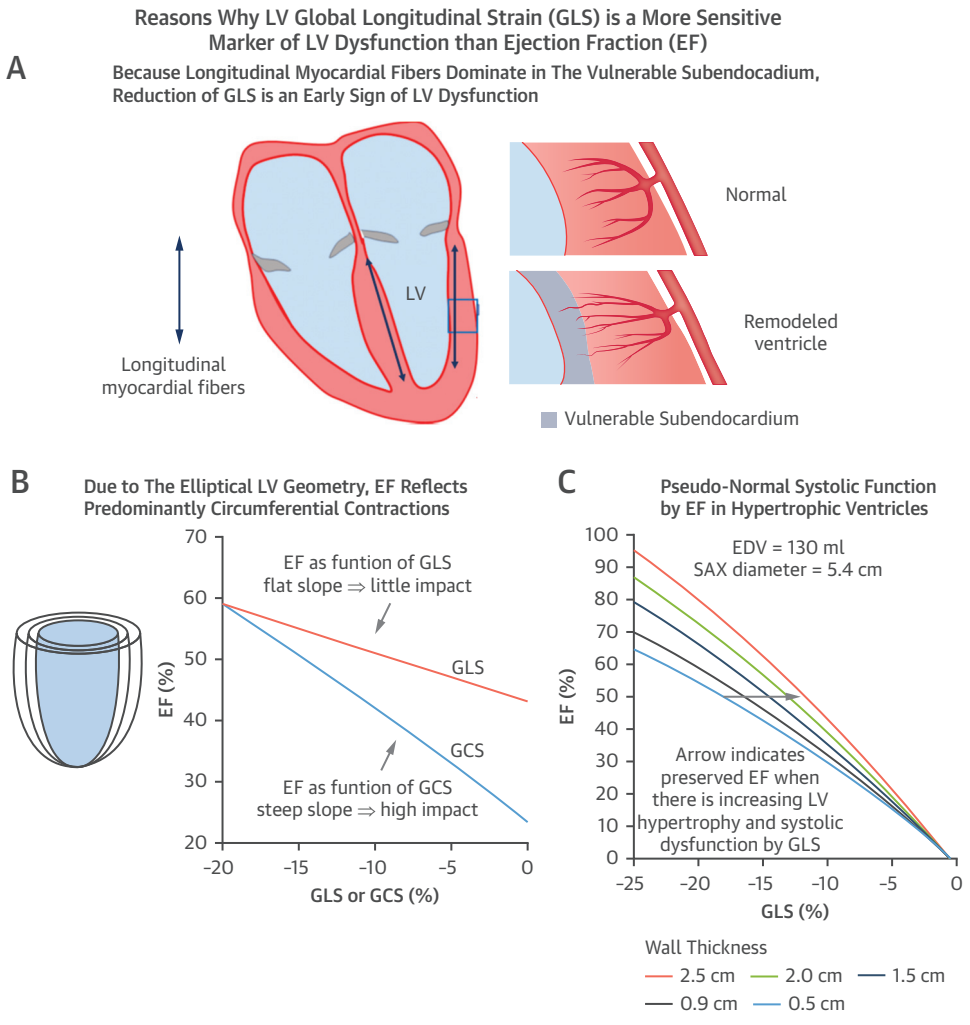

Mechanisms to explain why GLS is more sensitive than ejection fraction (EF) as a marker of systolic dysfunction. (A) Illustration of the LV in a normal heart and a remodeled LV. The double arrows inside the myocardium symbolize that longitudinally oriented fibers dominate in the subendocardium. (B) Relationships between EF and LV strains, showing much flatter slope for GLS vs EF than for global circumferential strain (GCS) vs EF. This illustrates that EF reflects predominantly circumferential contractions. (C) Simulation study of EF as a function of GLS and LV wall thickness. As illustrated by the arrow, EF is preserved at 50% when there is combined LV hypertrophy and reduction in absolute GLS. In the simulation shown in C, there were similar changes in GLS and GCS. Adapted under CC BY-NC-ND 4.0 license from Stokke et al.[62] d = delta; EDV = end-diastolic volume; other abbreviations as in Figures 1 and 12.

magnitude than RV global strain by about 5% strain units.[42,100,116] The normal reference ranges are much wider for RV free wall strain than for LV GLS, meaning the between-subject variability is larger than for LV GLS.[87] Data from 2 large cohorts of healthy subjects suggested that absolute RV free wall strain < 20% is likely pathologic,[117,118] while a recent large cohort study reported a lower limit of normal of 17% for absolute RV free wall strain.[87]

Consistent with previous results on LV strain, RV free wall strain and RV GLS are both reproducible measurements. Using dedicated RV tracking software is more convenient but does not increase measurement reproducibility.[100] Segmental RV strain measurements have an unacceptable level of variability (up to 30%)[42,95,100] and should be used with caution.

The complex anatomy of the RV makes the concept of 3D STE analysis attractive, as it allows

comprehensive assessment of the whole RV myocardium with multiple strain components. The results are promising, but the superiority of 3D strain over 2D strain has not yet been proved.[45,119,120]

The right atrium. Few data exist on the clinical utility of right atrial strain.[121,122] Practically, an RV-focused apical 4-chamber view is used,[24] while the technical principles of strain analysis are applied in analogy to LA strain. A recent meta-analysis demonstrated very wide ranges of right atrial strain values among healthy subjects,[123] which might limit the clinical utility of this parameter.

STRAIN IMAGING IN LV DYSFUNCTION: INCREMENTAL VALUE TO EJECTION FRACTION

WHY IS GLS A MORE SENSITIVE THAN EJECTION FRACTION AS PARAMETER OF SYSTOLIC DYSFUNCTION?

LV GLS is more sensitive than ejection fraction (EF) to diagnose mild systolic dysfunction, as shown in different patient populations, including heart failure with preserved EF, coronary artery disease, diabetes, hypertensive heart disease, and cardiomyopathies with LV hypertrophy.[124-129] Figure 20 illustrates 3 different mechanisms that may explain why GLS is superior to EF as measure of mild systolic dysfunction.

First, longitudinally oriented myofibers, which determine GLS, dominate in the LV subendocardium, whereas myofibers with circumferential orientation are dominant in the midlayer of the wall. The inner layer of the LV wall tends to develop ischemia earlier than the outer layers, and therefore the subendocardium is the most vulnerable part of the wall. Because myocardial fibers in different LV wall layers are tethered together, reduced shortening in the subendocardium leads to reduced shortening in all layers in the wall. This is suggested as an explanation for why reduction of GLS is an early sign of LV dysfunction (Figure 20A).

The tendency to develop subendocardial infarctions in acute coronary syndrome is well known and reflects the vulnerability of the inner wall layers. The subendocardium is susceptible to ischemia also in the absence of epicardial coronary artery stenosis. This is attributed to higher compressive forces on the intramyocardial vessels in the subendocardium than in the outer layers[130] and longer distance from the epicardial coronary arteries. These effects are enhanced in hypertrophic ventricles. Furthermore, subendocardial perfusion may be impaired because of microvascular remodeling and fibrosis, which tend to occur first in the subendocardium.[126] Therefore, several factors may contribute to subendocardial dysfunction and cause reduction in LV longitudinal shortening.

Second, because of the elliptical geometry of the ventricle, longitudinal contractions have less impact on LV volume and LVEF than circumferential contractions. This is illustrated in Figure 20B by a much flatter slope for the relationship between GLS and EF than for global circumferential strain and EF. As shown in a simulation study, the contributions from circumferential and longitudinal shortening to stroke volume were 67% and 33%, respectively.[131] With the ventricle as an approximate ellipsoid, circumferential contraction implies shortening of the entire LV short-axis area (ie, 2 spatial dimensions, x and y), whereas longitudinal shortening causes reduction in only 1 dimension (z). Using a cube as analogy makes this distinction more obvious. As an example, when contracting by 20% in both the x and y dimensions, volume is reduced to 64% (0.8×0.8) of the initial volume. When contracting only in the z-axis (equivalent to GLS), a 20% shortening results in a volume that is 80% of the initial volume. For patients with EFs in the lower normal range, one would predict that a moderate reduction in GLS will cause a small reduction in EF to a subnormal value. However, for ventricles with EFs in the midnormal or upper normal range, EF may remain within the relatively wide normal range, although GLS is mildly reduced. When considering the 2 mechanisms illustrated in Figures 20A and 20B together, they may explain why mild LV systolic dysfunction is reflected in reduced GLS, whereas EF may remain in the normal range.

Third, LV hypertrophy is an additional mechanism that tends to preserve EF (pseudonormal function) when there is impaired systolic function.[131,132] This is in part because hypertrophic and thick LV walls tend to cause small LV diastolic cavity volumes. Therefore, in hypertrophic LVs with reduced cavity size, a small contraction and a small stroke volume may represent a large relative change in cavity volume, and therefore EF may be normal in a dysfunctional ventricle. In addition, the same percentage thickening results in more absolute thickening when the wall is thicker prior to contraction (Figure 20C). Therefore, hypertrophic ventricles with thick walls may have normal EFs despite reduced systolic function. In some cases, a hypertrophic ventricle with reduced contractility may show almost complete closure of the cavity in end-systole, which is measured as a supernormal EF.

FIGURE 21 Segmental LV Strain Curves in Ischemia and Dyssynchrony

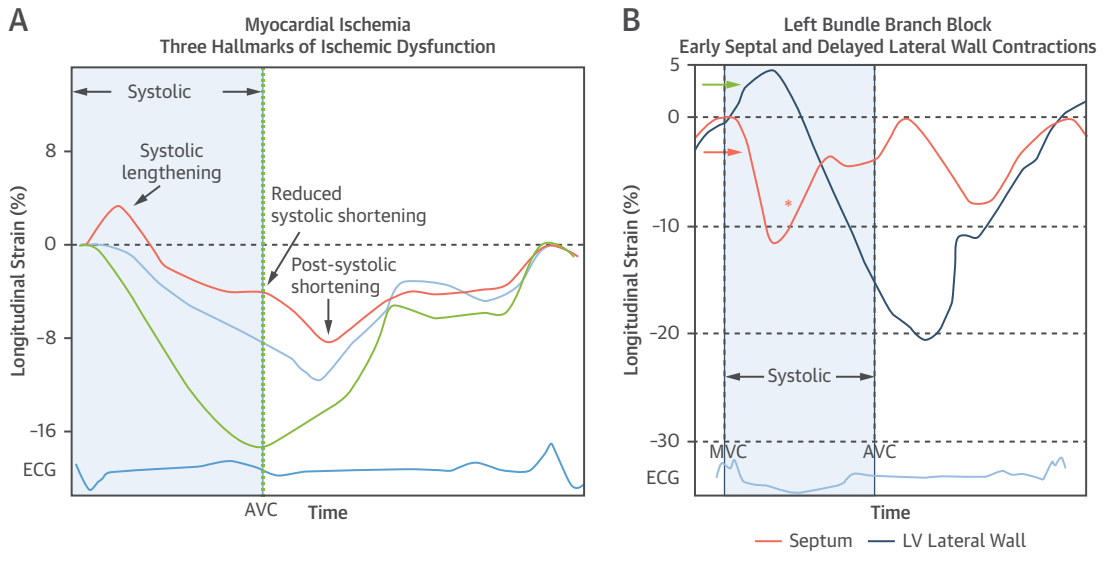

(A) Schematic illustration of LV segmental strains in a heart with myocardial ischemia. Measurements from 3 different segments are shown. The red-colored trace shows recordings from a severely ischemic segment with systolic lengthening, reduced net systolic shortening (measured at AVC), and marked postsystolic shortening. The green-colored trace shows recordings from a nonischemic segment. The blue trace is from a segment with mild ischemia, as indicated by reduced systolic shortening and postsystolic shortening. (B) Example of segmental strain curves in the septum (red) and LV lateral wall (blue) in typical left bundle branch block. The early activated septum shows early systolic shortening (red arrow), followed by systolic rebound stretch (red asterisk). After AVC, during isovolumic relaxation, there is further septal lengthening, probably reflecting earlier relaxation in the septum than in the LV lateral wall. The late activated lateral segment is initially stretched by the septum (green arrow) and has then a delayed onset of shortening. Abbreviations as in Figures 1, 2, and 17.

In these cases, the systolic dysfunction is confirmed by reduction in GLS. Typical examples are hypertrophic cardiomyopathy and amyloidosis. A similar mechanism may explain normal EF but reduced long-axis shortening in patients with hypertensive LV hypertrophy.[133]

The results from the simulations shown in Figures 20B and 20C are based upon a simplified model that does not incorporate torsional deformation, and there are assumptions about LV geometry. Therefore, the magnitude of effects on the different cardiac parameters that are discussed previously and presented in Figures 20B and 20C may be different in real life.

In theory, reduced absolute GLS could be compensated for by increased global circumferential strain to maintain EF. However, studies have reported preserved EF in cases with both reduced GLS and global circumferential strain,[128,134,135] which can be explained as shown in Figure 20C, in which both GLS and global circumferential strain are reduced but EF is maintained because of a thicker wall. The mathematical model shows how EF is less sensitive to changes in GLS because of the geometric relations. Nevertheless, it is not definitely determined if a compensatory increase in global circumferential strain exists in some cases, making EF even less sensitive to reduced GLS.

LV GLS AND MECHANICAL DISPERSION AS PROGNOSTIC MARKERS. As discussed under different topics in this review, LV GLS is a strong prognostic marker. This includes prognostic value in heart failure.[136,137] As shown by Park et al[136] in patients with acute heart failure, GLS has greater prognostic value than LVEF. Furthermore, Haugaa et al[82] showed in a study of patients with previous myocardial infarction that myocardial mechanical dispersion by strain imaging was an independent predictor of arrhythmic events. Both mechanical dispersion and GLS were markers of arrhythmias in patients with non-ST-segment elevation myocardial infarction and in those with LVEFs >35%, whereas LVEF was not. A combination of mechanical dispersion and global strain showed the best positive predictive value for arrhythmic events.

Future studies should explore whether GLS and mechanical dispersion may be used to guide therapeutic choices.

APPLICATION OF STRAIN IN SPECIFIC DISORDERS

MYOCARDIAL ISCHEMIA. Strain imaging may be applied to diagnose ischemia by showing reduction in systolic shortening (hypokinesia), but equally important is the demonstration of systolic lengthening (dyskinesia) and postsystolic shortening, which are the characteristic features of myocardial ischemic injury (**Figure 21A**).[138,139] Importantly, these features are not specific to myocardial ischemia, as similar abnormalities may be observed in cardiomyopathies and in other disorders with myocardial dysfunction. Furthermore, postsystolic shortening can also be found in about one-third of myocardial segments in healthy subjects. However, such physiological postsystolic shortening that follows a normal systolic strain is of minor amplitude and has no detrimental effects on cardiac function.[140]

In the center of an ischemic region, there is the most severe dysfunction, often reflected in systolic lengthening. Neighboring segments with less marked ischemia may have reduced systolic shortening and postsystolic shortening. The postsystolic shortening is often a reflection of elastic recoil in segments that have been stretched in systole, whereas in other cases, postsystolic shortening represents delayed active contraction of an ischemic segment.[141] There is no easy way to differentiate passive from active postsystolic shortening, as in most cases, invasive LV pressure is needed to make the distinction.[141] In segments with transmural scar, postsystolic shortening reflects passive contraction in myocardium that was stretched in the preceding systole.

Myocardial strain imaging is not widely implemented as a modality to diagnose coronary artery disease. The use of STE during stress echocardiography is still a matter of debate, as there are challenges with quality of measurements when there is excessive myocardial motion, higher heart rates, and lack of definition of cutoff levels of strain for the major coronary artery regions.

In the 2019 European Society of Cardiology guideline on management of coronary artery disease, however, a role for strain imaging was suggested in patients with normal EFs, as regional dysfunction would increase suspicion of ischemic myocardial damage.[142] Furthermore, a recommendation (Class 2b)[142] was given regarding risk assessment, stating that GLS provides incremental information to LVEF and may be of value when assessing risk in patients with LVEFs >35%.

DYSSYNCHRONY. In principle, there are 2 different mechanisms of LV dyssynchrony: electrical conduction delay, such as in left bundle branch block, and contractile disparity,[143] which has nonelectrical etiologies such as myocardial ischemia, scarring, and nonuniformities of myocardial loading. Importantly, only dyssynchrony caused by electrical conduction delay is amenable to cardiac resynchronization therapy. Therefore, distinction between the 2 fundamentally different mechanisms of LV dyssynchrony is important and was facilitated by the introduction of strain imaging as a clinical tool.

In hearts with left bundle branch block, there is early activation of the septum and delayed activation of the LV lateral wall. Therefore, in typical left bundle branch block cases, there is early contraction of the septum ("septal flash")[144] inducing mitral valve closure.[145] Furthermore, LV pressure rises slowly, as active septal contraction coincides with lengthening of the late activated, passive LV lateral wall (**Figure 21B**). Because the hyperextended lateral wall has increased preload, it contracts forcefully, and the associated increase in the transseptal pressure gradient pushes the septum rightward, causing "septal rebound stretch."[146]

Another characteristic feature of hearts with left bundle branch block is "apical rocking,"[147] which is a translational motion of the distal parts of the LV. The motion starts with the early activated septum pulling the apex toward the septum, and when the LV lateral wall is activated, the apex is pulled back toward the lateral wall. This motion can be measured but also assessed visually.[147] As these abnormal motions are caused by active contractions, they are attenuated or abolished when there is septal or LV lateral wall scarring.[148]

Because electrical dyssynchrony and contractile disparity interact, the resulting regional deformation patterns are not always clearly attributable to one or the other cause. Important modifiers of myocardial strains patterns are regional dysfunction due to ischemia or scar and progressive remodeling with changes in LV structure.[97,99,149] Particularly in a severely remodeled septum, strain patterns caused by scar and electrical conduction delay may be difficult to distinguish.

A series of studies of LV dyssynchrony by Prinzen and Lumens and coworkers[97,150] have shown how strain imaging may be applied to quantify dyssynchrony. Furthermore, they have shown how nonelectrical factors such as regional contractile dysfunction and myocardial scarring modify

FIGURE 22 Strain and Work Indexes in Patients Receiving CRT

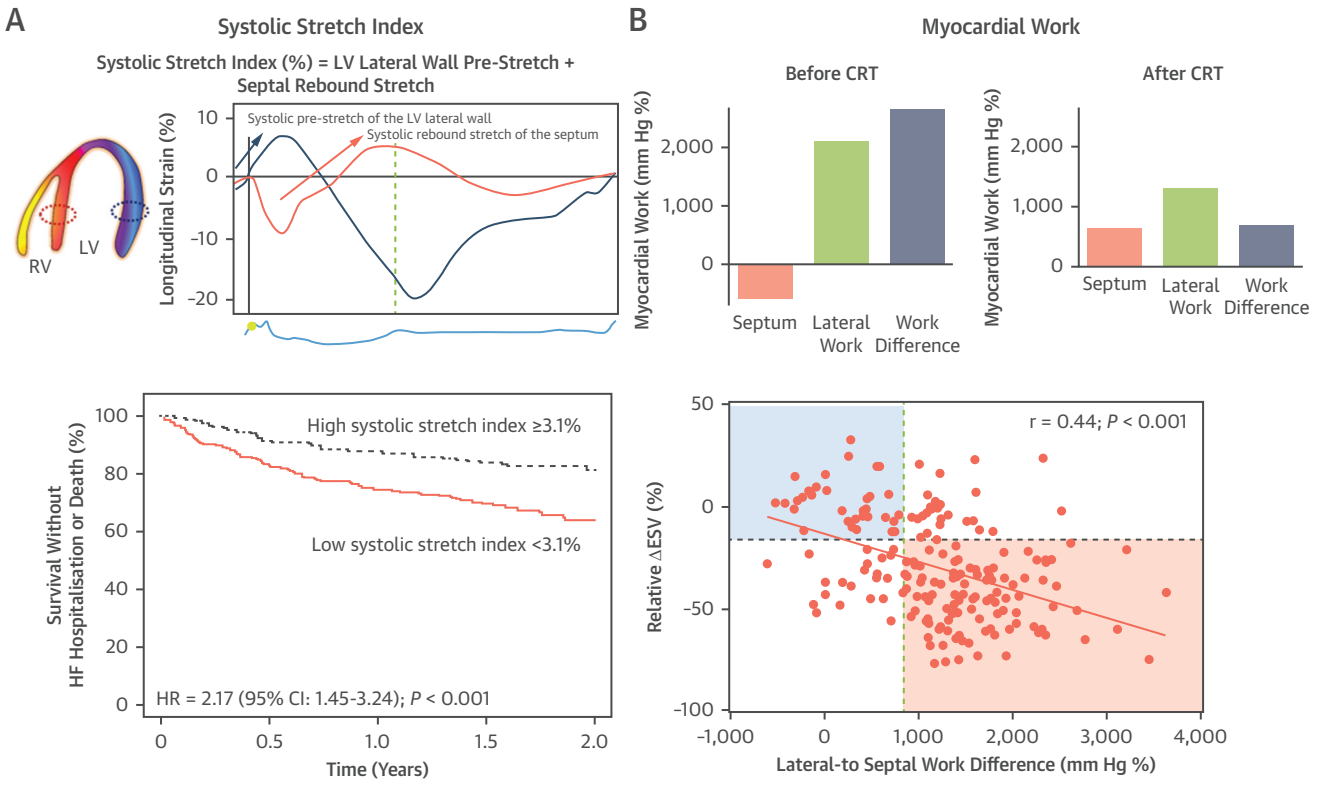

(A) Longitudinal systolic stretch index and its association with clinical outcome after cardiac resynchronization therapy (CRT) device implantation. Longitudinal systolic stretch index is calculated from the apical 4-chamber view as the sum of systolic prestretch (blue arrow) of the mid and basal segments of the lateral wall and systolic rebound stretch (red arrow) of the mid and basal segments of the septal wall. Kaplan-Meier plots demonstrate significant associations of high systolic stretch index with favorable clinical outcome after CRT. The cutoff was based on the median value in the study population. The vertical dashed green line in the top panel indicates aortic valve closure. Adapted with permission from Gorcsan et al.[156] (B) Regional myocardial work and reverse remodeling after CRT. Prior to CRT, a large difference in myocardial work between the septal and lateral walls is detected, which is diminished with successful resynchronization. The lateral-to-septal myocardial work differences before implantation correlate with the degree of reverse remodeling following CRT. The black-dotted horizontal line indicates a relative reduction of end-systolic volume (ESV) of 15%. The green-dotted vertical line indicates the proposed cutoff of myocardial work difference of 860 mm Hg %, which has been found as a predictor of response in the study population. Adapted under CC BY-NC 4.0 license from Aalen et al.[155] HF= heart failure; other abbreviations as in Figures 1 and 18.

parameters of dyssynchrony. The clinical utility of these novel insights should be explored in future clinical studies of optimal diagnostic work-up in cardiac resynchronization therapy candidates.

Likewise, the use of nuclear imaging to diagnose impaired myocardial perfusion and the assessment of myocardial viability are challenging in the presence of left bundle branch block. Currently, CMR late gadolinium enhancement is the modality of choice for imaging myocardial scar in patients with left bundle branch block.[151] To what extent high-frame rate echocardiography-based elastography may be used in this context should be explored.[152]

Echocardiographic parameters focusing on peak-to-peak time differences (eg, in tissue Doppler curves) do not have the specificity needed to identify dyssynchrony patterns that can be amended by cardiac resynchronization therapy. There is growing evidence, however, that specific patterns that can be analyzed visually (septal flash, apical rocking) or quantified by segmental strain or work analysis (see subsequent discussion) have a prognostic value in cardiac resynchronization therapy candidates.[97-99,153-155] Next to the purely visual analysis of septal flash and apical rocking,[154] the electromechanical substrate amendable by cardiac resynchronization therapy can be identified by measuring (antero)septal and (infero)lateral strain patterns. A quantitative assessment is possible with a combination of systolic prestretch of the LV

FIGURE 23 Longitudinal Strain Bull's-Eye Plots in Left Ventricular Hypertrophy With Different Etiologies

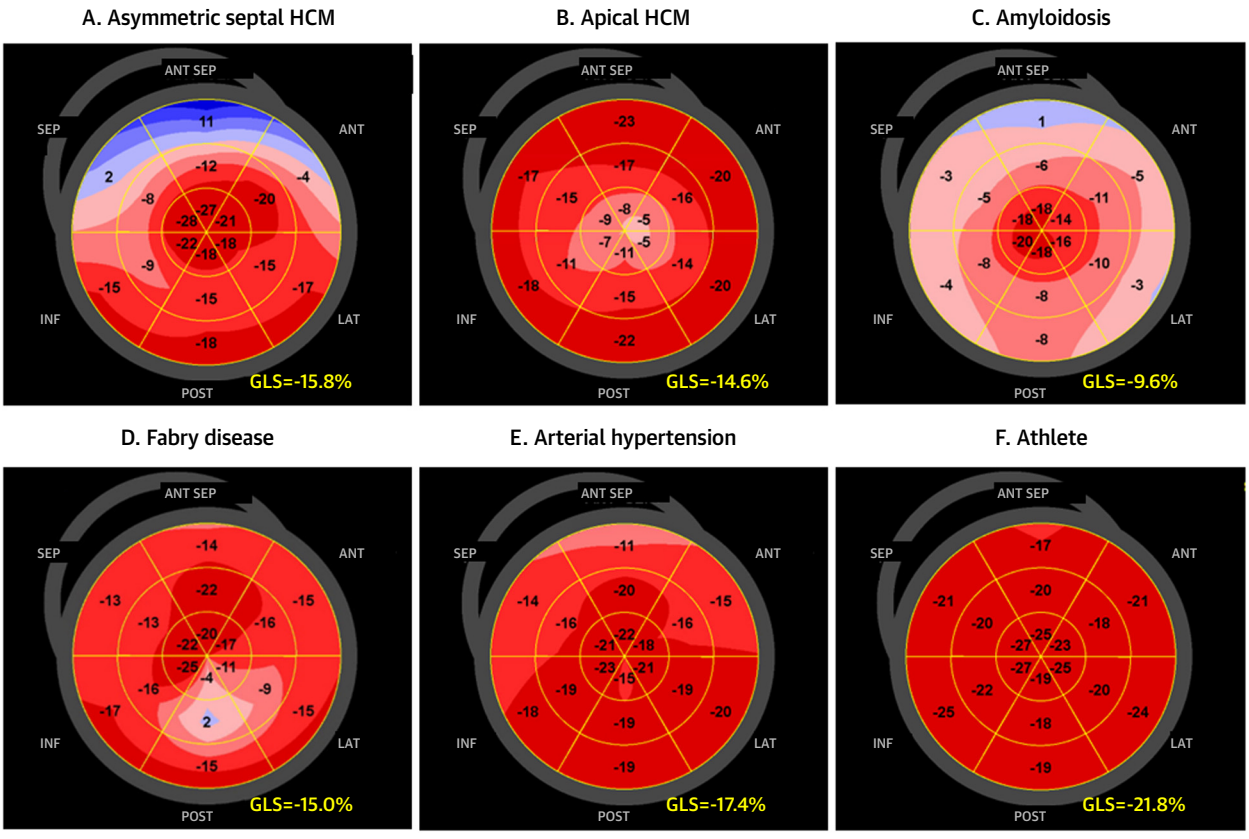

Examples of longitudinal strain bull's-eye plots in subjects with left ventricular hypertrophy of different etiologies. (A) A 34-year-old woman with asymmetrical septal hypertrophic cardiomyopathy (HCM). Hypertrophic septal segments deform less (mid and basal segments), whereas the rest appear spared. (B) A 59-year-old man with isolated apical HCM has impaired longitudinal strain in the apex, surrounded by the normal strain values at the basal and middle levels. (C) An 85-year-old man with wild-type transthyretin amyloidosis presents with typical apical-sparing pattern. (D) A 45-year-old women with Fabry disease with local impaired longitudinal strain at the middle level of the lateral wall. (E) A 54-year-old man with arterial hypertension has a normal average GLS with slightly impaired longitudinal strain at the basal septal segments. (F) A 28-year-old man, a professional rower, has a homogeneous segmental longitudinal strain pattern and normal GLS. Abbreviations as in Figure 17.

lateral wall and systolic rebound stretch of the septum, known as systolic stretch index, using longitudinal, circumferential, or radial strain (Figure 22A).[156,157] High values of baseline systolic stretch index were associated with favorable clinical outcomes after cardiac resynchronization therapy, and GLS was additive to systolic stretch index in predicting clinical outcomes (heart failure hospitalization or death).

Furthermore, dyssynchronous contraction causes a redistribution of myocardial work, with reduced work in the early activated septum and increased work in late activated lateral wall.[158] The larger the baseline myocardial work differences between the lateral wall and septum, the higher the reverse remodeling after cardiac resynchronization therapy[155] (Figure 22B). When myocardial work difference is combined with septal viability (eg, from CMR), it can accurately predict remodeling and long-term survival after cardiac resynchronization therapy (AUC: 0.88 [95% CI: 0.81-0.95]).

The importance of longitudinal strain curve features over classical clinical and echocardiographic characteristics to discriminate cardiac resynchronization therapy responders was recently demonstrated also in an unsupervised machine learning study.[159] However, using strain-guided LV lead placement targeting the latest mechanically activated viable segment did not increase response rate or survival in a small randomized study.[160] Although several retrospective and prospective nonrandomized studies strongly support mechanical dyssynchrony as

a marker of cardiac resynchronization therapy response that appears additive or even superior to guideline-based patient selection,[99,153,161] there is currently no guideline indication for using any of these parameters. The commonly mentioned reason is the lack of randomized studies. The ongoing prospective randomized AMEND-CRT (Assessment of Mechanical Dyssynchrony as Selection Criterion for Cardiac Resynchronization Therapy; NCT04225520) trial may provide this missing evidence.

SPECIFIC CARDIOMYOPATHIES. In the context of cardiomyopathies, strain imaging can be useful for identifying early functional abnormalities, especially in ventricles with hypertrophy and normal EFs, providing incremental information in diagnostic evaluation, identifying patients with risk for arrhythmias, and predicting outcomes.

Hypertrophic cardiomyopathy. Despite preserved LVEF, GLS is impaired in patients with hypertrophic cardiomyopathy. Segments with reduction of absolute longitudinal strain typically correspond to sites of hypertrophy or late gadolinium enhancement on CMR.[162,163] A bull's-eye display of peak systolic strain facilitates analysis in the clinic (**Figure 23**). Regional longitudinal strain may also be abnormal in patients with genotype-positive hypertrophic cardiomyopathy without phenotypic expression, suggesting that subtle functional and structural alterations are present even before the development of increased wall thickness.[164] In patients with hypertrophic cardiomyopathy, impaired GLS is associated with an increased risk for ventricular arrhythmias, heart failure hospitalization, heart transplantation, and death.[165] There are currently not sufficient data to propose a specific GLS cutoff for making clinical decisions regarding implantable cardioverter-defibrillator therapy. Mechanical dispersion metrics significantly improved risk stratification for malignant ventricular arrhythmias when added to conventional scores. Reduced absolute GLS was also a marker of risk for arrhythmic events but was inferior to mechanical dispersion.[166]

Amyloidosis. Basal systolic strain and strain rate have been shown to be impaired in cardiac amyloidosis even without signs of heart failure. Once heart failure is present, strain abnormalities may also extend to other LV segments. Several indexes focusing on the LV base-to-apex longitudinal strain gradient are clinically useful in diagnosing cardiac amyloidosis.[167,168] Also, differential changes in EF and GLS as well as LA reservoir strain have been proposed for differentiating cardiac amyloidosis from other hypertrophic substrates.[169,170] A relative apical sparing phenomenon was present in nearly three-quarters of patients with histologic cardiac amyloid infiltration, while a significant base-to-apex gradient of longitudinal strain was observed in all cases.[171] No differences in strain patterns exist in the various subtypes of amyloidosis.[172] Observing a pattern of apical sparing on longitudinal strain polar maps may be used as a first indication for a possible amyloidosis but has limited specificity in clinical routine, as it may sometimes also occur in other causes of LV hypertrophy (eg, aortic stenosis).[169,173,174] The importance of strain parameters in the diagnostic work-up of cardiac amyloidosis was recognized in the 2023 guideline recommendation for cardiomyopathies, with relative apical sparing pattern and an EF/GLS ratio >5 as the only echocardiographic parameters on the list of clinical red flags.[175]

In patients with transthyretin amyloidosis cardiomyopathy, average peak longitudinal strain from apical 4-chamber view was independently associated with mortality unrelated to the distinct genotype and severity of the disease.[176] Additionally, GLS and myocardial work indexes might be used as potential markers of monitoring treatment response to tafamidis in transthyretin amyloidosis cardiomyopathy.[177] Similarly, in light-chain amyloidosis with cardiac involvement, GLS or average peak longitudinal strain from 4-chamber view correlated with disease severity and was a strong, independent predictor of survival beyond the existing Mayo staging model.[178,179] An absolute improvement of average longitudinal strain from a 4-chamber view by 2 percentage points at 1 or 2 years after the initiation of chemotherapy was associated with improved survival and might serve as a measure of response to therapy.[179] Recently, strain data from all 4 chambers demonstrated prognostic utility in patients with biopsy-confirmed cardiac amyloidosis.[180] LA and RV strain data had additive prognostic value to GLS and clinical or conventional echocardiographic parameters.

Arrhythmogenic RV cardiomyopathy. In case of a clinical suspicion of arrhythmogenic RV cardiomyopathy, CMR is the preferred imaging technique for the evaluation of RV dilatation and dysfunction. However, echocardiographic RV strain has also been shown to be a promising parameter at an early stage of the disease.[181,182] Abnormal RV strain was present in 71% of asymptomatic carriers of a pathogenic mutation, predominantly in the basal segment of the RV free wall, while conventional parameters such as tricuspid annular plane systolic excursion and RV fractional area change were comparable with those among healthy control subjects. Normal segmental RV strain patterns were associated with an absence of

TABLE 2 Cancer Therapy-Related Cardiovascular Toxicity Definitions

Symptomatic CTRCD (HF)[a,b]	Very severe	HF requiring inotropic support, mechanical circulatory support, or consideration of transplantation
	Severe	HF hospitalization
	Moderate	Need for outpatient intensification of diuretic and HF therapy
	Mild	Mild HF symptoms, no intensification of therapy required
Asymptomatic CTRCD	Severe	New LVEF reduction to <40%
	Moderate	New LVEF reduction by ≥10 percentage points to an LVEF of 40%-49% or New LVEF reduction by <10 percentage points to an LVEF of 40%-49% and either new relative decline in LV GLS by >15% from baseline or new increases in cardiac biomarkers
	Mild	LVEF ≥ 50% and new relative decline in LV GLS >15% from baseline and/or new increases in cardiac biomarkers

Reproduced with permission from Lyon et al.[198] [a]The definitions are based on LVEF and supportive diagnostic biomarkers according to the 2021 European Society of Cardiology guidelines for the diagnosis and treatment of acute and chronic HF. [b]Symptomatic CTRCD represents HF, defined as a clinical syndrome as defined by Lyon et al.[198]

CTRCD = cancer therapy-related cardiac dysfunction; GLS = global longitudinal strain; HF = heart failure.; LV = left ventricular; LVEF = left ventricular ejection fraction.

disease progression during 4-year follow-up in these individuals.[181] Both abnormal RV strain patterns and prolonged RV mechanical dispersion have been shown to be associated with arrhythmic events.[183,184] A recent expert consensus document therefore proposed using RV free wall and/or RV GLS and RV mechanical dispersion in family screening and follow-up of early arrhythmogenic RV cardiomyopathy, considering RV mechanical dispersion more than 25 ms (3-segment model) or 30 ms (6-segment model) as an indicator for further investigation.[185]

Dilated cardiomyopathy. The diagnostic role of strain imaging is limited when there is already overt dilated cardiomyopathy with reduced EF. However, it might be used for screening of relatives of patients with dilated cardiomyopathy with normal EFs.[186] Abnormal GLS could identify those relatives at risk for EF deterioration and adverse events who would benefit from close follow-up. In patients with dilated cardiomyopathy who do not fulfil current indications for implantable cardioverter-defibrillator placement, both GLS and mechanical dispersion showed greater value than EF to identify patients at risk for ventricular arrhythmias.[80] Absolute GLS < 7.1% and mechanical dispersion more than 72 ms were associated with arrhythmic events during a median of 22 months' follow-up. Results from a recent CMR study demonstrated that LA strain could further improve risk stratification in dilated cardiomyopathy, incremental to LV GLS or late gadolinium enhancement.[187] In patients with dilated cardiomyopathy and LV conduction delays, segmental strain and work analysis has, next to the visual assessment of septal flash and apical rocking, a predictive value for cardiac resynchronization therapy response.[98,154,155]

Other rare cardiomyopathies. In storage diseases, such as Fabry disease and Danon disease, GLS is already impaired in early disease, before the development of LV hypertrophy, and it is related to worse clinical outcomes.[188-190] In Fabry disease, longitudinal strain is typically reduced and shows the characteristics pattern of postsystolic shortening, predominantly in the basal inferolateral segments, which are prone to replacement fibrosis.[191]

Distinguishing cardiomyopathies from athlete's heart. Differentiating pathologic LV hypertrophy or RV remodeling from that of physiological adaptation in athletes is challenging. GLS and RV strain in competitive athletes are usually relatively preserved.[192,193] In contrast, patients with hypertrophic cardiomyopathy show reduction in absolute GLS, and regional strain and may present significant heterogeneity of regional function (**Figure 23**).[194] Similarly, absolute global RV strain is typically reduced in patients with arrhythmogenic RV cardiomyopathy, whereas it is normal in athletes.[195] Nevertheless, the discriminatory ability of LV strain to distinguish an athletic heart from hypertensive heart disease is low, while LA strain might have added value.[194,196] Morphologic and tissue Doppler parameters as well as CMR data are complementary for a clinical distinction between athlete's hearts and cardiomyopathies.[194,195,197]

CARDIO-ONCOLOGY. Myocardial toxic effects from chemotherapy have become a leading cause of morbidity and mortality in cancer survivors. Therefore, protection of the heart during chemotherapy by risk assessment, evaluation of cardiac function prior to therapy, and monitoring during and after therapy are important. Recently published international guidelines summarize available evidence and provide recommendations for the optimal care of oncology patients with respect to cardiovascular health.[198]

According to the new guidelines,[198] cardiovascular imaging has an important role in identifying patients with subclinical cardiovascular disease, determining

FIGURE 24 LV Strains in Hypertension and HFpEF

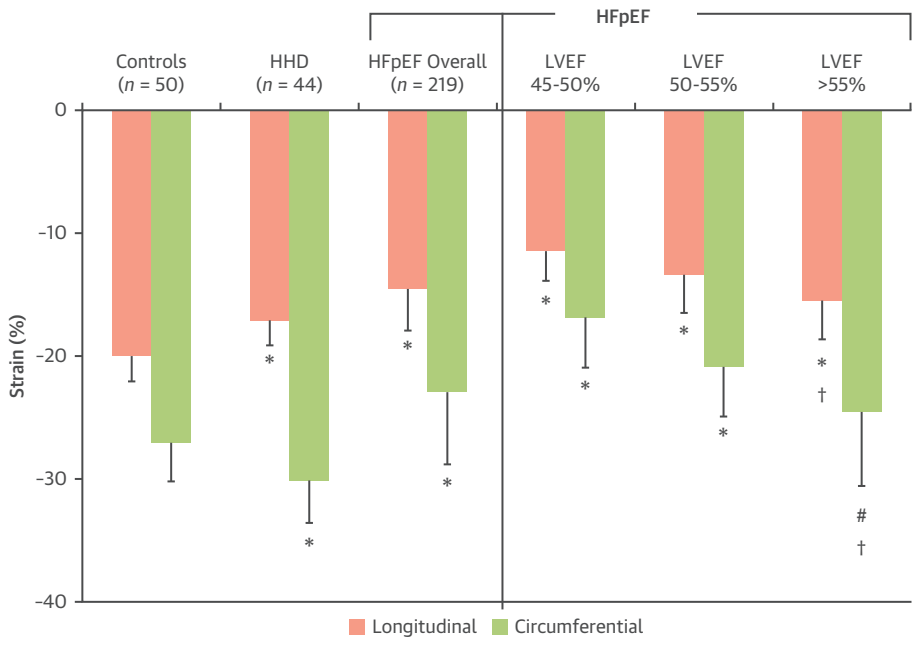

Left ventricular (LV) strain (longitudinal and circumferential) in hypertension and heart failure with preserved ejection fraction (HFpEF). (Left) Average longitudinal and circumferential systolic strain among normal control subjects, patients with hypertensive heart disease (HHD), and patients with HFpEF. (Right) LV strains in 3 categories of HFpEF on the basis of LV ejection fraction (LVEF). *$P < 0.0001$ vs control subjects and between patients with HHD and those with HFpEF overall for longitudinal strain and circumferential strain. †LVEF-adjusted $P < 0.001$ vs control subjects. #$P < 0.0002$ vs control subjects. Reproduced with permission from Kraigher-Krainer et al.[128]

the degree of preexisting cardiac comorbidity prior to decisions regarding cancer therapy, and serves as a reference for the identification of changes during treatment and long-term follow-up. As stated in the guidelines, echocardiography is the preferred imaging technique for baseline risk stratification, as it provides quantitative assessment of LV and RV function, chamber dilation, LV hypertrophy, regional wall motion abnormalities, diastolic function, valvular heart disease, pulmonary arterial pressure, and pericardial disease, which may influence the therapeutic decision. **Table 2** shows imaging criteria used in the guideline to define cancer therapy-related cardiovascular toxicity in patients with symptomatic as well as asymptomatic cardiac dysfunction. The criteria are based on the measurement of both EF and GLS.

Measurement of GLS is recommended in all patients with cancer undergoing echocardiography, if available. See the guidelines for details.[198] Further recommendations regarding the use of imaging in screening for cardiac dysfunction before, during, and after cancer therapy differ between therapeutic agents and pretreatment risk for complications.

VALVULAR HEART DISEASE. When evaluating patients with valvular disease, it is not only clinical condition and degree of valve dysfunction that matter but also the impact of valve dysfunction on the ventricle. Strain imaging and measurement of GLS are well suited to the evaluation of LV function in mitral and aortic valve disease and may in some cases detect myocardial dysfunction at an early stage, prior to a reduction in EF. Several studies suggest that strain may have added clinical value when evaluating LV function in patients with valve disease.[199-206]

In the current American College of Cardiology and American Heart Association clinical practice guidelines for the management of patients with valvular heart disease, GLS by STE is referred to as a method to identify LV dysfunction and remodeling and for risk stratification.[207] In asymptomatic patients with severe primary mitral regurgitation who require periodic transthoracic echocardiography to determine optimal timing of intervention, it is stated that GLS may be considered as an adjunct to guide timing of intervention. Furthermore, it is stated that GLS appears more sensitive than EF to detect LV dysfunction in patients with chronic mitral regurgitation and, as

FIGURE 25 Determinants of LA Strain

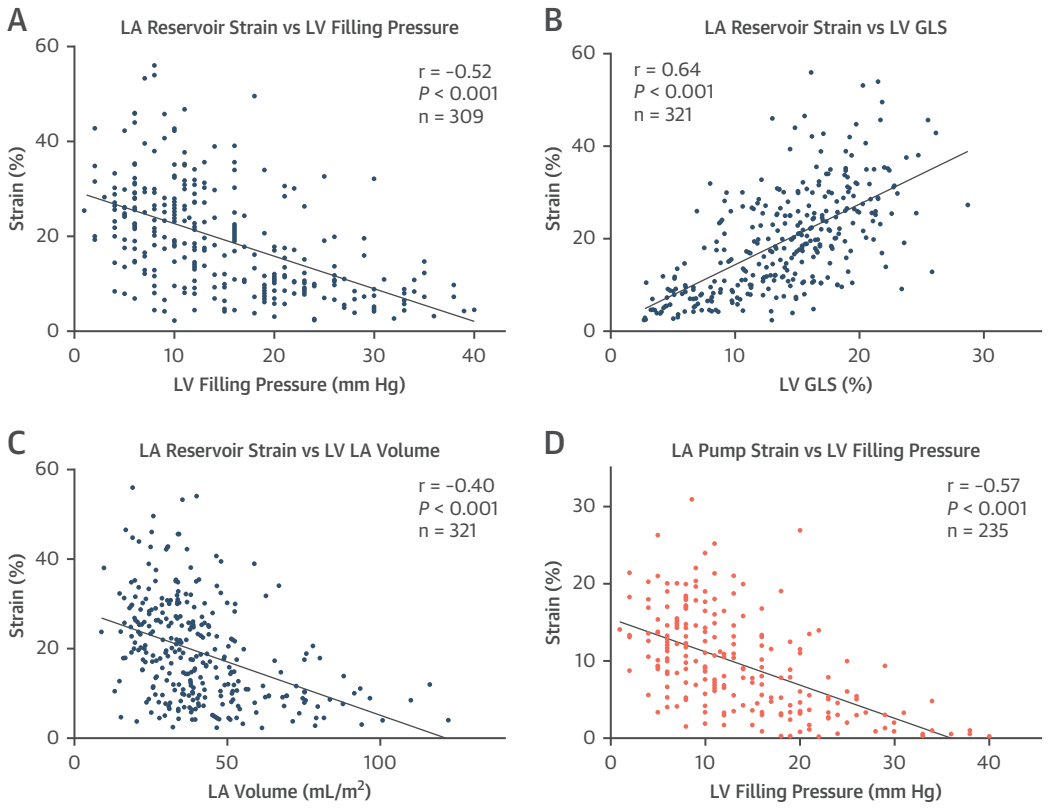

(A) LV filling pressure as a determinant of LA reservoir strain. (B) LV GLS as a determinant of LA reservoir strain. (C) LA volume as a determinant of LA reservoir strain. (D) LV filling pressure as a determinant of LA pump strain. Adapted under CC BY-NC 4.0 license from Inoue et al.[111] Abbreviations as in Figures 1, 12, and 19.

such, might give warning that LV function is declining before EF becomes abnormal.

In patients with aortic regurgitation, the European Society of Cardiology and European Association for Cardio-Thoracic Surgery guidelines for the management of valvular heart disease[208] recommend considering measuring GLS in patients with borderline LVEFs to help in the decision of timing for surgery. In patients with asymptomatic aortic stenosis, the measurement of GLS has a role. In addition to transvalvular velocities and the calculation of pressure gradient and aortic valve area, several diagnostic and prognostic parameters are recommended. This includes GLS as a measure of LV function, and a threshold of 15% for absolute GLS is suggested to identify patients with severe asymptomatic aortic stenosis who are at higher risk for clinical deterioration or premature mortality.

There is a need for additional clinical outcome studies on the role of strain imaging in valve patients. These studies should test if decisions based on the addition of strain imaging to quantify LV function result in better health outcomes. Whether GLS as a supplement to EF can improve decisions regarding the timing of valve interventions and surgery, measured as short- and long-term outcomes, should be tested.

HEART FAILURE WITH PRESERVED EF AND DIASTOLIC FUNCTION. LV GLS. In patients referred for suspected heart failure with preserved EF, the evaluation should include strain imaging by STE, as a large fraction of patients with heart failure with preserved EF have mild reductions in LV systolic function measured as GLS (Figure 24).[128,209] Therefore, when conventional parameters of diastolic function are nonconclusive, a finding of reduced absolute GLS strengthens the suspicion of heart failure with preserved EF. Furthermore, there are several specific cardiomyopathies with normal EF, for which segmental strain maps provide clues about the

substrate of heart failure with preserved EF. Some of these cardiomyopathies are discussed in other parts of this document (eg, cardiac amyloidosis).

LA strain by echocardiography. LA strain imaging was recently introduced as a method to evaluate LA function. Both LA reservoir strain and pump strain are closely related to LV mechanical function and may be used clinically as markers of LV filling pressure. Figure 25 illustrates the strong association between LA reservoir strain and LV systolic function measured as GLS. This association is explained by the tethering of both chambers to the mitral ring so that LV longitudinal shortening exerts a direct stretching effect on the atrium.[28,111,210] In addition to GLS, LV filling pressure is an independent determinant of LA reservoir strain. This may reflect stiffening of the atrial wall due to chronic remodeling in response to long-standing high LA pressures. In addition, because of the curvilinear shape of the LA passive pressure-volume curve, there is an increase in LA operative stiffness when LA pressure becomes elevated and therefore less increase in LA volume for a given increase in pressure. Finally, LA volume is a third independent determinant of LA reservoir strain.[210] This is because strain is relative change, and therefore a larger atrium can accommodate a given blood volume with less strain than a smaller atrium. As illustrated in Figure 25, LV GLS was the strongest determinant of reservoir strain, followed by LV filling pressure, and LA volume was only a weak determinant.

As illustrated in Figure 25, LA pump strain is also associated with LV filling pressure. This reflects that LA active shortening is determined by atrial preload, afterload, and contractility. LA preload may be represented by LA pressure at onset atrial contraction and LA afterload by LV end-diastolic pressure. The afterload dependency implies that the elevation of end-diastolic pressure leads to a reduction in LA pump strain. Furthermore, reduced LA contractility, as in atrial myopathy or atrial stunning following atrial arrhythmia, is associated with low values of LA pump strain, which are an important confounder when using LA pump strain to evaluate LV filling pressure.

Figure 25 illustrates determinants of LA reservoir and pump strain in a study that included patients with a wide range of cardiac diseases.[111]

LA pump strain has essentially similar correlation with LV filling pressure as reservoir strain, and when tested as predictors of LV filling pressure, accuracy was similar for the 2 strains.[111] A limitation of pump strain, however, is that measurements are sometimes not feasible when heart rate exceeds 100 to 105 beats/min, because of loss of the inflection point that defines the onset of atrial contraction. LA reservoir strain has the largest body of evidence supporting its diagnostic and prognostic value.[122,211-214] In atrial fibrillation, pump strain is absent, and there is need for further studies to determine the utility of measuring reservoir strain.[111] In a recent study it was suggested that LA reservoir strain may be used in combination with other echocardiographic parameters to assess LV filling pressure in atrial fibrillation.[215]

When using LA strain to assess diastolic function, elevated LV filling pressure is reflected in reductions in LA reservoir and pump strain (Figure 25).[216,217] Recent studies have shown that LA strain has a stronger correlation with LV filling pressure than LA volume index.[111] Whereas reservoir strain <19% to 23% is considered abnormally low, somewhat lower values are used as marker of elevated LV filling pressure. Values of reservoir strain <18% may be used as sign of elevated LV filling pressure, defined as pulmonary capillary wedge pressure >12 mm Hg.[111] When using pulmonary capillary wedge pressure ≥15 mm Hg as a criterion for elevated filling pressure, LA reservoir strain <16% may be used as sign of elevated filling pressure. For LA pump strain in young individuals (<40 years), the lower limit for normal reference values is markedly lower than in older individuals,[108] which complicates the use of this parameter. However, in middle-aged and older individuals, values of LA pump strain <8% are considered a sign of elevated LV filling pressure.[111] The association between LA strain and LV filling pressure is strongest in patients with reduced LVEFs.[111]

High normal absolute values for LA pump strain (>14%) in combination with normal LV GLS (>18%) identified normal LV filling pressure with high accuracy.[111] Apart from this combination of LA pump strain and GLS values, pump strain provides essentially similar information as reservoir strain.[111] Importantly, the associations between LA strains and LV filling pressure are not sufficiently strong to allow LA strain to be used as single parameter of for the assessment of LV filling pressure when making clinical decisions.[209] A recent study suggested using a combination of mitral E/A ratio and LA reservoir strain to differentiate between normal and elevated LV filling pressures in patients suspected of having precapillary pulmonary hypertension.[218]

LA strain by CMR. In addition to the role of CMR as reference method for measurement of LA volume, there is increasing clinical interest in using CMR FT to measure LA strain. LA strain by CMR FT has high feasibility and good reproducibility and is increasingly used in research studies.[219] As CMR FT provides

comprehensive and accurate diagnostic information on both LA volume and function, it may have a large potential as a method for use in clinical routine for the evaluation of patients suspected of heart failure as well as other cardiovascular disorders.

COMPARISON OF CMR AND ECHOCARDIOGRAPHY

The technical advantages and limitations of clinically used strain methods are summarized in **Table 1**. STE is considered an accurate and convenient method to assess myocardial strain and is widely available. It provides angle-independent and objective quantification of myocardial deformation. Despite this, echocardiography can be affected by poor acoustic windows, as in patients with lung disease and in obese patients. Although CMR techniques are independent of acoustic window, have larger fields of view, and allow good data acquisition independent of body habitus, they tend to have longer acquisition times and poorer spatial and temporal resolution. High cost, limited availability, and patient factors such as claustrophobia or implanted cardiac devices limit the widespread use of CMR FT.

As shown by Amzulescu et al[220] in a study comparing 2D STE and CMR tagging, overall accuracy was confirmed for both methods, as they agreed well when measuring global systolic longitudinal and circumferential strains. For regional strains, however, CMR tagging was superior to STE to detect infarcted segments. An additional advantage of CMR, when combined with late gadolinium enhancement, is diagnostic information regarding scarring and fibrosis, which can be obtained with little prolongation of the study.

Currently, CMR FT is the most widely applied CMR technique. In large clinical cohorts, CMR FT yields relatively good inter- and intrareader reproducibility for both LV and RV systolic and diastolic global parameters.[221] As with STE, strain values derived from CMR FT show a significant intervendor difference.[222] STE and CMR FT strain parameters show in general a good correlation, although CMR FT strain values tend to be lower.[223] In CMR images, tracking algorithms cannot rely on intramyocardial speckles as in STE, as the myocardium appears as a homogeneous structure. On the contrary, myocardial contours (endocardium or epicardium) are relatively sharp and detailed and are therefore used for tracking in CMR FT. Segmental strain measurements assessed using CMR FT show high variability due to a lack of trackable features within the myocardium and should not be used in the clinic.

VENDOR DEPENDENCY OF STRAIN MEASUREMENTS

For both echocardiography and CMR, strain measurements are subject to clinically relevant intervendor variability.[30,40,95,222,224] In an intervendor comparison of strain by STE, GLS values were reported to differ up to 3.7 percentage points (strain units)[40] among different vendors, indicating differing performance of different tracking algorithms. A very recent repetition of this study showed a favorable convergence of measurements of clinical strain tracking software solutions.[225] Furthermore, different tracking approaches (endo- and/or epicardial vs full wall tracking) lead to different results.[40,88] As illustrated in **Figure 18B**, an ROI that includes only the endocardium and the inner layer of the LV wall gives higher absolute strain values than an ROI that includes the entire wall thickness (full wall tracking). Normative recommendations from professional societies based on available evidence are needed to overcome this problem.

Limited data exist regarding vendor differences in RV and atrial strain assessment. So far, intervendor variability does not seem to dominate over the measurement variability of the parameters,[95] but larger studies on this issue are ongoing.

Echocardiographic 3D LV data acquisition and postprocessing are strongly vendor specific. The intervendor variability of strain measurements is very high, and the degree of variability varies among different 3D strain parameters, with the highest variability for twist and the lowest for GLS.[30]

CMR FT has limited accuracy in regional strain analysis, whereas GLS measurements show acceptable accuracy. Nevertheless, intervendor differences of CMR global strain measurements are significant, and repetitive measurements should be compared only when performed using the same vendor's equipment and software.[222,226] Segmental strain analysis with CMR cannot be recommended.

FUTURE DIRECTIONS

The clinical application of 2D strain imaging has grown tremendously in recent years, and measuring global strain by echocardiography has become widely adopted as A standard parameter for the assessment of myocardial function. Efforts of the imaging societies to provide guidance on how strain should be assessed in a standardized manner may have contributed to this success.[23,24] However, several challenges remain. Most important, companies still use different default settings for strain acquisition

HIGHLIGHTS

- LV GLS by STE is a sensitive method to diagnose mild systolic dysfunction.
- LV segmental strain maps can provide diagnostic clues in several cardiomyopathies.
- LA strain is a strong marker of LV filling pressure.
- Myocardial strain imaging by STE and CMR is ready for clinical implementation.

and reporting. A new joint consensus document of the European Association of Cardiovascular Imaging and the American Society of Echocardiography is in preparation that will further clarify the recommendation from the user's perspective. Furthermore, measurement of strain in single LV segments has relatively high variability. Potentially, analytical approaches that focus on the shape of segmental strain curves and supported by artificial intelligence will be more useful than just measuring a single segmental strain value. Furthermore, segmental strain maps, which are already implemented in the study of patients with suspected cardiomyopathy, may have potential in the diagnostic work-up of other cardiac diseases as well.

The potential of using myocardial strain rate in clinical routine is limited by the frame rate of the technology. Technological advancements, such as high-frame rate imaging,[35] may help overcoming this limitation. This would allow the reliable assessment of strain rate and provide a parameter that is more closely linked to contractility than strain. Furthermore, short-lived events, as during LV isovolumetric phases, and cardiac function during stress echocardiography could be better analyzed. Current experience with high-frame rate STE is limited to a few research laboratories, but first attempts have been made to translate the technology to clinical practice.

Both 3D STE and CMR strain imaging have the potential to overcome some limitations of 2D STE in the assessment of complex cardiac mechanics. The establishment of normal reference values are essential before the widespread clinical use of 3D STE and CMR strain imaging.

Advances in artificial intelligence technology will further improve reproducibility and workflow efficiency of CMR and echocardiographic measurements, including strain. Artificial intelligence-automated segmentation of the LV myocardium for FT or DENSE-derived strains provide comparable strain values as manual segmentation.[227,228] Fully automated measurements of GLS using deep learning technology remove the need for user interaction and may help increasing efficiency, precision, and reproducibility of strain measurements.[229,230] Open-source, vendor-independent artificial intelligence-based strain measurement approaches are promising[231] and might promote the widespread use of strain imaging in clinical practice. Furthermore, artificial intelligence algorithms integrating strain information may in the future aid in determination of diagnosis and prognosis of patients.[159,232,233]

Future studies should explore how strain imaging can be combined efficiently with imaging of cardiac structure, myocardial perfusion, and metabolism. Furthermore, the implementation of strain imaging in point-of-care settings and in first-line health care is a growing demand that should be met by the use of semiautomated approaches, artificial intelligence, and telemedicine guidance for image interpretation.

Ultimately, the clinical value of applying strain imaging technologies depends upon their contribution to patient management in terms of cost efficiency and impact on health outcome. Relatively few of the large number of imaging modalities presently available have proven added value on top of conventional and simpler diagnostic methods. There is a need for prospective clinicals studies that explore and define the added value of strain imaging when making clinical decisions.

FUNDING SUPPORT AND AUTHOR DISCLOSURES

Dr Rider is supported by a British Heart Foundation Senior Clinical Research Fellowship (FS/SCRF/22/32014). Dr Valkovič is supported by a Sir Henry Dale Fellowship from The Wellcome Trust and Royal Society (221805/Z/20/Z). Both authors acknowledge the support of the British Heart Foundation Center of Research Excellence Oxford. Dr Smiseth is a coinventor of "Method for Myocardial Segment Work Analysis" and holds a patent on "Estimation of Blood Pressure in the Heart;" and has received a speaker honorarium from GE Healthcare. Dr Voigt has received speaker honoraria and/or consultancy fees from GE Healthcare, Philips Healthcare, and TomTec Imaging Systems. All other authors have reported that they have no relationships relevant to the contents of this paper to disclose.

ADDRESS FOR CORRESPONDENCE: Dr Otto A. Smiseth, Institute for Surgical Research, Division of Cardiovascular and Pulmonary Diseases, Oslo University Hospital, Rikshospitalet, and University of Oslo, Trondheimsveien 235, NO-0514 Oslo, Norway. E-mail: otto.smiseth@gmail.com.

REFERENCES

1. Bugge-Asperheim B, Leraand S, Kiil F. Local dimensional changes of the myocardium measured by ultrasonic technique. *Scand J Clin Lab Invest*. 1969;24:361-371.

2. Waldman LK, Fung YC, Covell JW. Transmural myocardial deformation in the canine left ventricle. Normal in vivo three-dimensional finite strains. *Circ Res*. 1985;57:152-163.

3. Zerhouni EA, Parish DM, Rogers WJ, Yang A, Shapiro EP. Human heart: tagging with MR imaging—a method for noninvasive assessment of myocardial motion. *Radiology*. 1988;169:59-63.

4. Kramer CM, Lima JA, Reichek N, et al. Regional differences in function within noninfarcted myocardium during left ventricular remodeling. *Circulation*. 1993;88:1279-1288.

5. Axel L, Dougherty L. MR imaging of motion with spatial modulation of magnetization. *Radiology*. 1989;171:841-845.

6. Clark NR, Reichek N, Bergey P, et al. Circumferential myocardial shortening in the normal human left ventricle. Assessment by magnetic resonance imaging using spatial modulation of magnetization. *Circulation*. 1991;84:67-74.

7. Kramer CM, Reichek N, Ferrari VA, Theobald T, Dawson J, Axel L. Regional heterogeneity of function in hypertrophic cardiomyopathy. *Circulation*. 1994;90:186-194.

8. Hennig J, Markl M, Schneider B, Peschl S. Regional myocardial function with tissue phase mapping. *MAGMA*. 1998;6:145-146.

9. Jung B, Foll D, Bottler P, Petersen S, Hennig J, Markl M. Detailed analysis of myocardial motion in volunteers and patients using high-temporal-resolution MR tissue phase mapping. *J Magn Reson Imaging*. 2006;24:1033-1039.

10. Heimdal A, Støylen A, Torp H, Skjaerpe T. Real-time strain rate imaging of the left ventricle by ultrasound. *J Am Soc Echocardiogr*. 1998;11:1013-1019.

11. Urheim S, Edvardsen T, Torp H, Angelsen B, Smiseth OA. Myocardial strain by Doppler echocardiography. Validation of a new method to quantify regional myocardial function. *Circulation*. 2000;102:1158-1164.

12. Bohs LN, Trahey GE. A novel method for angle independent ultrasonic imaging of blood flow and tissue motion. *IEEE Trans Biomed Eng*. 1991;38:280-286.

13. Langeland S, D'Hooge J, Claessens T, et al. RF-based two-dimensional cardiac strain estimation: a validation study in a tissue-mimicking phantom. *IEEE Trans Ultrason Ferroelectr Freq Control*. 2004;51:1537-1546.

14. Leitman M, Lysyansky P, Sidenko S, et al. Two-dimensional strain-a novel software for real-time quantitative echocardiographic assessment of myocardial function. *J Am Soc Echocardiogr*. 2004;17:1021-1029.

15. Amundsen BH, Helle-Valle T, Edvardsen T, et al. Noninvasive myocardial strain measurement by speckle tracking echocardiography: validation against sonomicrometry and tagged magnetic resonance imaging. *J Am Coll Cardiol*. 2006;47:789-793.

16. Auger DA, Bilchick KC, Gonzalez JA, et al. Imaging left-ventricular mechanical activation in heart failure patients using cine DENSE MRI: validation and implications for cardiac resynchronization therapy. *J Magn Reson Imaging*. 2017;46:887-896.

17. Gupta V, Lantz J, Henriksson L, et al. Automated three-dimensional tracking of the left ventricular myocardium in time-resolved and dose-modulated cardiac CT images using deformable image registration. *J Cardiovasc Comput Tomogr*. 2018;12:139-148.

18. Ibrahim el SH. Myocardial tagging by cardiovascular magnetic resonance: evolution of techniques—pulse sequences, analysis algorithms, and applications. *J Cardiovasc Magn Reson*. 2011;13:36.

19. Hor KN, Baumann R, Pedrizzetti G, et al. Magnetic resonance derived myocardial strain assessment using feature tracking. *J Vis Exp*. 2011;(48):2356.

20. Mor-Avi V, Lang RM, Badano LP, et al. Current and evolving echocardiographic techniques for the quantitative evaluation of cardiac mechanics: ASE/EAE consensus statement on methodology and indications endorsed by the Japanese Society of Echocardiography. *Eur J Echocardiogr*. 2011;12:167-205.

21. Jasaityte R, Heyde B, D'Hooge J. Current state of three-dimensional myocardial strain estimation using echocardiography. *J Am Soc Echocardiogr*. 2013;26:15-28.

22. Claus P, Omar AMS, Pedrizzetti G, Sengupta PP, Nagel E. Tissue tracking technology for assessing cardiac mechanics: principles, normal values, and clinical applications. *JACC Cardiovasc Imaging*. 2015;8:1444-1460.

23. Voigt JU, Pedrizzetti G, Lysyansky P, et al. Definitions for a common standard for 2D speckle tracking echocardiography: consensus document of the EACVI/ASE/Industry Task Force to Standardize Deformation Imaging. *Eur Heart J Cardiovasc Imaging*. 2015;16:1-11.

24. Badano LP, Kolias TJ, Muraru D, et al. Standardization of left atrial, right ventricular, and right atrial deformation imaging using two-dimensional speckle tracking echocardiography: a consensus document of the EACVI/ASE/Industry Task Force to Standardize Deformation Imaging. *Eur Heart J Cardiovasc Imaging*. 2018;19:591-600.

25. Dobrovie M, Bezy S, Unlu S, et al. How does regional hypertrophy affect strain measurements with different speckle-tracking methods? *J Am Soc Echocardiogr*. 2019;32:1444-1450.

26. Unlu S, Duchenne J, Mirea O, et al. Impact of apical foreshortening on deformation measurements: a report from the EACVI-ASE Strain Standardization Task Force. *Eur Heart J Cardiovasc Imaging*. 2020;21:337-343.

27. Saito K, Okura H, Watanabe N, et al. Comprehensive evaluation of left ventricular strain using speckle tracking echocardiography in normal adults: comparison of three-dimensional and two-dimensional approaches. *J Am Soc Echocardiogr*. 2009;22:1025-1030.

28. Voigt JU, Cvijic M. 2- and 3-Dimensional myocardial strain in cardiac health and disease. *JACC Cardiovasc Imaging*. 2019;12:1849-1863.

29. Negishi K, Negishi T, Agler DA, Plana JC, Marwick TH. Role of temporal resolution in selection of the appropriate strain technique for evaluation of subclinical myocardial dysfunction. *Echocardiography*. 2012;29:334-339.

30. Gayat E, Ahmad H, Weinert L, Lang RM, Mor-Avi V. Reproducibility and inter-vendor variability of left ventricular deformation measurements by three-dimensional speckle-tracking echocardiography. *J Am Soc Echocardiogr*. 2011;24:878-885.

31. Ferferieva V, Van den Bergh A, Claus P, et al. The relative value of strain and strain rate for defining intrinsic myocardial function. *Am J Physiol Heart Circ Physiol*. 2012;302:H188-H195.

32. Voigt JU, Exner B, Schmiedehausen K, et al. Strain-rate imaging during dobutamine stress echocardiography provides objective evidence of inducible ischemia. *Circulation*. 2003;107:2120-2126.

33. Lyseggen E, Rabben SI, Skulstad H, Urheim S, Risoe C, Smiseth OA. Myocardial acceleration during isovolumic contraction: relationship to contractility. *Circulation*. 2005;111:1362-1369.

34. Remme EW, Lyseggen E, Helle-Valle T, et al. Mechanisms of preejection and postejection velocity spikes in left ventricular myocardium: interaction between wall deformation and valve events. *Circulation*. 2008;118:373-380.

35. Orlowska M, Bezy S, Ramalli A, Voigt JU, D'Hooge J. High-Frame-Rate Speckle Tracking for Echocardiographic Stress Testing. *Ultrasound Med Biol*. 2022;48:1644-1651.

36. Orlowska M, Ramalli A, Petrescu A, et al. A novel 2-D speckle tracking method for high-frame-rate echocardiography. *IEEE Trans Ultrason Ferroelectr Freq Control*. 2020;67:1764-1775.

37. Risum N, Ali S, Olsen NT, et al. Variability of global left ventricular deformation analysis using vendor dependent and independent two-dimensional speckle-tracking software in adults. *J Am Soc Echocardiogr*. 2012;25:1195-1203.

38. Yingchoncharoen T, Agarwal S, Popovic ZB, Marwick TH. Normal ranges of left ventricular strain: a meta-analysis. *J Am Soc Echocardiogr*. 2013;26:185-191.

39. Smith BC, Dobson G, Dawson D, Charalampopoulos A, Grapsa J, Nihoyannopoulos P. Three-dimensional speckle tracking of the right ventricle: toward optimal

quantification of right ventricular dysfunction in pulmonary hypertension. *J Am Coll Cardiol*. 2014;64:41–51.

40. Farsalinos KE, Daraban AM, Unlu S, Thomas JD, Badano LP, Voigt JU. Head-to-head comparison of global longitudinal strain measurements among nine different vendors: the EACVI/ASE Inter-Vendor Comparison Study. *J Am Soc Echocardiogr*. 2015;28:1171–1181.e2.

41. Pathan F, D'Elia N, Nolan MT, Marwick TH, Negishi K. Normal ranges of left atrial strain by speckle-tracking echocardiography: a systematic review and meta-analysis. *J Am Soc Echocardiogr*. 2017;30:59–70.e8.

42. Genovese D, Mor-Avi V, Palermo C, et al. Comparison between four-chamber and right ventricular-focused views for the quantitative evaluation of right ventricular size and function. *J Am Soc Echocardiogr*. 2019;32:484–494.

43. Perez de Isla L, Balcones DV, Fernandez-Golfin C, et al. Three-dimensional-wall motion tracking: a new and faster tool for myocardial strain assessment: comparison with two-dimensional-wall motion tracking. *J Am Soc Echocardiogr*. 2009;22:325–330.

44. Badano LP, Cucchini U, Muraru D, Al Nono O, Sarais C, Iliceto S. Use of three-dimensional speckle tracking to assess left ventricular myocardial mechanics: inter-vendor consistency and reproducibility of strain measurements. *Eur Heart J Cardiovasc Imaging*. 2013;14:285–293.

45. Ishizu T, Seo Y, Atsumi A, et al. Global and regional right ventricular function assessed by novel three-dimensional speckle-tracking echocardiography. *J Am Soc Echocardiogr*. 2017;30:1203–1213.

46. Santoro C, Arpino G, Esposito R, et al. 2D and 3D strain for detection of subclinical anthracycline cardiotoxicity in breast cancer patients: a balance with feasibility. *Eur Heart J Cardiovasc Imaging*. 2017;18:930–936.

47. Wang J, Khoury DS, Yue Y, Torre-Amione G, Nagueh SF. Left ventricular untwisting rate by speckle tracking echocardiography. *Circulation*. 2007;116:2580–2586.

48. Opdahl A, Remme EW, Helle-Valle T, Edvardsen T, Smiseth OA. Myocardial relaxation, restoring forces, and early-diastolic load are independent determinants of left ventricular untwisting rate. *Circulation*. 2012;126:1441–1451.

49. Buchalter MB, Weiss JL, Rogers WJ, et al. Noninvasive quantification of left ventricular rotational deformation in normal humans using magnetic resonance imaging myocardial tagging. *Circulation*. 1990;81:1236–1244.

50. Helle-Valle T, Crosby J, Edvardsen T, et al. New noninvasive method for assessment of left ventricular rotation: speckle tracking echocardiography. *Circulation*. 2005;112:3149–3156.

51. Notomi Y, Lysyansky P, Setser RM, et al. Measurement of ventricular torsion by two-dimensional ultrasound speckle tracking imaging. *J Am Coll Cardiol*. 2005;45:2034–2041.

52. Sugimoto T, Dulgheru R, Bernard A, et al. Echocardiographic reference ranges for normal left ventricular 2D strain: results from the EACVI NORRE study. *Eur Heart J Cardiovasc Imaging*. 2017;18:833–840.

53. Opdahl A, Helle-Valle T, Remme EW, et al. Apical rotation by speckle tracking echocardiography: a simplified bedside index of left ventricular twist. *J Am Soc Echocardiogr*. 2008;21:1121–1128.

54. Hong SJ, Shim CY, Kim D, et al. Dynamic change in left ventricular apical back rotation: a marker of diastolic suction with exercise. *Eur Heart J Cardiovasc Imaging*. 2018;19:12–19.

55. Sengupta PP, Tajik AJ, Chandrasekaran K, Khandheria BK. Twist mechanics of the left ventricle: principles and application. *JACC Cardiovasc Imaging*. 2008;1:366–376.

56. Unlu S, Mirea O, Pagourelias ED, et al. Layer-specific segmental longitudinal strain measurements: capability of detecting myocardial scar and differences in feasibility, accuracy, and reproducibility, among four vendors. A report from the EACVI-ASE Strain Standardization Task Force. *J Am Soc Echocardiogr*. 2019;32:624–632.e11.

57. Weidemann F, Jamal F, Sutherland GR, et al. Myocardial function defined by strain rate and strain during alterations in inotropic states and heart rate. *Am J Physiol Heart Circ Physiol*. 2002;283:H792–H799.

58. Donal E, Bergerot C, Thibault H, et al. Influence of afterload on left ventricular radial and longitudinal systolic functions: a two-dimensional strain imaging study. *Eur J Echocardiogr*. 2009;10:914–921.

59. Lumens J, Prinzen FW, Delhaas T. Longitudinal strain: "think globally, track locally.". *JACC Cardiovasc Imaging*. 2015;8:1360–1363.

60. Mentias A, Naji P, Gillinov AM, et al. Strain echocardiography and functional capacity in asymptomatic primary mitral regurgitation with preserved ejection fraction. *J Am Coll Cardiol*. 2016;68:1974–1986.

61. Negishi K, Borowski AG, Popovic ZB, et al. Effect of gravitational gradients on cardiac filling and performance. *J Am Soc Echocardiogr*. 2017;30:1180–1188.

62. Stokke TM, Hasselberg NE, Smedsrud MK, et al. Geometry as a confounder when assessing ventricular systolic function: comparison between ejection fraction and strain. *J Am Coll Cardiol*. 2017;70:942–954.

63. Genovese D, Singh A, Volpato V, et al. Load dependency of left atrial strain in normal subjects. *J Am Soc Echocardiogr*. 2018;31:1221–1228.

64. Sletten OJ, Aalen JM, Smiseth OA, et al. Mental stress reduces left ventricular strain: can it lead to misinterpretation of cancer therapy-related cardiac dysfunction? *J Am Soc Echocardiogr*. 2024;37(5):564–566.

65. Støylen A, Mølmen HE, Dalen H. Regional motion of the AV-plane is related to the cardiac anatomy and deformation of the AV-plane. Data from the HUNT study. *Clin Physiol Funct Imaging*. 2023;43(6):453–462.

66. Støylen A, Mølmen HE, Dalen H. Relation between mitral annular plane systolic excursion and global longitudinal strain in normal subjects: the HUNT study. *Echocardiography*. 2018;35:603–610.

67. Johansson Blixt P, Chew MS, Ahman R, et al. Left ventricular longitudinal wall fractional shortening accurately predicts longitudinal strain in critically ill patients with septic shock. *Ann Intensive Care*. 2021;11:52.

68. Russell K, Eriksen M, Aaberge L, et al. A novel clinical method for quantification of regional left ventricular pressure-strain loop area: a non-invasive index of myocardial work. *Eur Heart J*. 2012;33:724–733.

69. Suga H. Total mechanical energy of a ventricle model and cardiac oxygen consumption. *Am J Physiol*. 1979;236:H498–H505.

70. Tyberg JV, Forrester JS, Wyatt HL, Goldner SJ, Parmley WW, Swan HJ. An analysis of segmental ischemic dysfunction utilizing the pressure-length loop. *Circulation*. 1974;49:748–754.

71. Russell K, Eriksen M, Aaberge L, et al. Assessment of wasted myocardial work: a novel method to quantify energy loss due to uncoordinated left ventricular contractions. *Am J Physiol Heart Circ Physiol*. 2013;305:H996–H1003.

72. Batzner A, Hahn P, Morbach C, et al. Non-invasive estimation of left ventricular systolic peak pressure: a prerequisite to calculate myocardial work in hypertrophic obstructive cardiomyopathy. *Eur Heart J Cardiovasc Imaging*. 2024;25:213–219.

73. Fortuni F, Butcher SC, van der Kley F, et al. Left ventricular myocardial work in patients with severe aortic stenosis. *J Am Soc Echocardiogr*. 2021;34:257–266.

74. Jain R, Bajwa T, Roemer S, et al. Myocardial work assessment in severe aortic stenosis undergoing transcatheter aortic valve replacement. *Eur Heart J Cardiovasc Imaging*. 2021;22:715–721.

75. Ribic D, Remme EW, Smiseth OA, et al. Non-invasive myocardial work in aortic stenosis—validation and improvement of left ventricular pressure estimation. *Eur Heart J Cardiovasc Imaging*. 2024;25(2):201–212.

76. Duchenne J, Turco A, Unlu S, et al. Left ventricular remodeling results in homogenization of myocardial work distribution. *Circ Arrhythm Electrophysiol*. 2019;12:e007224.

77. Manganaro R, Marchetta S, Dulgheru R, et al. Echocardiographic reference ranges for normal non-invasive myocardial work indices: results from the EACVI NORRE study. *Eur Heart J Cardiovasc Imaging*. 2019;20:582–590.

78. Haugaa KH, Amlie JP, Berge KE, Leren TP, Smiseth OA, Edvardsen T. Transmural differences in myocardial contraction in long-QT syndrome: mechanical consequences of ion channel dysfunction. *Circulation*. 2010;122, 1355-1263.

79. Leren IS, Hasselberg NE, Saberniak J, et al. Cardiac mechanical alterations and genotype specific differences in subjects with long QT syndrome. *JACC Cardiovasc Imaging*. 2015;8:501–510.

80. Haugaa KH, Goebel B, Dahlslett T, et al. Risk assessment of ventricular arrhythmias in patients with nonischemic dilated cardiomyopathy by strain echocardiography. *J Am Soc Echocardiogr*. 2012;25:667–673.

81. Ersboll M, Valeur N, Andersen MJ, et al. Early echocardiographic deformation analysis for the prediction of sudden cardiac death and life-

threatening arrhythmias after myocardial infarction. *JACC Cardiovasc Imaging*. 2013;6:851–860.

82. Haugaa KH, Grenne BL, Eek CH, et al. Strain echocardiography improves risk prediction of ventricular arrhythmias after myocardial infarction. *JACC Cardiovasc Imaging*. 2013;6:841–850.

83. Reisner SA, Lysyansky P, Agmon Y, Mutlak D, Lessick J, Friedman Z. Global longitudinal strain: a novel index of left ventricular systolic function. *J Am Soc Echocardiogr*. 2004;17:630–633.

84. D'Elia N, Caselli S, Kosmala W, et al. Normal global longitudinal strain: an individual patient meta-analysis. *JACC Cardiovasc Imaging*. 2020;13:167–169.

85. Asch FM, Miyoshi T, Addetia K, et al. Similarities and differences in left ventricular size and function among races and nationalities: results of the World Alliance Societies of Echocardiography Normal Values Study. *J Am Soc Echocardiogr*. 2019;32:1396–1406.e2.

86. Skaarup KG, Lassen MCH, Johansen ND, et al. Age- and sex-based normal values of layer-specific longitudinal and circumferential strain by speckle tracking echocardiography: the Copenhagen City Heart Study. *Eur Heart J Cardiovasc Imaging*. 2022;23:629–640.

87. Nyberg J, Jakobsen EO, Ostvik A, et al. Echocardiographic reference ranges of global longitudinal strain for all cardiac chambers using guideline-directed dedicated views. *JACC Cardiovasc Imaging*. 2023;16:1516–1531.

88. Unlu S, Mirea O, Duchenne J, et al. Comparison of feasibility, accuracy, and reproducibility of layer-specific global longitudinal strain measurements among five different vendors: a report from the EACVI-ASE Strain Standardization Task Force. *J Am Soc Echocardiogr*. 2018;31:374–380.e1.

89. Mirea O, Pagourelias ED, Duchenne J, et al. Variability and reproducibility of segmental longitudinal strain measurement: a report from the EACVI-ASE Strain Standardization Task Force. *JACC Cardiovasc Imaging*. 2018;11:15–24.

90. Negishi K, Negishi T, Kurosawa K, et al. Practical guidance in echocardiographic assessment of global longitudinal strain. *JACC Cardiovasc Imaging*. 2015;8:489–492.

91. Badano LP, Muraru D, Parati G, Haugaa K, Voigt JU. How to do right ventricular strain. *Eur Heart J Cardiovasc Imaging*. 2020;21:825–827.

92. Voigt JU, Malaescu GG, Haugaa K, Badano L. How to do LA strain. *Eur Heart J Cardiovasc Imaging*. 2020;21:715–717.

93. Rosner A, Barbosa D, Aarsaether E, Kjonas D, Schirmer H, D'Hooge J. The influence of frame rate on two-dimensional speckle-tracking strain measurements: a study on silico-simulated models and images recorded in patients. *Eur Heart J Cardiovasc Imaging*. 2015;16:1137–1147.

94. Mada RO, Lysyansky P, Daraban AM, Duchenne J, Voigt JU. How to define end-diastole and end-systole? Impact of timing on strain measurements. *JACC Cardiovasc Imaging*. 2015;8:148–157.

95. Il'Giovine ZJ, Mulder H, Chiswell K, et al. Right ventricular longitudinal strain reproducibility using vendor-dependent and vendor-independent software. *J Am Soc Echocardiogr*. 2018;31:721–732.e5.

96. Jamal F, Kukulski T, Sutherland GR, et al. Can changes in systolic longitudinal deformation quantify regional myocardial function after an acute infarction? An ultrasonic strain rate and strain study. *J Am Soc Echocardiogr*. 2002;15:723–730.

97. Leenders GE, Lumens J, Cramer MJ, et al. Septal deformation patterns delineate mechanical dyssynchrony and regional differences in contractility: analysis of patient data using a computer model. *Circ Heart Fail*. 2012;5:87–96.

98. Risum N, Jons C, Olsen NT, et al. Simple regional strain pattern analysis to predict response to cardiac resynchronization therapy: rationale, initial results, and advantages. *Am Heart J*. 2012;163:697–704.

99. Calle S, Duchenne J, Beela AS, et al. Clinical and experimental evidence for a strain-based classification of left bundle branch block-induced cardiac remodeling. *Circ Cardiovasc Imaging*. 2022;15:e014296.

100. Mirea O, Duchenne J, Voigt JU. Comparison between nondedicated and novel dedicated tracking tool for right ventricular and left atrial strain. *J Am Soc Echocardiogr*. 2022;35:419–425.

101. Hoit BD. Left atrial size and function: role in prognosis. *J Am Coll Cardiol*. 2014;63:493–505.

102. Hoit BD, Gabel M. Influence of left ventricular dysfunction on the role of atrial contraction: an echocardiographic-hemodynamic study in dogs. *J Am Coll Cardiol*. 2000;36:1713–1719.

103. Giubertoni A, Boggio E, Ubertini E, et al. Atrial conduit function quantitation pre-cardioversion predicts early arrhythmia recurrence in persistent atrial fibrillation patients. *J Cardiovasc Med (Hagerstown)*. 2019;20:169–179.

104. Bowman AW, Kovacs SJ. Left atrial conduit volume is generated by deviation from the constant-volume state of the left heart: a combined MRI-echocardiographic study. *Am J Physiol Heart Circ Physiol*. 2004;286:H2416–H2424.

105. Nappo R, Degiovanni A, Bolzani V, et al. Quantitative assessment of atrial conduit function: a new index of diastolic dysfunction. *Clin Res Cardiol*. 2016;105:17–28.

106. Smiseth OA, Baron T, Marino PN, Marwick TH, Flachskampf FA. Imaging of the left atrium: pathophysiology insights and clinical utility. *Eur Heart J Cardiovasc Imaging*. 2021;23:2–13.

107. Gillebert TC, Smiseth OA. Left atrial reservoir strain in prognosis of heart failure. Time for getting terminology straight. *Eur Heart J Cardiovasc Imaging*. 2024;25(3):325–327.

108. Singh A, Carvalho Singulane C, Miyoshi T, et al. Normal values of left atrial size and function and the impact of age: results of the World Alliance Societies of Echocardiography Study. *J Am Soc Echocardiogr*. 2022;35:154–164.e3.

109. Cameli M, Lisi M, Mondillo S, et al. Left atrial longitudinal strain by speckle tracking echocardiography correlates well with left ventricular filling pressures in patients with heart failure. *Cardiovasc Ultrasound*. 2010;8:14.

110. Cameli M, Miglioranza MH, Magne J, et al. Multicentric Atrial Strain Comparison Between Two Different Modalities: MASCOT HIT study. *Diagnostics (Basel)*. 2020;10(11):946.

111. Inoue K, Khan FH, Remme EW, et al. Determinants of left atrial reservoir and pump strain and use of atrial strain for evaluation of left ventricular filling pressure. *Eur Heart J Cardiovasc Imaging*. 2021;23:61–70.

112. Singh A, Medvedofsky D, Mediratta A, et al. Peak left atrial strain as a single measure for the non-invasive assessment of left ventricular filling pressures. *Int J Cardiovasc Imaging*. 2019;35:23–32.

113. Santoro C, Donal E, Magne J, et al. Inter-center reproducibility of standard and advanced echocardiographic parameters in the EACVI-AFib echo registry. *Echocardiography*. 2023;40:775–783.

114. Muraru D, Haugaa K, Donal E, et al. Right ventricular longitudinal strain in the clinical routine: a state-of-the-art review. *Eur Heart J Cardiovasc Imaging*. 2022;23:898–912.

115. Sanz J, Sanchez-Quintana D, Bossone E, Bogaard HJ, Naeije R. Anatomy, function, and dysfunction of the right ventricle: *JACC* state-of-the-art review. *J Am Coll Cardiol*. 2019;73:1463–1482.

116. Morris DA, Krisper M, Nakatani S, et al. Normal range and usefulness of right ventricular systolic strain to detect subtle right ventricular systolic abnormalities in patients with heart failure: a multicentre study. *Eur Heart J Cardiovasc Imaging*. 2017;18:212–223.

117. Park JH, Choi JO, Park SW, et al. Normal references of right ventricular strain values by two-dimensional strain echocardiography according to the age and gender. *Int J Cardiovasc Imaging*. 2018;34:177–183.

118. Addetia K, Miyoshi T, Citro R, et al. Two-dimensional echocardiographic right ventricular size and systolic function measurements stratified by sex, age, and ethnicity: results of the World Alliance of Societies of Echocardiography Study. *J Am Soc Echocardiogr*. 2021;34:1148–1157.e1.

119. Vitarelli A, Mangieri E, Terzano C, et al. Three-dimensional echocardiography and 2D-3D speckle-tracking imaging in chronic pulmonary hypertension: diagnostic accuracy in detecting hemodynamic signs of right ventricular (RV) failure. *J Am Heart Assoc*. 2015;4:e001584.

120. Li Y, Zhang L, Gao Y, et al. Comprehensive assessment of right ventricular function by three-dimensional speckle-tracking echocardiography: comparisons with cardiac magnetic resonance imaging. *J Am Soc Echocardiogr*. 2021;34:472–482.

121. Hasselberg NE, Kagiyama N, Soyama Y, et al. The Prognostic value of right atrial strain imaging in patients with precapillary pulmonary hypertension. *J Am Soc Echocardiogr*. 2021;34:851–861.e1.

122. Tomaselli M, Badano LP, Cannone V, et al. Incremental value of right atrial strain analysis to predict atrial fibrillation recurrence after electrical cardioversion. *J Am Soc Echocardiogr*. 2023;36:945–955.

123. Krittanawong C, Maitra NS, Hassan Virk HU, et al. Normal ranges of right atrial strain: a systematic review and meta-analysis. *JACC Cardiovasc Imaging*. 2023;16:282–294.

124. Fang ZY, Yuda S, Anderson V, Short L, Case C, Marwick TH. Echocardiographic detection of early diabetic myocardial disease. *J Am Coll Cardiol*. 2003;41:611–617.

125. Yang H, Sun JP, Lever HM, et al. Use of strain imaging in detecting segmental dysfunction in patients with hypertrophic cardiomyopathy. *J Am Soc Echocardiogr*. 2003;16:233–239.

126. Stanton T, Marwick TH. Assessment of subendocardial structure and function. *JACC Cardiovasc Imaging*. 2010;3:867–875.

127. Smedsrud MK, Sarvari S, Haugaa KH, et al. Duration of myocardial early systolic lengthening predicts the presence of significant coronary artery disease. *J Am Coll Cardiol*. 2012;60:1086–1093.

128. Kraigher-Krainer E, Shah AM, Gupta DK, et al. Impaired systolic function by strain imaging in heart failure with preserved ejection fraction. *J Am Coll Cardiol*. 2014;63:447–456.

129. Hasselberg NE, Haugaa KH, Sarvari SI, et al. Left ventricular global longitudinal strain is associated with exercise capacity in failing hearts with preserved and reduced ejection fraction. *Eur Heart J Cardiovasc Imaging*. 2015;16:217–224.

130. Stein PD, Marzilli M, Sabbah HN, Lee T. Systolic and diastolic pressure gradients within the left ventricular wall. *Am J Physiol*. 1980;238:H625–H630.

131. Maciver DH. The relative impact of circumferential and longitudinal shortening on left ventricular ejection fraction and stroke volume. *Exp Clin Cardiol*. 2012;17:5–11.

132. Maciver DH. A new method for quantification of left ventricular systolic function using a corrected ejection fraction. *Eur J Echocardiogr*. 2011;12:228–234.

133. Aurigemma GP, Silver KH, Priest MA, Gaasch WH. Geometric changes allow normal ejection fraction despite depressed myocardial shortening in hypertensive left ventricular hypertrophy. *J Am Coll Cardiol*. 1995;26:195–202.

134. Serri K, Reant P, Lafitte M, et al. Global and regional myocardial function quantification by two-dimensional strain: application in hypertrophic cardiomyopathy. *J Am Coll Cardiol*. 2006;47:1175–1181.

135. Mizuguchi Y, Oishi Y, Miyoshi H, Iuchi A, Nagase N, Oki T. Concentric left ventricular hypertrophy brings deterioration of systolic longitudinal, circumferential, and radial myocardial deformation in hypertensive patients with preserved left ventricular pump function. *J Cardiol*. 2010;55:23–33.

136. Park JJ, Park JB, Park JH, Cho GY. Global longitudinal strain to predict mortality in patients with acute heart failure. *J Am Coll Cardiol*. 2018;71:1947–1957.

137. Sengelov M, Jorgensen PG, Jensen JS, et al. Global longitudinal strain is a superior predictor of all-cause mortality in heart failure with reduced ejection fraction. *JACC Cardiovasc Imaging*. 2015;8:1351–1359.

138. Kumada T, Karliner JS, Pouleur H, Gallagher KP, Shirato K, Ross J Jr. Effects of coronary occlusion on early ventricular diastolic events in conscious dogs. *Am J Physiol*. 1979;237:H542–H549.

139. Lew WY, Ban-Hayashi E. Mechanisms of improving regional and global ventricular function by preload alterations during acute ischemia in the canine left ventricle. *Circulation*. 1985;72:1125–1134.

140. Voigt JU, Lindenmeier G, Exner B, et al. Incidence and characteristics of segmental postsystolic longitudinal shortening in normal, acutely ischemic, and scarred myocardium. *J Am Soc Echocardiogr*. 2003;16:415–423.

141. Skulstad H, Edvardsen T, Urheim S, et al. Postsystolic shortening in ischemic myocardium: active contraction or passive recoil? *Circulation*. 2002;106:718–724.

142. Knuuti J, Wijns W, Saraste A, et al. 2019 ESC guidelines for the diagnosis and management of chronic coronary syndromes. *Eur Heart J*. 2020;41:407–477.

143. Kass DA. Pathobiology of cardiac dyssynchrony and resynchronization. *Heart Rhythm*. 2009;6:1660–1665.

144. Parsai C, Bijnens B, Sutherland GR, et al. Toward understanding response to cardiac resynchronization therapy: left ventricular dyssynchrony is only one of multiple mechanisms. *Eur Heart J*. 2009;30:940–949.

145. Remme EW, Niederer S, Gjesdal O, et al. Factors determining the magnitude of the preejection leftward septal motion in left bundle branch block. *Europace*. 2016;18:1905–1913.

146. De Boeck BW, Teske AJ, Meine M, et al. Septal rebound stretch reflects the functional substrate to cardiac resynchronization therapy and predicts volumetric and neurohormonal response. *Eur J Heart Fail*. 2009;11:863–871.

147. Voigt JU, Schneider TM, Korder S, et al. Apical transverse motion as surrogate parameter to determine regional left ventricular function inhomogeneities: a new, integrative approach to left ventricular asynchrony assessment. *Eur Heart J*. 2009;30:959–968.

148. Steelant B, Stankovic I, Roijakkers I, et al. The impact of infarct location and extent on LV motion patterns: implications for dyssynchrony assessment. *JACC Cardiovasc Imaging*. 2016;9:655–664.

149. Calle S, Kamoen V, De Buyzere M, De Pooter J, Timmermans F. A strain-based staging classification of left bundle branch block-induced cardiac remodeling. *JACC Cardiovasc Imaging*. 2021;14:1691–1702.

150. Lumens J, Leenders GE, Cramer MJ, et al. Mechanistic evaluation of echocardiographic dyssynchrony indices: patient data combined with multiscale computer simulations. *Circ Cardiovasc Imaging*. 2012;5:491–499.

151. Larsen CK, Galli E, Duchenne J, et al. Scar imaging in the dyssynchronous left ventricle: accuracy of myocardial metabolism by positron emission tomography and function by echocardiographic strain. *Int J Cardiol*. 2023;372:122–129.

152. Wouters L, Duchenne J, Bezy S, et al. Septal scar detection in patients with left bundle branch block using echocardiographic shear wave elastography. *JACC Cardiovasc Imaging*. 2023;16:713–715.

153. Risum N, Tayal B, Hansen TF, et al. Identification of typical left bundle branch block contraction by strain echocardiography is additive to electrocardiography in prediction of long-term outcome after cardiac resynchronization therapy. *J Am Coll Cardiol*. 2015;66:631–641.

154. Stankovic I, Prinz C, Ciarka A, et al. Relationship of visually assessed apical rocking and septal flash to response and long-term survival following cardiac resynchronization therapy (PREDICT-CRT). *Eur Heart J Cardiovasc Imaging*. 2016;17:262–269.

155. Aalen JM, Donal E, Larsen CK, et al. Imaging predictors of response to cardiac resynchronization therapy: left ventricular work asymmetry by echocardiography and septal viability by cardiac magnetic resonance. *Eur Heart J*. 2020;41:3813–3823.

156. Gorcsan J III, Anderson CP, Tayal B, et al. Systolic stretch characterizes the electromechanical substrate responsive to cardiac resynchronization therapy. *JACC Cardiovasc Imaging*. 2019;12:1741–1752.

157. Lumens J, Tayal B, Walmsley J, et al. Differentiating electromechanical from non-electrical substrates of mechanical discoordination to identify responders to cardiac resynchronization therapy. *Circ Cardiovasc Imaging*. 2015;8:e003744.

158. Cvijic M, Duchenne J, Unlu S, et al. Timing of myocardial shortening determines left ventricular regional myocardial work and regional remodelling in hearts with conduction delays. *Eur Heart J Cardiovasc Imaging*. 2018;19:941–949.

159. Gallard A, Bidaut A, Hubert A, et al. Characterization of responder profiles for cardiac resynchronization therapy through unsupervised clustering of clinical and strain data. *J Am Soc Echocardiogr*. 2021;34:483–493.

160. Borgquist R, Carlsson M, Markstad H, et al. Cardiac resynchronization therapy guided by echocardiography, MRI, and CT imaging: a randomized controlled study. *JACC Clin Electrophysiol*. 2020;6:1300–1309.

161. Beela AS, Unlu S, Duchenne J, et al. Assessment of mechanical dyssynchrony can improve the prognostic value of guideline-based patient selection for cardiac resynchronization therapy. *Eur Heart J Cardiovasc Imaging*. 2019;20:66–74.

162. Popovic ZB, Kwon DH, Mishra M, et al. Association between regional ventricular function and myocardial fibrosis in hypertrophic cardiomyopathy assessed by speckle tracking echocardiography and delayed hyperenhancement magnetic resonance imaging. *J Am Soc Echocardiogr*. 2008;21:1299–1305.

163. Pagourelias ED, Mirea O, Vovas G, et al. Relation of regional myocardial structure and function in hypertrophic cardiomyopathy and amyloidosis: a combined two-dimensional speckle tracking and cardiovascular magnetic resonance

analysis. *Eur Heart J Cardiovasc Imaging*. 2019;20:426–437.

164. Yiu KH, Atsma DE, Delgado V, et al. Myocardial structural alteration and systolic dysfunction in preclinical hypertrophic cardiomyopathy mutation carriers. *PLoS One*. 2012;7:e36115.

165. Tower-Rader A, Mohananey D, To A, Lever HM, Popovic ZB, Desai MY. Prognostic value of global longitudinal strain in hypertrophic cardiomyopathy: a systematic review of existing literature. *JACC Cardiovasc Imaging*. 2019;12:1930–1942.

166. Haland TF, Almaas VM, Hasselberg NE, et al. Strain echocardiography is related to fibrosis and ventricular arrhythmias in hypertrophic cardiomyopathy. *Eur Heart J Cardiovasc Imaging*. 2016;17:613–621.

167. Phelan D, Collier P, Thavendiranathan P, et al. Relative apical sparing of longitudinal strain using two-dimensional speckle-tracking echocardiography is both sensitive and specific for the diagnosis of cardiac amyloidosis. *Heart*. 2012;98:1442–1448.

168. Liu D, Hu K, Niemann M, et al. Effect of combined systolic and diastolic functional parameter assessment for differentiation of cardiac amyloidosis from other causes of concentric left ventricular hypertrophy. *Circ Cardiovasc Imaging*. 2013;6:1066–1072.

169. Pagourelias ED, Mirea O, Duchenne J, et al. Echo parameters for differential diagnosis in cardiac amyloidosis: a head-to-head comparison of deformation and nondeformation parameters. *Circ Cardiovasc Imaging*. 2017;10:e005588.

170. Brand A, Frumkin D, Hubscher A, et al. Phasic left atrial strain analysis to discriminate cardiac amyloidosis in patients with unclear thick heart pathology. *Eur Heart J Cardiovasc Imaging*. 2021;22:680–687.

171. De Gaspari M, Sinigiani G, De Michieli L, et al. Relative apical sparing in cardiac amyloidosis is not always explained by an amyloid gradient. *Eur Heart J Cardiovasc Imaging*. 2023;24:1258–1268.

172. Ternacle J, Bodez D, Guellich A, et al. Causes and consequences of longitudinal lv dysfunction assessed by 2D strain echocardiography in cardiac amyloidosis. *JACC Cardiovasc Imaging*. 2016;9:126–138.

173. Phelan D, Thavendiranathan P, Popovic Z, et al. Application of a parametric display of two-dimensional speckle-tracking longitudinal strain to improve the etiologic diagnosis of mild to moderate left ventricular hypertrophy. *J Am Soc Echocardiogr*. 2014;27:888–895.

174. Abecasis J, Lopes P, Santos RR, et al. Prevalence and significance of relative apical sparing in aortic stenosis: insights from an echo and cardiovascular magnetic resonance study of patients referred for surgical aortic valve replacement. *Eur Heart J Cardiovasc Imaging*. 2023;24:1033–1042.

175. Arbelo E, Protonotarios A, Gimeno JR, et al. 2023 ESC guidelines for the management of cardiomyopathies. *Eur Heart J*. 2023;44:3503–3626.

176. Chacko L, Martone R, Bandera F, et al. Echocardiographic phenotype and prognosis in transthyretin cardiac amyloidosis. *Eur Heart J*. 2020;41:1439–1447.

177. Giblin GT, Cuddy SAM, Gonzalez-Lopez E, et al. Effect of tafamidis on global longitudinal strain and myocardial work in transthyretin cardiac amyloidosis. *Eur Heart J Cardiovasc Imaging*. 2022;23:1029–1039.

178. Lee Chuy K, Drill E, Yang JC, et al. Incremental value of global longitudinal strain for predicting survival in patients with advanced AL amyloidosis. *JACC CardioOncol*. 2020;2:223–231.

179. Cohen OC, Ismael A, Pawarova B, et al. Longitudinal strain is an independent predictor of survival and response to therapy in patients with systemic AL amyloidosis. *Eur Heart J*. 2022;43:333–341.

180. Huntjens PR, Zhang KW, Soyama Y, Karmpalioti M, Lenihan DJ, Gorcsan J III. Prognostic utility of echocardiographic atrial and ventricular strain imaging in patients with cardiac amyloidosis. *JACC Cardiovasc Imaging*. 2021;14:1508–1519.

181. Mast TP, Taha K, Cramer MJ, et al. The prognostic value of right ventricular deformation imaging in early arrhythmogenic right ventricular cardiomyopathy. *JACC Cardiovasc Imaging*. 2019;12:446–455.

182. Teske AJ, Cox MG, Te Riele AS, et al. Early detection of regional functional abnormalities in asymptomatic ARVD/C gene carriers. *J Am Soc Echocardiogr*. 2012;25:997–1006.

183. Sarvari SI, Haugaa KH, Anfinsen OG, et al. Right ventricular mechanical dispersion is related to malignant arrhythmias: a study of patients with arrhythmogenic right ventricular cardiomyopathy and subclinical right ventricular dysfunction. *Eur Heart J*. 2011;32:1089–1096.

184. Kirkels FP, Lie OH, Cramer MJ, et al. Right ventricular functional abnormalities in arrhythmogenic cardiomyopathy: association with life-threatening ventricular arrhythmias. *JACC Cardiovasc Imaging*. 2021;14:900–910.

185. Haugaa KH, Basso C, Badano LP, et al. Comprehensive multi-modality imaging approach in arrhythmogenic cardiomyopathy—an expert consensus document of the European Association of Cardiovascular Imaging. *Eur Heart J Cardiovasc Imaging*. 2017;18:237–253.

186. Verdonschot JAJ, Merken JJ, Brunner-La Rocca HP, et al. Value of speckle tracking-based deformation analysis in screening relatives of patients with asymptomatic dilated cardiomyopathy. *JACC Cardiovasc Imaging*. 2020;13:549–558.

187. Raafs AG, Vos JL, Henkens M, et al. Left atrial strain has superior prognostic value to ventricular function and delayed-enhancement in dilated cardiomyopathy. *JACC Cardiovasc Imaging*. 2022;15:1015–1026.

188. Bui QM, Hong KN, Kraushaar M, et al. Myocardial strain and association with clinical outcomes in Danon disease: a model for monitoring progression of genetic cardiomyopathies. *J Am Heart Assoc*. 2021;10:e022544.

189. Lu DY, Huang WM, Wang WT, et al. Reduced global longitudinal strain as a marker for early detection of Fabry cardiomyopathy. *Eur Heart J Cardiovasc Imaging*. 2022;23:487–495.

190. Rob D, Marek J, Dostalova G, Linhart A. Heart failure in Fabry disease revisited: application of current heart failure guidelines and recommendations. *ESC Heart Fail*. 2022;9:4043–4052.

191. Weidemann F, Niemann M, Herrmann S, et al. A new echocardiographic approach for the detection of non-ischaemic fibrosis in hypertrophic myocardium. *Eur Heart J*. 2007;28:3020–3026.

192. Caselli S, Montesanti D, Autore C, et al. Patterns of left ventricular longitudinal strain and strain rate in Olympic athletes. *J Am Soc Echocardiogr*. 2015;28:245–253.

193. Dawkins TG, Curry BA, Wright SP, et al. Right ventricular function and region-specific adaptation in athletes engaged in high-dynamic sports: a meta-analysis. *Circ Cardiovasc Imaging*. 2021;14:e012315.

194. Afonso L, Kondur A, Simegn M, et al. Two-dimensional strain profiles in patients with physiological and pathological hypertrophy and preserved left ventricular systolic function: a comparative analyses. *BMJ Open*. 2012;2:e001390.

195. D'Ascenzi F, Solari M, Corrado D, Zorzi A, Mondillo S. Diagnostic differentiation between arrhythmogenic cardiomyopathy and athlete's heart by using imaging. *JACC Cardiovasc Imaging*. 2018;11:1327–1339.

196. D'Andrea A, De Corato G, Scarafile R, et al. Left atrial myocardial function in either physiological or pathological left ventricular hypertrophy: a two-dimensional speckle strain study. *Br J Sports Med*. 2008;42:696–702.

197. Petersen SE, Selvanayagam JB, Francis JM, et al. Differentiation of athlete's heart from pathological forms of cardiac hypertrophy by means of geometric indices derived from cardiovascular magnetic resonance. *J Cardiovasc Magn Reson*. 2005;7:551–558.

198. Lyon AR, Lopez-Fernandez T, Couch LS, et al. 2022 ESC guidelines on cardio-oncology developed in collaboration with the European Hematology Association (EHA), the European Society for Therapeutic Radiology and Oncology (ESTRO) and the International Cardio-Oncology Society (IC-OS). *Eur Heart J Cardiovasc Imaging*. 2022;23:e333–e465.

199. Kim HM, Cho GY, Hwang IC, et al. Myocardial strain in prediction of outcomes after surgery for severe mitral regurgitation. *JACC Cardiovasc Imaging*. 2018;11:1235–1244.

200. Vollema EM, Sugimoto T, Shen M, et al. Association of left ventricular global longitudinal strain with asymptomatic severe aortic stenosis: natural course and prognostic value. *JAMA Cardiol*. 2018;3:839–847.

201. Magne J, Cosyns B, Popescu BA, et al. Distribution and prognostic significance of left ventricular global longitudinal strain in asymptomatic significant aortic stenosis: an individual participant data meta-analysis. *JACC Cardiovasc Imaging*. 2019;12:84–92.

202. Alashi A, Khullar T, Mentias A, et al. Long-term outcomes after aortic valve surgery in

patients with asymptomatic chronic aortic regurgitation and preserved LVEF: impact of baseline and follow-up global longitudinal strain. *JACC Cardiovasc Imaging*. 2020;13:12–21.

203. Hiemstra YL, Tomsic A, van Wijngaarden SE, et al. Prognostic value of global longitudinal strain and etiology after surgery for primary mitral regurgitation. *JACC Cardiovasc Imaging*. 2020;13:577–585.

204. Namazi F, van der Bijl P, Hirasawa K, et al. Prognostic value of left ventricular global longitudinal strain in patients with secondary mitral regurgitation. *J Am Coll Cardiol*. 2020;75:750–758.

205. Dahl JS, Videbaek L, Poulsen MK, Rudbaek TR, Pellikka PA, Moller JE. Global strain in severe aortic valve stenosis: relation to clinical outcome after aortic valve replacement. *Circ Cardiovasc Imaging*. 2012;5:613–620.

206. Kamperidis V, Marsan NA, Delgado V, Bax JJ. Left ventricular systolic function assessment in secondary mitral regurgitation: left ventricular ejection fraction vs. speckle tracking global longitudinal strain. *Eur Heart J*. 2016;37:811–816.

207. Writing Committee Members, Otto CM, Nishimura RA, et al. 2020 ACC/AHA guideline for the management of patients with valvular heart disease: executive summary: a report of the American College of Cardiology/American Heart Association Joint Committee on Clinical Practice Guidelines. *J Am Coll Cardiol*. 2021;77(4):450–500.

208. Vahanian A, Beyersdorf F, Praz F, et al. 2021 ESC/EACTS guidelines for the management of valvular heart disease. *Eur Heart J*. 2022;43:561–632.

209. Smiseth OA, Morris DA, Cardim N, et al. Multimodality imaging in patients with heart failure and preserved ejection fraction: an expert consensus document of the European Association of Cardiovascular Imaging. *Eur Heart J Cardiovasc Imaging*. 2022;23:e34–e61.

210. Malaescu GG, Mirea O, Capota R, Petrescu AM, Duchenne J, Voigt JU. Left atrial strain determinants during the cardiac phases. *JACC Cardiovasc Imaging*. 2022;15:381–391.

211. Freed BH, Daruwalla V, Cheng JY, et al. Prognostic utility and clinical significance of cardiac mechanics in heart failure with preserved ejection fraction: importance of left atrial strain. *Circ Cardiovasc Imaging*. 2016;9:e003754.

212. Leung M, van Rosendael PJ, Abou R, et al. Left atrial function to identify patients with atrial fibrillation at high risk of stroke: new insights from a large registry. *Eur Heart J*. 2018;39:1416–1425.

213. Moon MG, Hwang IC, Lee HJ, et al. Reverse remodeling assessed by left atrial and ventricular strain reflects treatment response to sacubitril/valsartan. *JACC Cardiovasc Imaging*. 2022;15:1525–1541.

214. Nagueh SF, Khan SU. Left atrial strain for assessment of left ventricular diastolic function: focus on populations with normal LVEF. *JACC Cardiovasc Imaging*. 2023;16:691–707.

215. Khan FH, Zhao D, Ha JW, et al. Evaluation of left ventricular filling pressure by echocardiography in patients with atrial fibrillation. *Echo Res Pract*. 2024;11:14.

216. Kurt M, Tanboga IH, Aksakal E, et al. Relation of left ventricular end-diastolic pressure and N-terminal pro-brain natriuretic peptide level with left atrial deformation parameters. *Eur Heart J Cardiovasc Imaging*. 2012;13:524–530.

217. Cameli M, Sparla S, Losito M, et al. Correlation of left atrial strain and doppler measurements with invasive measurement of left ventricular end-diastolic pressure in patients stratified for different values of ejection fraction. *Echocardiography*. 2016;33:398–405.

218. Inoue K, Andersen OS, Remme EW, et al. Echocardiographic evaluation of left ventricular filling pressure in patients with pulmonary hypertension. *JACC Cardiovasc Imaging*. 2024;17(5):566–567.

219. Kowallick JT, Kutty S, Edelmann F, et al. Quantification of left atrial strain and strain rate using cardiovascular magnetic resonance myocardial feature tracking: a feasibility study. *J Cardiovasc Magn Reson*. 2014;16:60.

220. Amzulescu MS, Langet H, Saloux E, et al. Head-to-head comparison of global and regional two-dimensional speckle tracking strain versus cardiac magnetic resonance tagging in a multicenter validation study. *Circ Cardiovasc Imaging*. 2017;10(11):e006530.

221. Fischer K, Linder OL, Erne SA, et al. Reproducibility and its confounders of CMR feature tracking myocardial strain analysis in patients with suspected myocarditis. *Eur Radiol*. 2022;32:3436–3446.

222. Barreiro-Perez M, Curione D, Symons R, Claus P, Voigt JU, Bogaert J. Left ventricular global myocardial strain assessment comparing the reproducibility of four commercially available CMR-feature tracking algorithms. *Eur Radiol*. 2018;28:5137–5147.

223. Domenech-Ximenos B, Sanz-de la Garza M, Sepulveda-Martinez A, et al. Assessment of myocardial deformation with CMR: a comparison with ultrasound speckle tracking. *Eur Radiol*. 2021;31:7242–7250.

224. Pathan F, Zainal Abidin HA, Vo QH, et al. Left atrial strain: a multi-modality, multi-vendor comparison study. *Eur Heart J Cardiovasc Imaging*. 2021;22:102–110.

225. Balinisteanu A, Duchenne J, Puvrez A, et al. Inter-vendor differences in speckle tracking strain—a ten year follow-up on the Strain Standardization Task Force Inter-Vendor Comparison Study. London, United Kingdom: Paper presented at: European Society of Cardiology Congress; 2024.

226. Dobrovie M, Barreiro-Perez M, Curione D, et al. Inter-vendor reproducibility and accuracy of segmental left ventricular strain measurements using CMR feature tracking. *Eur Radiol*. 2019;29:6846–6857.

227. Groschel J, Kuhnt J, Viezzer D, et al. Comparison of manual and artificial intelligence based quantification of myocardial strain by feature tracking-a cardiovascular MR study in health and disease. *Eur Radiol*. 2024;34(2):1003–1015.

228. Barbaroux H, Kunze KP, Neji R, et al. Automated segmentation of long and short axis DENSE cardiovascular magnetic resonance for myocardial strain analysis using spatio-temporal convolutional neural networks. *J Cardiovasc Magn Reson*. 2023;25:16.

229. Salte IM, Ostvik A, Olaisen SH, et al. Deep learning for improved precision and reproducibility of left ventricular strain in echocardiography: a test-retest study. *J Am Soc Echocardiogr*. 2023;36:788–799.

230. Salte IM, Ostvik A, Smistad E, et al. Artificial intelligence for automatic measurement of left ventricular strain in echocardiography. *JACC Cardiovasc Imaging*. 2021;14:1918–1928.

231. Stowell CC, Howard JP, Ng T, et al. 2-dimensional echocardiographic global longitudinal strain with artificial intelligence using open data from a UK-wide collaborative. *JACC Cardiovasc Imaging*. 2024;17:865–876.

232. Backhaus SJ, Aldehayat H, Kowallick JT, et al. Artificial intelligence fully automated myocardial strain quantification for risk stratification following acute myocardial infarction. *Sci Rep*. 2022;12:12220.

233. Ntalianis E, Sabovcik F, Cauwenberghs N, et al. Unsupervised time-series clustering of left atrial strain for cardiovascular risk assessment. *J Am Soc Echocardiogr*. 2023;36:778–787.

234. Shehata ML, Cheng S, Osman NF, Bluemke DA, Lima JA. Myocardial tissue tagging with cardiovascular magnetic resonance. *J Cardiovasc Magn Reson*. 2009;11:55.

235. Backhaus SJ, Metschies G, Billing M, et al. Cardiovascular magnetic resonance imaging feature tracking: Impact of training on observer performance and reproducibility. *PLoS One*. 2019;14:e0210127.

236. Auger DA, Ghadimi S, Cai X, et al. Reproducibility of global and segmental myocardial strain using cine DENSE at 3 T: a multicenter cardiovascular magnetic resonance study in healthy subjects and patients with heart disease. *J Cardiovasc Magn Reson*. 2022;24:23.

237. Hayat D, Kloeckner M, Nahum J, et al. Comparison of real-time three-dimensional speckle tracking to magnetic resonance imaging in patients with coronary heart disease. *Am J Cardiol*. 2012;109:180–186.

238. Marwick TH, Leano RL, Brown J, et al. Myocardial strain measurement with 2-dimensional speckle-tracking echocardiography: definition of normal range. *JACC Cardiovasc Imaging*. 2009;2:80–84.

239. Reant P, Barbot L, Touche C, et al. Evaluation of global left ventricular systolic function using three-dimensional echocardiography speckle-tracking strain parameters. *J Am Soc Echocardiogr*. 2012;25:68–79.

240. Omar AM, Vallabhajosyula S, Sengupta PP. Left ventricular twist and torsion: research

observations and clinical applications. *Circ Cardiovasc Imaging*. 2015;8:e003029.

241. Tan YT, Wenzelburger F, Lee E, et al. The pathophysiology of heart failure with normal ejection fraction: exercise echocardiography reveals complex abnormalities of both systolic and diastolic ventricular function involving torsion, untwist, and longitudinal motion. *J Am Coll Cardiol*. 2009;54:36–46.

242. Zhu WX, Myers ML, Hartley CJ, Roberts R, Bolli R. Validation of a single crystal for measurement of transmural and epicardial thickening. *Am J Physiol*. 1986;251:H1045–H1055.

243. Hexeberg E, Homans DC, Bache RJ. Interpretation of systolic wall thickening. Can thickening of a discrete layer reflect fibre performance? *Cardiovasc Res*. 1995;29:16–21.

244. Smiseth OA, Torp H, Opdahl A, Haugaa KH, Urheim S. Myocardial strain imaging: how useful is it in clinical decision making? *Eur Heart J*. 2016;37:1196–1207.

245. Xu L, Pagano JJ, Haykowksy MJ, et al. Layer-specific strain in patients with heart failure using cardiovascular magnetic resonance: not all layers are the same. *J Cardiovasc Magn Reson*. 2020;22:81.

246. Smiseth OA, Aalen JM. Mechanism of harm from left bundle branch block. *Trends Cardiovasc Med*. 2019;29:335–342.

KEY WORDS cardiac magnetic resonance, cardiomyopathy, myocardial function, myocardial work, speckle-tracking echocardiography, strain imaging

APPENDIX For a supplemental video, please see the online version of this paper.